Assessment of hydrocarbon resource potential in Australian sedimentary basins:

development of fission track techniques

May 1988

END OF GRANT TECHNICAL REPORT
NERDDC Project No. 720

AJW Gleadow, IR Duddy,
PF Green & JF Lovering

Department of Geology,
University of Melbourne

Total Expenditure: $115,337

CONTENTS

ABSTRACT

This project has advanced the techniques of fission track analysis as a means of reconstructing the thermal evolution of sedimentary basins so that the conditions and timing of hydrocarbon generation can be assessed. It has been shown that the annealing of fission tracks in apatite is a more complex process than previously thought. A new quantitative description of apatite annealing has been developed which enables realistic predictions to be made of the annealing effects obtained from different kinds of thermal histories over geological time. These compare closely with fission track length measurements obtained on samples from a variety of well-understood geological environments. Application of the results of this research to the Cooper-Eromanga Basin indicates that the present high thermal gradients encountered in this area are a relatively recent phenomenon with the implication that hydrocarbon generation has been accelerating in the past few million years.

SUMMARY

Project Objectives

This report summarises the main research results obtained during the three years of support under NERDDC Project No 720 "Assessment of hydrocarbon resource potential in Australian sedimentary basins: development of fission track techniques". The broad objective of this project has been to develop the techniques of fission track analysis so that they can be used as a routine tool for thermal history reconstruction in hydrocarbon exploration. The importance of this arises from the relationship which we have previously demonstrated between fission track annealing in apatite and the thermal conditions required for oil generation in suitable hydrocarbon source rocks.

Specifically the project has combined two major objectives. These are firstly to define the annealing properties of fission tracks in the mineral apatite in terms of the fundamental physical process involved and to use this information as the basis for a quantitative annealing model Secondly the project has aimed to apply the concepts of fission track analysis so developed to Australian sedimentary basins and the Cooper-Eromanga Basin in particular. Another application of fission track analysis to sedimentary basins is the study of sedimentary provenance through dating of the detrital materials. Fission track ages of apatites (and other minerals) that have not been significantly heated since deposition will relate to their source areas and this aspect has also been investigated in rocks from the Cooper-Eromanga Basin.

Work Program and Findings

The first part of this project has involved research into the fundamental nature of the fission track annealing process in apatite as a basis for quantitative modelling. Extensive laboratory annealing studies have been carried out where fission tracks in apatite samples have been heated under accurately controlled conditions of temperature and time. These studies have enabled us to develop a rigorous mathematical description of track annealing in this mineral so that the annealing effect resulting from any given thermal history can now be calculated for comparison with that observed in naturally annealed apatite samples.

The results of this work have also led to a new description of the way in which fission tracks are gradually annealed during exposure to elevated temperatures. The mechanism appears to be a two-stage one whereby the dominant process is a progressive shrinking of the track from each end, with tracks perpendicular to the c-axis shortening more rapidly than those parallel to it. As annealing becomes more severe the tracks begin to break up into discontinuous portions by the appearance of essentially unetchable gaps in the track structure. Track length distributions in annealed apatites reflect the interplay of these processes.

These studies have included an examination of small variations in annealing properties which are found between individual apatite grains of different chemical composition. Electron microprobe studies show that apatite grains rich in chlorine are more resistant to annealing, while fluorapatite is more readily annealed. This compositional effect is an important consideration in achieving the maximum temperature resolution from apatite fission track modelling.

Formal statistical methods have been applied to the extensive set of laboratory annealing data to rigorously derive an empirical mathematical description of the annealing process. Older laboratory annealing studies have tended to show the reduction in fission track density during annealing in terms of a series of fanning lines on an Arrhenius plot, showing logarithm of time against inverse absolute temperature, implying a range of activation energies for different degrees of annealing. Our new results using the higher precision that is possible with track length measurements, rather than track densities, show that the degree of such fanning is much less than had generally been thought. The dependence of track length reduction on time and temperature suggests that contours of equal length reduction in an Arrhenius plot can be described by parallel or only slightly fanning straight lines. The best fitting model developed from this procedure is a slightly fanning model which can explain 98% of the variation in the experimental results for a single apatite composition, and makes realistic predictions for similar apatites undergoing geological annealing.

We have also conducted an extensive survey of fission track length distributions in apatites from a variety of different terrains where the style of thermal history may be constrained by the regional geology. This database provides a unique resource for testing and evaluating the validity of thermal history modelling based on an experimental understanding of the fission track annealing process. The continuous production of fission tracks through time, coupled with the fact that the length of each track shrinks to a value characteristic of the maximum temperature it has experienced, gives a final length distribution which directly reflects the nature of the variation of temperature with time. We have identified a series of commonly ocurring distribution types that are typical of particular thermal histories. The most distinctive of the various possible forms of the final distribution are bimodal distributions, which give clear evidence of a two-stage history, including high and low temperature phases. Samples that have undergone natural annealing during burial in sedimentary basins, especially the Otway Basin of southeastern Australia, also give comparable results to laboratory annealing studies on the same apatites. These observations give further confirmation that the fission track annealing process observable in the laboratory is the same as that which occurs at lower temperatures over geological time.

The major application of fission track techniques arising from this project is an assessment of the thermal history of the Cooper-Eromanga Basin. Modelling of fission track parameters in a number of hydrocarbon exploration wells indicates that the markedly high geothermal gradients present over much of the basin are a relatively recent phenomenon and have probably developed over only the last 1 to 10 Ma. This suggests that hydrocarbon generation within the basin has been enhanced in the recent geological past. These findings are in agreement with the suggestion of some earlier coalification studies but contrary to more recent ideas suggesting that the present gradients have been operating throughout the basin's history. The study has delineated important aspects of the thermal history of the basin that will form the basis of further fission track work.

This study has also revealed the presence of a dominant contemporaneous volcanogenic source for most of the Cretaceous units in the Eromanga Basin, providing an explanation for the nature of the boundaries between the quartzose basement derived reservoirs like the Hutton and Namur and the associated dirty (volcanogenic) reservoirs of the the Birkhead and Murta. The study gives an important example of how variations in apatite composition can affect its annealing response, confirming the generality of the concept first proposed from work in the Otway Basin. Apatites from two quite different types of provenance are found in the basin sequence, those of volcanogenic origin with a variable Cl/(Cl+F) ratio and an older basement source with a much more restricted range of F-rich compositions.

Industrial Application and Recommendations

Even at this relatively early stage in its development, Fission Track Analysis has very great potential for routine industrial application in petroleum exploration programs by giving new insights into questions of the thermal evolution of sedimentary basins and the timing of hydrocarbon generation. For some years now there has been a steadily growing demand for fission track analytical services on a commercial basis. Throughout the duration of this grant it was possible for the Melbourne Fission Track Research Group to meet this demand operating as a part-time consultancy under the auspices of the University of Melbourne. This had the major advantage that the results of the research activities could be progressively tested on actual exploration problems with benefits flowing back into the research program. Strong growth during 1987 for such services, however, particularly from major overseas markets, meant that this mode of operation was no longer possible without impinging in a deleterious way on the continuing research effort. This led directly to the launching of Geotrack International Pty Ltd as an independent company which is now actively marketing fission track services to the international oil exploration industry. Geotrack is acknowledged as the world leader in this field.

Much research work still remains to be done in order to realize the full potential of the fission track analysis and we are continuing this effort as a major focus of our continuing NERDDC-sponsored project. We believe that in its industrial application fission track analysis will remain a highly specialised technology that is best carried out by dedicated and experienced analysts. For this reason we consider it unlikely that many petroleum companies will choose to set up their own fission track analytical facilities in the near future but will rely on the expertise available through a specialist company such as Geotrack International. The skills involved in the interpretation of fission track data, however, should be readily transferable to exploration geologists throughout the industry. We believe that there is a need for an understanding of the principles involved in fission track analysis to become part of the training and continuing education of exploration staff. In this area of technology transfer we plan to continue the wide distribution of the results of our research through scientific publications and holding seminars and workshops.

Future Research and Development in this field needs to focus on quantifying further details of the fission track annealing process so that numerical modelling procedures can be fully developed. For example, further work is clearly needed to fully understand the relationship between the composition and thermal annealing properties of apatite. In addition further work is needed to carry out demonstration projects on selected sedimentary basins to test the applicability and advantages of fission track analysis in a variety of geological environments. These aspects are currently being addressed in our on-going NERDDC-sponsored research program.

TECHNOLOGY TRANSFER ACTIVITIES

Technology transfer has been pursued during the three years of this project by means of presentation of the results of our work at a number of Australian and overseas conferences, and through the publication of our research findings in the international scientific literature. A list of research publications arising from this project is given in the following bibliography. In addition to this we have conducted seminars on Fission Track Analysis for a number of major oil exploration companies, both in Australia and overseas, to explain our work and familiarise staff with interpretation procedures.

A major feature of this program of information exchange was the holding of a "Workshop on Fission Track Analysis" held at James Cook University, Townsville over three days in September, 1984. The scientific program for this workshop was organised entirely by our Melbourne Fission Track Research Group and costs were partly met by NERDDC. The Workshop was attended by 30 delgates from Universities, Oil Companies, State Geological Surveys, and the Bureau of Mineral Resources in Australia and there were overseas delegates from New Zealand and Papua New Guinea as well. The principal aim of the Workshop was to familiarise interested personnel with the methods, applications and current state of development of fission track techniques. Particular emphasis was given to areas of potentially important commercial application. It is planned to hold a similar Workshop during the latter part of the continuing NERRDC-sponsored resereach program.

BIBLIOGRAPHY

Major publications arising directly from the present project are listed below. Other publications in related fields are cited in the reference lists at the ends of Parts 2 and 3.

Gleadow, A.J.W. and Harrison T.M., 1988. Thermochronology: quantitative constraints on basin modelling and hydrocarbon maturation. *in* K. Sinding-Larsen (ed) *Extensional basin modelling and paleotemperature reconstruction*. International Union of geological Sciences (in press).

Gleadow, A.J.W., Duddy, I.R., Green P.F. and Hegarty, K.A., 1986a. Fission track lengths in the apatite annealing zone and the interpretation of mixed ages. *Earth Planet. Sci. Lett.* 78, 245-254.

Gleadow, A.J.W., Duddy, I.R., Green, P.F. and Lovering, J.F., 1986b. Confined fission track lengths in apatite - a diagnostic tool for thermal history analysis. *Contr. Miner. Petrol.* 94, 405-415.

Green, P.F., Duddy, I.R., Gleadow, A.J.W., Tingate, P.R. and Laslett, G.M., 1985. Fission track annealing in apatite: track length measurements and the form of the Arrhenius plot. *Nucl. Tracks* 10, 323-328.

Green, P.F., Duddy, I.R., Gleadow, A.J.W. and Laslett, G.M., 1986. Thermal annealing of fission tracks in apatite: 1- A qualitative description. *Isot Geosci.* 59, 237-253..

Green, P.F., Duddy, I.R., Gleadow, A.J.W. and Lovering, J. F., 1988. Apatite fission track analysis as a paleotemperature indicator for hydrocarbon exploration. *In* N.D Naeser, (ed.) *Thermal histories of sedimentary basins*. Springer-Verlag (in press).

Laslett, G.M., Green, P.F., Duddy, I.R. and Gleadow, A.J.W., 1987. Thermal annealing of fission tracks in apatite: II - A quantitative analysis. *Isot. Geosci.* 65, 1-13.

PART 1

BACKGROUND AND OBJECTIVES

THERMAL HISTORY ASSESSMENT IN SEDIMENTARY BASINS

Study of the low temperature thermal evolution of sedimentary basins has been motivated largely by the need to understand the thermal maturation of hydrocarbons in suitable source rocks within the basin environment. This has led to the development of a wide variety of techniques which use the record of thermally-activated processes preserved in the sedimentary rocks to assess their thermal evolution at the relatively low temperatures encountered during basin development. Some of these are mineralogical methods involving measurements of diagenetic reactions, fluid inclusions and other inorganic properties of the rocks, all of which may provide information on maximum palaeotemperatures, analogous to that obtained from the battery of organic geochemical techniques now in use for this purpose. The timing of the thermal maximum, however, can only be inferred indirectly from such evidence. Other approaches have used K-Ar and Rb-Sr dating of diagenetic minerals such as glauconite and illite, the results of which have usually been interpreted in terms of the timing of the diagenetic episode.

Fission track analysis of detrital apatites is a relatively new technique that combines many of these attributes by being able to give information simultaneously on both temperature and time (Gleadow *et al.*, 1983, Green *et al.*, 1986). This technique is based on a well-established method of geochronology, the radiometric clock of which is progressively reset between temperatures of about 60-130°C, leaving a record of heating in the temperature range of maximum generation of liquid hydrocarbons. This resetting occurs by a process of fission track *annealing* which is explained in more detail below. The technique can provide information on the age of basin cooling, the temperature, timing and, in some cases, the duration of a heating episode, and can also give an indication of age patterns in the sediment source area. The amount of this information that can be extracted from any one sample, or suite of samples, will vary depending on the particular circumstances, but it is already clear that the system contains an important record of thermal history in a temperature range relevant to basin modelling. By providing accurate constraints on the variation of temperature through time, this technique can provide new insights into mechanisms of basin evolution and direct information about the likely generation of hydrocarbons within suitable habitats.

Other methods of evaluating such information based on organic materials, such as vitrinite reflectance (e.g. Castaño and Sparks 1974; Waples, 1980) and conodont colouration indices (Epstein et al., 1977; Harris, 1979), give only a single parameter, integrated over the complete thermal history. Fission tracks, on the other hand, are formed continuously throughout time, and therefore the final track length distribution contains the full detail of the temperature variation with time below about 130°C. Understanding the fission track annealing process in terms of the temperature and time necessary to produce a given track length should enable the detailed thermal history below 130°C to be extracted from the track length distribution.

APATITE FISSION TRACK ANALYSIS

Fission Track Dating

Fission track dating depends on the accumulation of radiation damage in uranium-bearing minerals from the spontaneous fission of ^{238}U over geological time. The radiation damage occurs in the form of *fission tracks*, linear defects in the host crystal which are produced by the passage of the heavily-ionizing nuclear fragments resulting from the fission decay. The tracks are relatively large and can be made visible by chemically etching a polished surface on the crystal so that they can be observed and counted under an optical microscope at high magnification. The number of fission tracks will steadily increase through time, at least for the simplest case where the sample remains at low temperatures. If the rate of decay and the uranium concentration are known, then a geological age can be calculated from the number of tracks that have accumulated over the lifetime of the crystal. The uranium concentration is measured by irradiating the sample with thermal neutrons which induce fission in a small fraction of the ^{235}U nuclei, which are present as a constant proportion of natural uranium. The new induced fission tracks are most conveniently measured in an external track detector, such as a sheet of mica, held firmly in contact with the polished sample surface during the irradiation. This approach has the advantage that fission track ages can be measured on individual crystals within the sample mount. Useful summaries of various aspects of the fission track dating method may be found in Naeser (1979), Gleadow (1981), Wagner (1981), Hurford and Green (1983), Gleadow and Harrison (1988).

The most useful minerals for fission track dating are apatite, zircon and sphene the first two of which are common as trace detrital constituents in clastic sedimentary rocks as well as in a whole range of crystalline rocks. If temperatures have not been raised above about 60°C for apatite or 200°C for zircon (over millions of years) then these minerals will provide information on the fission track age distributions in the sedimentary provenance area. This can be extremely valuable, especially since apparent ages are obtained on individual ~100 μm sized grains in each sample. In

many cases it is possible to identify multiple sources in the sediment on the basis of the distribution of single-grain ages (*e.g.* Duddy *et al.*, 1984; Hurford *et al.* 1984). Sphene is much less common as a detrital component in sediments but is very useful when it does occur because of its relative resistance to thermal overprinting, greater even than that of zircon.

All these minerals are easily extracted from sedimentary rocks using conventional heavy liquid and magnetic separation techniques. As the minimum grainsize that can be analysed is about 50 μm, the method is most readily applied to sandstones and siltstones. Experience in the Melbourne Fission Track Laboratory over the past eight years has shown an 80% success rate in extracting usable apatite separates from many hundreds of samples of these rock types from a wide variety of sedimentary basins. Most of these samples have been about 1kg in size and have included conventional cores, composite sidewall cores and cuttings, as well as outcrop samples. Zircons are obtained from an even larger proportion of these samples although many, at least in older terrains, have too much uranium, giving radiation damage levels that are too high for analysis.

Fission Track Annealing

Of all the environmental factors which have been investigated for their effect on the stability of fission tracks over geological time, the most important by far is temperature. Like other forms of radiation damage, fission tracks begin to fade as the temperature is raised and are only stable for long time periods at relatively low temperatures. Other factors such as pressure, shock, deformation or fluids have been shown to have no effect or very little additional effect compared to that of temperature alone (*e.g.*Fleischer *et al*, 1965, 1975). Fission tracks have also been shown to remain stable under conditions of sample weathering (Gleadow and Lovering, 1974) which is important when interpreting the ages of detrital minerals that have already been through at least one weathering cycle prior to deposition.

The fading of the etchable fission tracks during heating is known as *thermal annealing* and occurs by a gradual shortening of the etchable tracks as the radiation damage is progressively repaired and eventually disappears. The temperatures required for this to occur depend on the duration of heating and the particular mineral, each having its own characteristic annealing properties. The same process which occurs during natural annealing in geological environments over long time periods can be reproduced and studied in the laboratory at higher temperatures for much shorter times. The kinetics of the annealing process are therefore much more accessible to systematic study than is the case for many other systems used for palaeotemperature reconstruction, especially ones depending on complex organic reaction pathways, for which it is doubtful whether laboratory studies can actually simulate the natural process.

The particular importance of fission track annealing in apatite for the study of thermal histories in sedimentary basins arises from the remarkably close co-incidence between the "track annealing zone" and the temperature window for maximum petroleum generation (Gleadow *et al.* 1983). Geological annealing actually takes place progressively from ambient surface temperatures up to about 150°C, depending on the time-scale of heating.

Much of the emphasis in this project has concerned firstly defining the full extent of the information contained within the fission track record (*e.g.* Green *et al.*, 1986; Gleadow *et al.* 1986a, 1986b), and secondly, developing techniques to extract this information as a quantitative thermal history (*e.g.* Green *et al.* 1985, Laslett *et al.*, 1987). Of particular importance in this regard has been a renewed emphasis on the study of fission track lengths which will be examined in detail in the following report.

PROJECT OBJECTIVES AND WORK PLAN

The general objective of this project has been to develop the techniques of apatite fission track analysis so that they can be used as a routine tool for thermal history reconstruction in hydrocarbon exploration and to apply these techniques to the assessment of hydrocarbon resource potential in Australian sedimentary basins. The close co-incidence which we have previously demonstrated between the temperature range for fission track annealing in apatite and that required for oil generation in sedimentary rocks makes the information which can be recovered from the fission track record of great significance to exploration programs. The project has therefore been directed towards enhancing our understanding of the response of fission tracks to geological heating in a quantitative way so that the full potential of fission track analysis can be realised.

The work plan for the project has addressed two principal objectives. These are firstly to define the annealing properties of fission tracks in the mineral apatite in terms of the fundamental physical processes involved and to use this information as the basis for a quantitative annealing model. This has been pursued by a combination of laboratory-based fission track annealing studies and the collection of data from apatite samples which have undergone natural annealing in a variety of different, but well-understood geological environments. Laboratory annealing experiments have involved subjecting apatite samples to carefully controlled heating experiments using a wide range of temperature-time combinations and then measuring the response of the fission tracks. These studies have also been designed to address details of the annealing process such as the effects of crystal anisotropy and compositional variation. Collection of data from naturally annealed samples has been carried out on apatites from many different surface outcrop terrains as well as samples at elevated temperatures in deep drill holes.

Secondly, the work plan has aimed to apply the concepts of fission track analysis to Australian sedimentary basins and the Cooper-Eromanga Basin in particular. In this preliminary study fission track analyses have been carried out on samples from nine exploration wells in the Cooper-Eromanga Basin. Applying the principles of interpretation and the quantitative annealing model developed in other parts of the project, these have been interpreted both from the point of view of their thermal history and also from that of the provenance of the sediment. The results obtained have proved to be of particular significance in evaluating this latter question of the origin of the sedimentary detritus in the basin sequence.

The structure of the report reflects this combined approach and the following description of the work program, main findings and conclusions has therefore been divided into two major parts. In addition to this report, most of the results of the project have either recently been published or will shortly be published as a series of papers describing the work in even more detail. These publications are listed in the Bibliography above and contain additional information on various aspects of the project.

PART 2

EVALUATION OF FISSION TRACK ANNEALING

FISSION TRACK LENGTHS

It has been known since the work of Bhandari *et al.* (1971) and Wagner and Storzer (1972) that the fission track annealing process in apatite is accompanied by shortening of the tracks, and that this preserves information about the thermal history experienced. Until the last few years, however, little use has been made of track length studies because of limited understanding of their behaviour during annealing and confusion over the most appropriate experimental procedure. It has been shown during this project that the greatest amount of information about past annealing can be obtained from the distribution of lengths of horizontal *confined* fission tracks (Laslett *et al.*, 1982; Gleadow *et al.*, 1986a, 1986b). These are tracks which do not intersect the polished surface, but are etched out wholly within the body of the mineral where the etchant has penetrated below the surface along other tracks or fractures (Lal *et al.* 1969). Procedures for measuring the lengths of such features are described below and have been detailed by Gleadow *et al.* (1986b).

The particular importance of fission track length studies arises from three properties of the spontaneous fission tracks. First, all tracks have a very similar length when first produced (Gleadow *et al.*, 1986b), which is controlled by the energetics of the fission decay and the nature of the track recording material. Second, fission tracks become progressively shorter during thermal annealing in a way that is controlled principally by the maximum temperature that each has experienced (Green et al. 1985). Third, new tracks are added to the sample progressively through time so that each has experienced a different fraction of the total thermal history. These three factors combine to give a final distribution of track lengths which contains a complete record of the temperatures experienced below about 130°C.

As considered in more detail below, quite distinct patterns of length distribution result from different styles of thermal history and, when combined with the apparent fission track age, these can be used to reconstruct the variation of temperature through time. A major part of this project has involved defining the relationship between annealing and the fission track length distribution both by quantitaive annealing studies and through observations on naturally annealed apatites.

TECHNIQUES

Annealing experiments

The studies reported here were carried out either on crushed grains or oriented slices cut from a large (~ 1cm) single crystal of Durango apatite (Young et al., 1969). Slices were cut parallel to a prismatic face (1010) with a thin-blade diamond saw. The grains and slices were annealed at 450°C for 5 hours to remove all spontaneous tracks and irradiated with ~10^{16} thermal neutrons/cm^2 in the X7 facility of HIFAR nuclear reactor at Lucas Heights, NSW. The samples were then annealed in a tube furnace, controlled to ±3°C in early work, and ±1°C in later studies. The temperature was monitored using a thermocouple inserted into the furnace in the vicinity of the samples. Annealing temperatures between 95°C and 400°C were used for times between 20 minutes and 500 days.

Sample Preparation

After annealing, samples were mounted in epoxy on microscope slides, ground using 400 and 600 grade silicon carbide papers, and polished for ~2 minutes with 0.3 μm alumina powder in water. The polished mounts were then etched in 5M HNO_3 for 20 seconds at 20 °C, rinsed in water to stop etching and washed first in water plus detergent, and then with alcohol. Unannealed control samples were prepared in the same way as for the annealed samples.

Track Length Measurements

The evaulation of track annealing in this study has concentrated on the meaurement of confined track lengths distributions, as considered in the previous section. Initially the track lengths were measured using an eyepiece scale-bar, divided into approximately 1 μm divisions, calibrated against a stage-micrometer ruled in 2 μm divisions, and/or against a diffraction grating ruled with 6378 lines per mm. Using this arrangement, tracks are assigned to 0.5 μm intervals, which can introduce a slight systematic difference to measurements by different observers. Reproducibility was nevertheless found to be very good, one of the pricipal drawbacks being the slowness of this approach and the necessity to manually record the results enter them into a computer for processing.

As part of this study a new semi-automated system for measuring track lengths was developed. This system consists of HIPAD™ digitising tablet directly connected to a microcomputer and placed adjacent to the microscope. An optical drawing tube attachment on the microscope is then used to superimpose an image of the digitising tablet on the microscope field of view. A small, high-intensity light emitting diode (LED) was fixed to the cross-hair of the digitising tablet's cursor, so that in normal lighting

conditions all that can be seen of the digitising tablet is the bright red spot of the LED. To measure the length of any track the cursor is simply clicked at each end of the track image and the length data are automatically registered in the microcomputer. Calibration is again carried out relative to the 2 μm stage-micrometer and software has been developed to automatically accumulate and process the track length information. The system has been highly successful and was developed at a fraction of the cost of several broadly comparable commercial systems that are now available.

Overall we estimate that this semi-automated approach has reduced the time required to carry out each length determination by a factor of approximately three. Using this arrangement, individual tracks can be measured with greater precision than the earlier manual measurements, to approximately ±0.2 μm. In addition, by developing our own software we are able to accumulate various other attributes of the tracks, such as their orientation, which are potentially useful in fully understanding and quantifying the track annealing process. The orientations of individual tracks in prismatic slices were defined relative to the direction of the c-axis, which is marked by the larger dimension of the openings of fission tracks intersecting the surface.

Lengths of confined fission tracks were measured following the recommendations of Laslett et al. (1982), the most important of which is that only horizontal tracks be measured. Such tracks can easily be identified from the strong reflection obtained from them when viewed in incident light, or by the constancy of focus along their length using a high-power objective in transmitted light. In addition, tracks were measured only in grains with polished surfaces parallel to a prismatic surface. This is of great importance because of the anisotropy of the annealing process in apatite, whereby tracks oriented parallel to the c-axis are more resistant to annealing, and are therefore longer than tracks perpendicular to the c-axis (Green and Durrani, 1977; Green, 1981; Laslett et al., 1984). Thus if horizontal confined tracks are measured in a basal section of annealed apatite all tracks will be perpendicular to the c-axis, and therefore will be shorter than tracks in other orientations. This would introduce severe bias to the measurements. In a prismatic section, however, horizontal confined tracks will be present in all orientations from 0° to 90° to the c-axis and therefore the anisotropy can be studied directly over any azimuthal interval.

In each sample the lengths of at least 50 confined tracks were measured wherever possible. Following Laslett et al. (1982) no distinction has been drawn between tracks-in-tracks and tracks-in-cleavage ("TINTS" and "TINCLES" of Lal et al., 1969).

LABORATORY ANNEALING RESULTS

Isochronal annealing experiments

The results of confined track length measurements in samples annealed for various time/temperature combinations are shown in Fig. 1, and have been fully tabulate dby Green *et al.* (1986, Table 1). Results are shown in Fig. 1 as reduced track length, l/l_0, where l is the mean length and l_0 the mean length of fresh induced tracks, plotted against temperature for five annealing times. Fig. 1 shows that the values of l/l_0 in annealed samples are, even at the lowest temperatures employed, always less than unity. That is, in the temperature range in which experimental data is available, no conditions have been identified in which tracks are totally stable. Also noticeable from Fig. 1 is the sudden fall off of l/l_0 from ~0.65 to zero over a very narrow temperature range of ~10°C, in contrast to the gentle fall off with temperature down to l/l_0 ~0.65. For this reason, values of l/l_0 <0.65 are very rarely encountered, and indeed only two values <0.5 (other than zero) have been measured in this study, from a total of over 70.

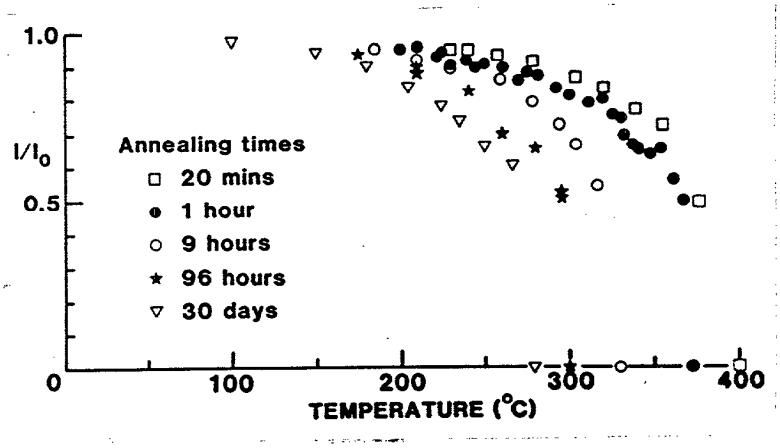

Fig. 1. Isochronal annealing data obtained in the present study for five annealing times as shown.

The distributions of confined track lengths in six samples at various degrees of annealing are shown in Fig. 2. These distributions are typical of those observed in other samples for similar degrees of annealing throughout this study. Length distributions are very similar in shape for mean lengths from 16 μm down to ~11 μm, being symmetrical and narrow, with standard deviations of ~ 0.9 to 1 μm. However, for mean lengths below ~11 μm, the distributions become noticeably broader, with a tail to very short lengths becoming increasingly evident as the mean length is reduced.

These observations are summarised and extended in Fig. 3, which shows the standard deviation of the annealed length distribution plotted against mean track length, for all the annealed samples. This plot shows a very gradual increase in standard deviation from ~0.9 μm for unannealed tracks, with a mean of ~16 μm, to ~1.0 μm for annealed tracks with mean length of ~10.5 μm (l/l_0 ~0.65). Below ~10.5 μm there is a rapid increase in standard deviation to values around 2.1 μm for mean lengths of ~8 μm. The skewness and kurtosis of the distributions of track lengths have also been investigated, but these are not particularly useful due to their sensitivity to outliers.

Thus we have evidence, in the abrupt drop in l/l_0 over a narrow range of temperature, and from the change in the form of the distribution of track lengths (as shown quantitatively by the standard deviation of the distribution) of some difference in the annealing process above and below reduction to a mean length of ~10.5 μm (l/l_0 ~ 0.65).

In seeking to understand these results, two factors have been found to be of particular significance. These are the anisotropy of annealing in apatite, and the presence of unetchable gaps in tracks in annealed apatites. These will be dealt with below and are discussed in more detail by Green *et al.* (1986, 1988) and Gleadow *et al.* (1986a, 1986b).

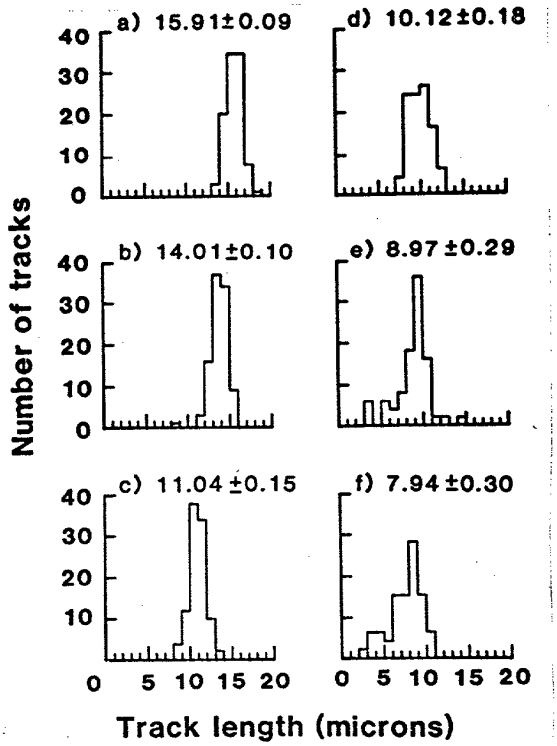

Fig. 2. Confined track length distributions in unannealed (a) and annealed (b-f) Durango apatite samples with mean lengths between 16 μm and 8 μm. All samples are taken from one hour annealing data, although distributions in samples annealed for other times, with similar degrees of annealing, are essentially identical. A total of 100 tracks were measured in each case.

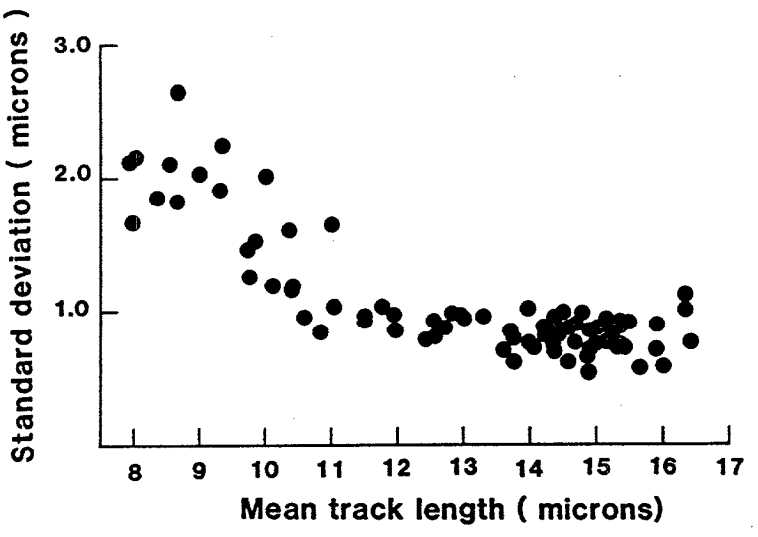

Fig. 3. Standard deviation of confined track length distributions plotted against mean track length. Note the sharp increase in the trend for mean lengths below ~10.5 μm.

Anisotropy of fission track annealing

That fission tracks in different orientations in apatite anneal at different rates has been known since the work of Green and Durrani (1977). They showed that fission tracks parallel to the c-axis were more resistant to annealing than were tracks perpendicular to the c-axis. These early studies have been supported by later studies (Green, 1981; Laslett et al., 1984), and there can be no doubt that as the degree of annealing increases, the anisotropy of the annealing process also increases. Despite these observations, no other study of fission track annealing in apatite has been designed to allow for this effect.

To study the anisotropy in detail, prismatic slices of Durango apatite were annealed at 260°C, 310°C, 336°C, 352°C and 366°C for 1 hour, in an attempt to achieve length reductions close to 0.9, 0.8, 0.7, 0.6 and 0.5 (based on the results shown in Fig. 1). These slices and an unannealed control were then etched for 20 seconds, and the length and orientation of confined tracks measured in each slice. Because of the quality of the parent crystal, these slices were almost devoid of cracks which would produce TINCLES and therefore the confined tracks measured in this part of our study were predominantly TINTS.

Microscopic examination of fission tracks in these slices, clearly shows the increasingly anisotropic nature of the annealing process (Green *et al.* 1986 Fig 4)). At 336°C for 1 hour (l/l_o ~0.7) it is readily apparent that the longest tracks etched in the surface are parallel to the c-axis. At 352°C for 1 hour (l/l_o ~0.6) this trend is strongly emphasised, while at 366°C for 1 hour

(l/l_0 ~0.5) only very few tracks remain visible, all of which are parallel to the c-axis, with lengths up to 8 μm.

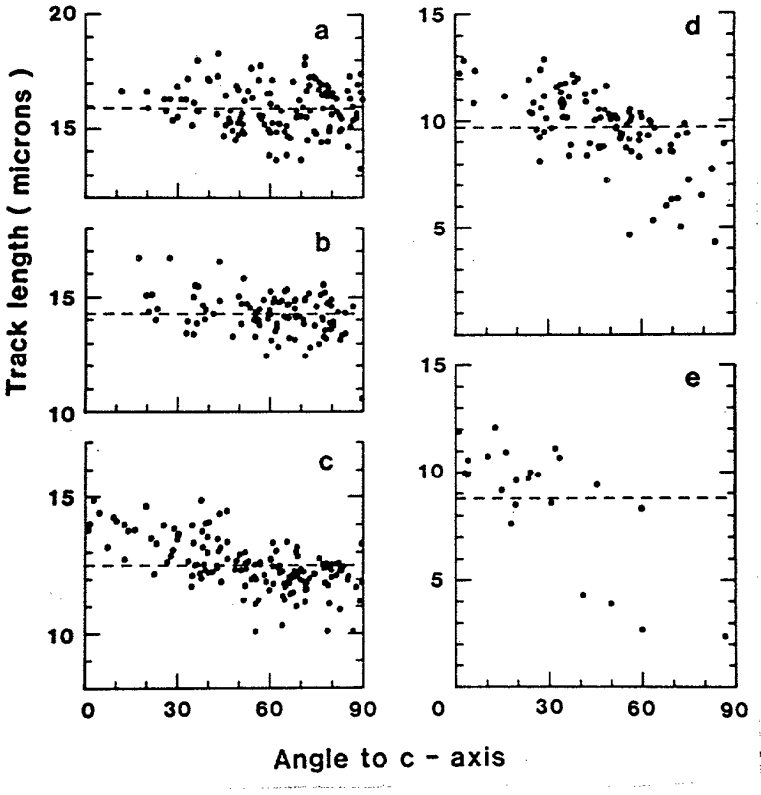

Fig. 4. Variation of the lengths of individual confined tracks with angle to the c-axis in Durango apatite slices etched for 20 seconds. (a) Unannealed mean = 15.92 ± 0.09 μm; standard deviation = 1.02 μm, (b) annealed 260°C, 1 hour. Mean = 14.26 ± 0.09 μm; s.d. = 0.90 μm, (c) 310°C, 1 hour. Mean = 12.52 ± 0.07 μm; s.d.= 0.92 μm, (d) 336°C, 1 hour. Mean = 9.69 ± 0.18 μm; s.d. = 1.75 μm, (e) 352°C, 1 hour. Mean = 8.78 ± 0.58 μm, s.d. = 2.80 μm.

Fig. 4 shows the lengths of individual tracks in these slices, plotted against the orientation of these tracks relative to the c-axis (the azimuthal angle in the plane of observation). No data are presented for the sample annealed at 366°C because insufficient tracks were present to act as hosts for TINTs. The data from the unannealed control sample in Fig. 4a show only a small degree of anisotropy, with a noticable lack of tracks at small angles to the c-axis. This is thought to be due to the anisotropy of bulk etch rates in apatite. The bulk etch rate is higher parallel to the c-axis than perpendicular to this axis. This causes tracks perpendicular to the c-axis to be wider than those parallel to the c-axis by a factor of ~3. Thus the characteristic knife-blade shape of confined tracks perpendicular to the c-axis makes these tracks much easier to identify than the thinner profile of

tracks parallel to the c-axis. As the degree of annealing increases (Fig. 4b and 4c) the length becomes more strongly anisotropic until in Fig. 4d, the track length falls rapidly with angle above a value of ~45°. Fig. 4e shows still stronger anisotropy, although because of the small number of suitable host tracks, few TINTS were found in this sample, and it is difficult to define a clear trend.

The length distributions corresponding to the data of Fig. 4 are of the same form as those in the samples illustrated in Figs. 1-3. The samples shown in Figs. 4d and e, which are strongly anisotropic, have mean lengths below 10.5 μm and lie in the part of the trend in Fig. 3 where the standard deviation increases rapidly. Thus this sharp increase of standard deviation below ~10.5 μm (l/l_0<0.65) is associated with an increase in the degree of anisotropy of annealing, with tracks of lengths <8 μm becoming increasingly significant.

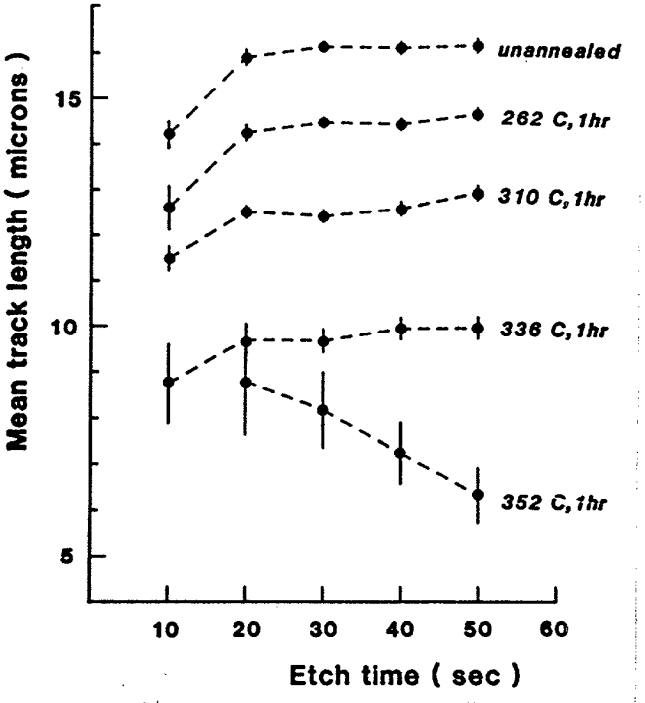

Fig. 5. Mean confined track length in the samples corresponding to Fig. 4, plotted against etch time. The small rate of increase of mean length with etch time suggests that at each step, most of the TINTS measured have been freshly created, since confined tracks, once formed, will increase in length at between 0.3 and 1.0 μm per 20 seconds, depending on orientation. The decrease of mean length with increasing etch time in the sample annealed at 352°C for 1 hour results from the increasing presence of short TINTS (see Fig. 6 and 7).

Because of the small number of TINTS observed in the sample annealed for one hour at 352°C, this slice, together with the others, was etched sequentially to produce more TINTS and also to study the effect of

longer etch times on the observed length distributions. Fig. 5 shows the mean lengths of confined tracks observed in the slices with increasing etch time. A surprising observation from Fig. 5 is that the mean length in all but the most annealed samples shows only a small increase with increasing etch time. Individual confined tracks, once revealed, will continue to increase in size at a rate determined by the component of bulk etch rate parallel to the track orientation, ranging from ~0.3 μm to ~1 μm per 20 seconds increase in etch time (Laslett et al., 1984). Clearly none of the mean lengths in Fig. 5 increase at anywhere near this rate once their full etchable length has been reached, and most show no significant increase after 20 seconds of etching. This indicates that after each etching step, the measured tracks largely represent a new generation of TINTS. The standard deviations of the distribution of track lengths in each sample also show no increase from 20 sec to 50 sec.

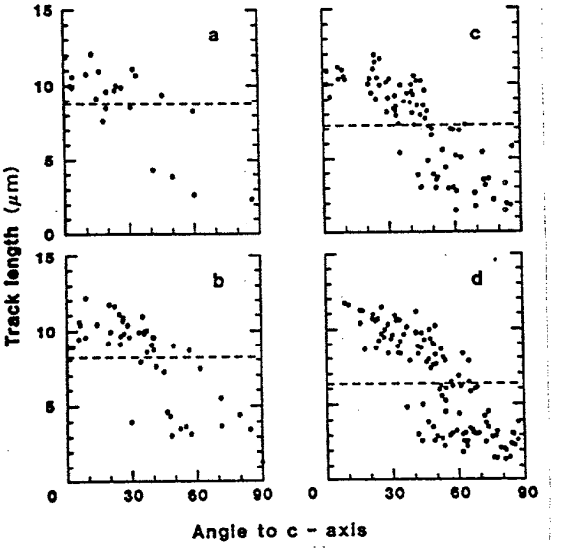

Fig. 6. Variation of the lengths of individual confined tracks with angle to the c-axis in a slice of Durango apatite annealed at 352°C for 1 hour, and etched for (a) 20 seconds, (b) 30 seconds, (c) 40 seconds and (d) 50 seconds. As the etching time increases, more TINTS become visible, and the anisotropic trend becomes more distinct.

Another surprising observation comes from the data for the sample annealed at 352°C, in which the mean length actually shows a decrease

with increased etch time. Fig. 6 shows the length of individual tracks plotted against orientation in this slice for etch times from 20 sec to 50 sec, and the corresponding track length distributions are shown in Fig. 7. As the etch time increases, the number of TINTS observed shows a marked increase, and in particular the number of very short TINTS (<5 μm) at high angles to the c-axis increases, thereby reducing the mean observed track length. The track length distribution in Fig. 7d after 50 seconds etching shows an unusual bimodal distribution which by reference to Fig. 6d, seems to represent a component of long tracks, above ~7 μm, at small angles to the c-axis,and another component of shorter tracks at high angles to the c-axis. The progression in Fig. 6 shows the two components becoming increasingly distinct, and this is echoed in Fig. 7. The increase in the number of short tracks observed as etch time is increased results from an observational bias, in that tracks as short as ~2 μm must be widened appreciably before they can be detected. On the other hand, tracks longer than ~8 μm can easily be detected even when quite thin. Note that geometrical bias of the sort discussed by Laslett et al. (1982) is present to the same degree in Figs. 6a-d, so that the increase in number of short tracks must be purely observational. It should be stressed that the width of potential host tracks for confined tracks will always be >1 μm and this precludes the observation of TINTS much below 2 μm in length. Therefore it is possible that the lower peaks in the track length distributions of Fig. 7 are truncated due to this further bias, and that in fact the lower peak represents a continuum extending towards zero.

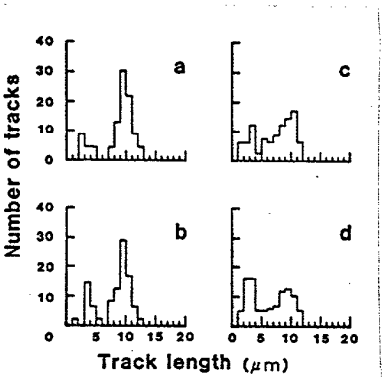

Fig. 7. Confined track length distributions corresponding to the data of Fig. 6. As etching proceeds, more and more short tracks become visible. (a) 20 seconds, (b) 30 seconds, (c) 40 seconds and (d) 50 seconds.

Fission track structure and the annealing process

Little is known of the actual structure of unetched ("latent") fission tracks, and consequently even less is known about the physical processes taking place during annealing. Apart from the earliest observations of latent fission tracks in mica by transmission electron microscopy, as summarised by Fleischer et al. (1975), probably the only significant advance in understanding these aspects has come from small angle X-ray scattering studies of heavy ion tracks in silicate minerals (Dartyge et al., 1978, 1981). These studies suggest that latent tracks are composed of two components - large (15Å-40Å) clusters of atomic defects termed "extended defects", which are linked by a large number of much smaller "point defects". The extended defects cause a much greater enhancement of the etch rate along the track than the point defects. During low temperature annealing, only the point defects are removed, leaving the extended defects separated by essentially undamaged regions which etch at the bulk etch rate of the undamaged mineral. This leads to the concept of "gaps" in the etchability of annealed tracks, in which the etchant is held up in its progress along the track by these undamaged regions. Dartyge et al. (1978, 1981) show convincing proof of the presence of these gaps, in the form of length distributions of heavy ion tracks in mica and labradorite.

We have extended the gap model to apatite by investigating the annealing behaviour of tracks in prismatic slices of Durango apatite produced by 220 MeV Ni ions. These ions were obtained from the Tandem Van der Graaf accelerator of the Physics Department, Australian National University. Samples were irradiated with collimated beams, at 45° to the surface, in three orientations with respect to the c-axis: parallel, perpendicular and at 45°. After irradiation,slices were annealed at various temperatures, for one hour, and others were left unannealed. Fig. 8 shows the length distributions of the horizontal projection of unannealed Ni tracks in three orientations, after etching for 40 seconds. Tracks in all orientations are completely etched to their terminations and have a very narrow range of lengths (which is to be expected since the ions are monoenergetic). Fig. 9 shows similar distributions for Ni tracks in samples anneale dat 275°C for 1 hour, after etch times of 40 seconds and 60 seconds. After 40 seconds, tracks parallel to the c-axis (Fig. 9c) have etched through to their ends whereas a significant proportion of those at 45° to the c-axis (Fig. 9b) have only etched through part of the total range. None of the tracks perpendicular to the c-axis (Fig. 9a) are fully etched, and most have etched less than one third of their total range. After 60 seconds, the length distribution of tracks parallel to the c-axis (Fig. 9f) is unchanged, while the majority of tracks at 45° to the c-axis (Fig. 9e) are now completely etched. Of the tracks perpendicular to the c-axis (Fig. 9d) about half are now completely etched.

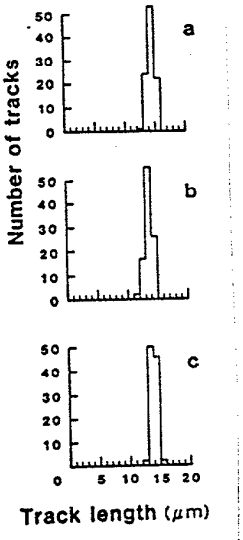

Fig. 8. Distributions of projected lengths of unannealed 220 MeV Ni ions in Durango apatite in three orientations. a) Perpendicular to c-axis, b) 45° to c-axis, c) parallel to c-axis. All samples etched 40 seconds. Tracks in different orientations have roughly equal lengths.

These results suggest the presence of gaps in the etchability of annealed tracks which delay the progress of the etchant, although the etchable ranges are still roughly equal in each sample and are eventually reached after prolonged etching. Thus these results support the gap model of Dartyge et al. (1978, 1981), and emphasize the generality of the concept.

A search was carried out to identify gaps in fission tracks in the five annealed slices of Durango apatite, by measuring the lengths of individual confined tracks during sequential etching in 10 second steps. Fission tracks in which the etchant was delayed by the presence of gaps were only found in the slices annealed for 1 hour at 336°C and 352°C. In neither case was the presence of observable gaps a common occurrence. Only 2 out of 14 tracks at 336°,and 2 out of 11 tracks at 352° showed gaps. Those tracks in which gaps were present were always at angles >45° to the c-axis where annealing is most severe.

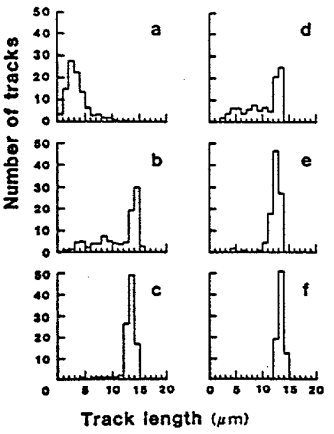

Fig. 9 Distributions of projected lengths of annealed 220 MeV Ni tracks in Durango apatite. a) perpendicular to c-axis, b) 45° to c-axis, c) parallel to c-axis. All samples were annealed at 275° for 1 hour and etched for 40 seconds. The distributions in d), e) and f) correspond to the samples in a), b) and c) respectively but are etched for 60 seconds.

These observations suggest that for a given degree of annealing, there is a maximum length over which a confined track may be etched, this maximum length decreasing with increasing angle to the c-axis. When annealing becomes very severe the etchable portions of tracks at high angles (>45°) to the c-axis may become separated by non-etchable gaps, which cause these tracks to take longer to become fully etched, although the maximum etchable length is still defined by the overall anisotropic "envelope" and cannot be breached by etching through further gaps at the ends of the track. The rarity of gaps in tracks lying at small angles to the c-axis presumably results from the greater stability of such tracks, and/or the greater bulk etch rate in this direction, which will etch through undamaged material faster than in tracks perpendicular to the c-axis.

A picture thus emerges of two stages in the annealing of fission tracks in apatite. The dominant process causes a shrinking of the etchable portion of the track from each end, with the rate of shortening increasing with increasing angle to the c-axis. For a given combination of temperature and

time there is a characteristic maximum etchable length, which depends on the orientation of the track. As annealing becomes increasingly severe, gaps may appear in the etchable portions which delay the progress of the etchant. With continued etching the gaps may be breached, allowing the characteristic etchable length to be revealed.

The observed length distributions in annealed apatites shown in Fig. 2 thus result from a combination of the anisotropy of annealing, and to a lesser degree, the presence of gaps. For mean lengths above ~10.5 μm (l/l_0 ~0.65) the form of the distribution changes only slightly with the degree of annealing (Fig. 3) because the anisotropy is not very pronounced. However, below ~10.5 μm, the form of the confined track length distribution changes rapidly as annealing progresses, and is profoundly affected by the processes discussed above.

Quantitative annealing models

Systematic studies of the annealing behaviour of apatite under laboratory conditions date from the work of Naeser and Faul (1969) and Wagner (1968). These, and most other annealing studies since that time, have concentrated on measurements of track density, the number of tracks per unit of area, which is proportional to the fission track age. In a typical experiment, samples are heated for various times at different temperatures and the reduction in track density observed. Results are typically displayed in the form of an Arrhenius plot showing log(time) against inverse absolute temperature. These studies have agreed in general terms, concluding that extrapolation of the Arrhenius relationship indicates that about half the tracks would be lost at temperatures of the order of 80-100°C over millions of years.

Studies of the natural annealing of tracks in apatites from deep boreholes (Naeser, 1981; Gleadow and Duddy, 1981a) have been used to complement the laboratory studies and to test their predictions. This has shown that the range of temperatures for annealing over geological time is actually much narrower than had been predicted from the laboratory experiments alone. In part this is due to the particular model selected to describe the annealing kinetics and also to the difficulty of judging the point at which annealing effectively begins and ends. In this study we have shown that part of this discrepancy is also due to the increasingly well-demonstrated dependence of annealing properties on the small compositional differences observed between apatite samples (see below).

By assigning the observed annealing in borehole samples to estimated time-temperature combinations the borehole data have been used to constrain the laboratory results in order to arrive at a more realistic description of the annealing kinetics (Naeser, 1981; Gleadow *et al.*, 1983; Harrision, 1985). These studies give an indication of the relationship between time and temperature in fission track annealing in apatite suggesting that an order of magnitude increase in heating time would

produce a decrease of about 15°C in the temperature required for a given degree of annealing.

The exact form of the annealing relationship is extremely important if fission track studies are to form the basis of rigorous quantitative modelling of thermal histories in sedimentary basins, and there has been much discussion about this in the literature (*e.g.* Märk *et al.*, 1973; Zimmerman and Gaines, 1978; Burchart *et al.*, 1979; Chaillou and Chambaudet, (1981); Green *et al.*, 1985). A difficulty in deciding between the various alternatives proposed has been that the experimental data have seldom been of sufficient precision. One of the limiting factors in this has been the exclusive reliance in many studies on track density measurements, the precision of which is limited by the number of tracks counted and is usually no better than 3-5%. Track lengths, on the other hand, can be measured to a precision of about 1% and have recently offered some new insights into the fission track annealing process (Green *et al.*, 1986). They are also the more fundamental fission track parameter in that reduction in observed track density is actually a consequence of the track shortening during annealing.

We have derived a new empirical model for track annealing in apatite which is based on the extensive set of laboratory annealing experiments reported here which relate the reduction in mean track length to various conditions of temperature and time. The derivation of this model has been described in detail by Green *et al.*, (1985) and Laslett *et al.* (1987).

Firstly, Laplacian smoothing splines were used to reveal the gross nature of the dependence of the length reduction, r (i.e. l/l_0), on logarithm of time (ln(t)) and inverse absolute temperature (1/T). This suggested that contours of equal length reduction in an Arrhenius plot can be described by parallel or only slightly fanning straight lines. In seeking a more rigorous description, we constructed a series of models relating some function g(r) and another function f{ln(t),1/T}, which contain most previously published relationships, as well as a number of novel forms. Within this composite model, both parallel and fanning Arrhenius plots were considered.

The models were fitted and compared using formal statistical methods. None of the previously suggested relationships satisfactorily describe the data, and a novel form is proposed with g(r) = ln(1-r) for the parallel Arrhenius plot. The best fitting model is given by the following:

$$\ln(1-r) = 3.87 + 0.219\,(\ln(t) - 19270/T), \qquad -(1)$$

and accounts for 96.7% of the variation of g(r). However residual plots showed some structure, suggesting that some improvement in the model was possible. The best fanning model is given by:

$$\{[(1-r^{2.7})/2.7]^{0.35}-1\}/0.35 = -4.87+0.000168T\{\ln(t)+28.12\} \quad -(2)$$

which accounts for 98.0% of the variation in g(r), and gives a significantly better fit than the parallel model, with residual plots showing no obvious structure.

Thus, we have shown that while equation (1), containing within it a constant activation energy (parallel Arrhenius plot), describes the data quite well, equation (2) with the activation energy increasing with decreasing r (fanning Arrhenius plot) provides a significantly better fit. However, there are good reasons why the parallel Arrhenius plot should not be immediately abandoned. First, the parallel model has the practical advantage that it may easily be extended to deal with variable temperature annealing. In addition, although the fanning model is superior, the parallel model still accounts for 96.7% of the variation within the data set, and gives a useful approximation within a limited range of temperatures and values of r.

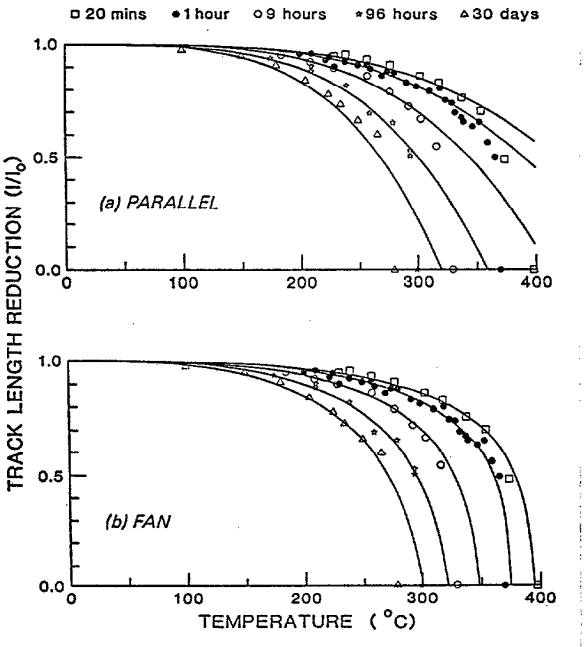

Fig. 10. Isochronal laboratory annealing data, together with fitted curves, corresponding to the five annealing times indicated. In a), the fitted curves are predicted from the parallel Arrhenius model, equation(1), while in b), the curves are fitted using the fanning model, equation (2). Major differences between the two models appear below values of r ~ 0.65.

To illustrate the comparison of the best fanning and parallel models, Figure 10 shows isochronal annealing data for five different annealing

times, as indicated, on which are superimposed fitted curves for each time calculated from the above two models (equations (1) and (2)). The major difference between the two sets of fitted curves is the way in which they approach zero, this being much steeper for the fan than for the parallel model. In this respect, the fan model more closely mimics the data. However, in the range of length reductions above r ~0.65, the two models both describe the data well.

Figure 11 shows the full data set from our annealing studies (Green et al., 1986) presented in Arrhenius plot form, with contours of equal length reduction predicted from both models, as above. This emphasises the exceptionally small difference between the two models for r> 0.65, so that even if we accept the fanning model as superior, the parallel Arrhenius plot appears to give a good approximation within a restricted temperature range.

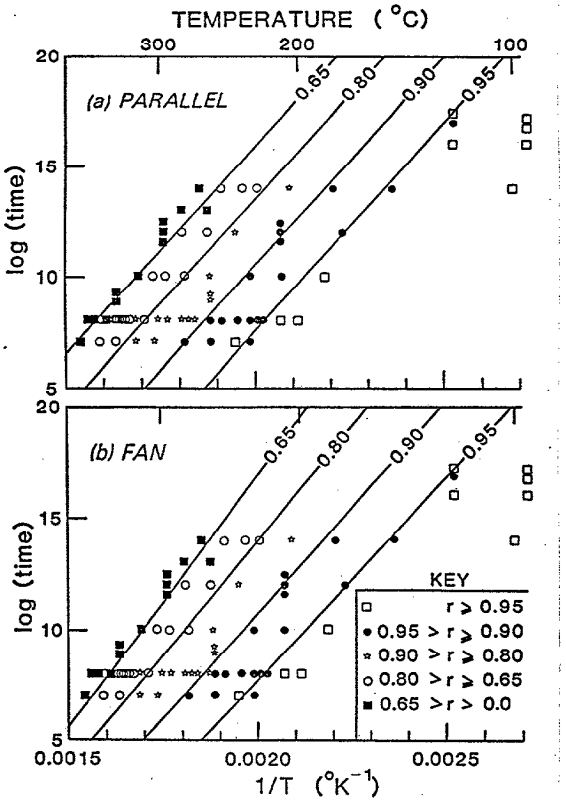

Fig. 11. Full laboratory annealing data set, presented in Arrhenius plot form. In a), contours of equal length reduction are predicted from the parallel Arrhenius model, equation (1), while in b), the contours are fitted using the fanning model, equation (2). The parallel model gives a useful approximation to the fanning model.

Figure 12 shows contours of equal length reduction predicted from the rival models (equations (1) and (2)) plotted to extend from laboratory to geological time scales. The slight difference between the two models is magnified by extrapolation, and it is possible that attempts to place geological constraints on annealing kinetics could be useful in refining the model. Note, however, that any such geological constraints must be obtained from similar apatites to those for which laboratory data is available, because of the influence of apatite composition on annealing properties (see below and the discussion by Green et al. 1985 & 1986).

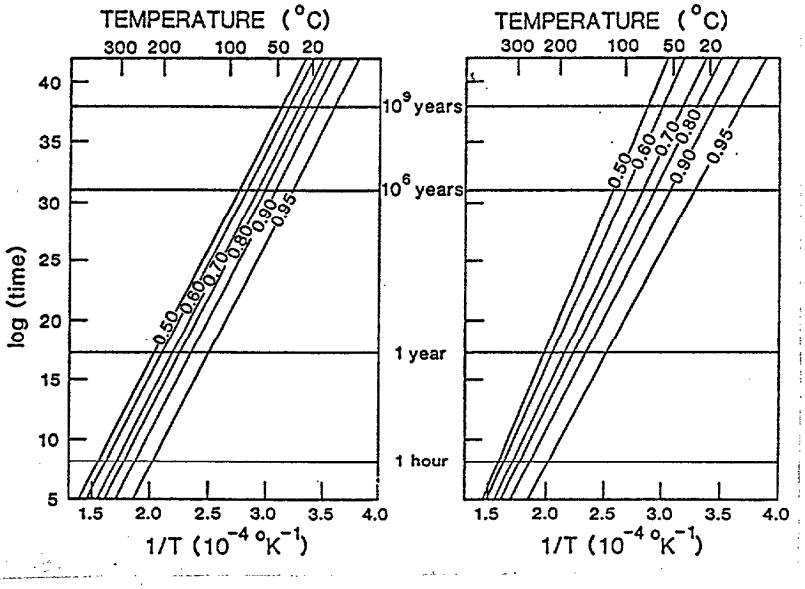

Fig. 12. Comparison of the parallel and fanning models from equation (1) and equation (2), extrapolated from laboratory to geological timescales. Differences between the two models are magnified by extrapolation, and it is possible that geological annealing studies could be useful in further refining the description of annealing.

It is commonly assumed that annealing is dominantly a diffusive process, in which displaced atoms return to lattice sites under the influence of thermal conditions. It is reasonable to suppose that the diffusion of individual chemical species might be controlled by a single activation energy. However in a mineral such as apatite, there are a number of chemical species present, each of which might possess a slightly different activation energy for annealing. Furthermore, since the diffusion process in apatite is markedly anisotropic (as shown by the anisotropy of annealing), different orientations may be characterised by different activation energies.

In addition, the measured parameter i.e., track length, is merely a large-scale manifestation of the fundamental processes taking place on the atomic scale. Therefore, an interpretation of the preferred model in terms of a single process, for which the activation energy increases continuously with the degree of annealing, seems overly simplistic. Instead, we suggest that the small amount of fanning in the preferred model could be viewed as an artefact, reflecting the interplay of the complicating factors listed above. In fact there seems to be no good reason why contours in the fanning Arrhenius plot need be straight, if indeed the fanning is only an artefact. Nevertheless, the straight line fanning model gives a convenient, statistically satisfactory description of all the available data. In general, when constructing empirical models to be used as the basis of prediction, simple models with few fitted parameters are generally preferable, and therefore more complex models have not been pursued.

The quantitative analysis of our annealing data thus suggests that contours of equal length reduction on an Arrhenius plot can be described by a set of parallel, or more probably, a slightly fanning array of straight lines. Even with the preferred fanning model, however, the degree of fanning is much less than predicted by most previous laboratory studies, but is in much closer agreement with the natural annealing observed in borehole samples. This may be due to the presence of apatites of various compositions in the earlier studies, whereas the present study relates to only a single composition. The slight amount of fanning observed in our study may be an artefact introduced by several intermediate steps between the physical processes taking place during annealing and their manifestation as the reduction in mean track length.

This quantitative annealing relationship can be used, together with the observed relationship between track length and track density reduction (see Laslett *et al.*, 1984; Green *et al.* 1988), as a basis for modelling studies which can predict the various fission track parameters which will result from any given thermal history. The development of this numerical modelling capability is being continued as part of our on-going NERRDC-sponsored research program.

OBSERVATIONS ON NATURAL APATITES

Outcrop Samples

Observations of track lengths from nearly 200 apatite samples from a wide variety of outcropping rocks show that distinctive patterns of track length characterise different geological environments. The results of this part of our work have been reported in detail by Gleadow *et al.*, (1986b).

The starting point for this study is that induced fission tracks in all the apatites investigated have mean track lengths within a very narrow range,

and are statistically indistinguishable from each other. Furthermore, the form of the length distribution is also very similar in all the samples studied, being approximately normal, with a standard deviation of approximately 0.9 μm, with the majority of track lengths falling between 15 μm and 17 μm. This distribution is termed the *induced* type and a representative example, produced by summing distributions for six apatites chosen at random (and normalised to 100 tracks), is shown in Fig. 13 It seems reasonable to conclude that induced tracks in all apatite samples will have a distribution which is typified by a mean of near 16.3 μm and a standard deviation of approximately 0.9 μm. This observation is highly significant as it means that the track length distributions of spontaneous tracks in any of a wide variety of apatites can be discussed in their own right, without the need for reference to the lengths of induced tracks in the same sample.

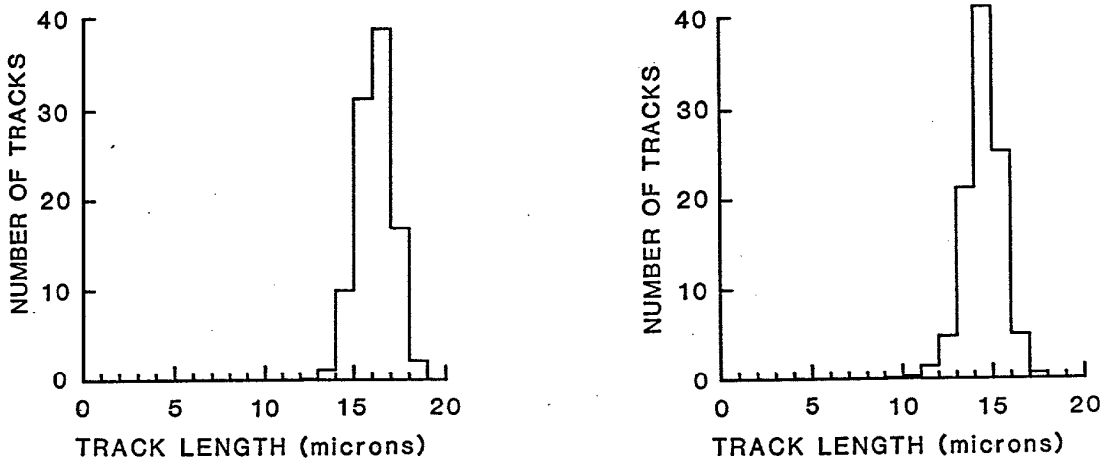

Fig. 13. Typical length distribution of (a) confined induced tracks and (b) confined spontaneous tracks in rapidly cooled volcanic apatites, obtained by summing the distributions from six oindividual samples in each case.

The nearest that may be observed to the induced type in natural apatites is what may be termed an *undisturbed volcanic* type (Fig 13). As its name implies, this type of distribution is characteristic of volcanic rocks that have remained undisturbed and at relatively low surface temperatures since their formation. A similar pattern will result in any rock which has cooled rapidly and not been re-heated thereafter. Although this type of distribution is similar to that shown by fresh induced tracks, the mean is slightly lower indicating that some shortening of spontaneous tracks occurs over geological time even at ambient surface temperatures.

Apatites that have spent a significant period of time within the fission track annealing zone will have broader distributions of various kinds, such as those shown in Fig. 14. The most common of these is an *undisturbed basement* type, which is typical of many old basement terrains which have been in a long-term erosional environment. This type of distribution is

interpreted to reflect a simple monotonic cooling from temperatures above about 130°C. More complex, multi-stage thermal histories will produce the even broader *mixed* distributions. When the peaks in such a distribution are clearly resolved, as in the *bimodal* case, the distribution is indicative of a two-stage history with an older generation of tracks shortened during a thermal event, and a new generation of long tracks produced subsequently. This latter type of distribution is particularly useful, giving information on the timing as well as the severity of the thermal event. The relationship between the various distribution types can be seen in Fig. 15 which shows how the breadth of the length distribution varies with mean track length.

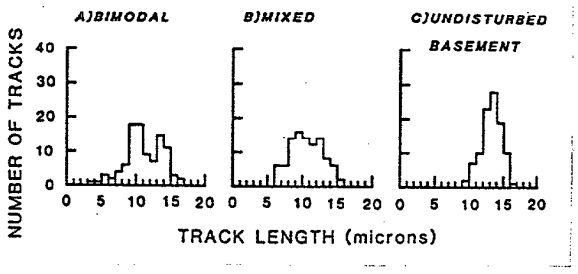

Fig. 14. Typical track length distributions from the three characteristic types identified from the large number of apatites studied. These types are a) bimodal, b) mixed, and c) undisturbed basement. The bimodal is a special case of the mixed distributions where two separate components can be readily identified.

Subsurface samples

Early Cretaceous sediments in the Otway Basin of southeastern Australia have proved invaluable in understanding the behaviour of fission tracks in apatite at temperatures between about 20° and 130°C over times of the order of tens of Millions of years. Apatites from these Otway Group sediments had a contemporaneous volcanogenic origin and therefore had essentially no inherited tracks at the time of their deposition. In this section we concentrate on the change in form of the length distribution as the mean track length decreases due to annealing with increasing downhole temperature in a group of selected deep exploration wells. Four wells, Flaxmans-1, Eumeralla-1, Port Campbell-4 and Banyula-1 were selected for this purpose on the basis that their burial histories argued that temperatures have increased through time and are now at their maximum (Gleadow et al., 1986a, Green et al. 1988). One sample from Eumeralla-1 was excluded as it appears to have been slightly hotter in the past (Gleadow et al 1983).

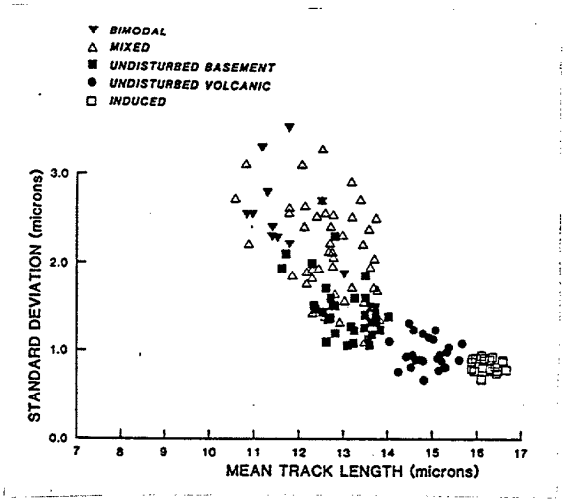

Fig. 15. Relationship between standard deviation and mean track length for the length distribution types that we have identified. The data for induced tracks and spontaneous tracks in undisturbed volcanic apatites form distinct groups, emphasising that the two types of tracks possess distinct and characterictic distributions. The remaining data form an obvious trend, with a progressive broadening of the distribution as the mean track length decreases. The bimodal distributions are much broader than any of those for the undisturbed samples, while the mixed distributions span the range between the bimodals and the undisturbed samples.

Figure 16 shows distributions of confined fission-track lengths in Otway Group apatites in outcrop samples and from the four selected Otway Basin wells. In these distributions, data from samples within approximately 10°C intervals have been pooled. In each interval, the distributions obtained in individual samples were essentially identical. These distributions show that as the mean track length falls the distribution maintains the narrow, symmetric form at first, but as the mean length is reduced below about 13 μm, the distributions become increasingly broad, until at temperatures between 102°C and 110°C tracks of lengths from about 1 or 2 μm up to 16 μm are present, in a very broad, almost flat, distribution. The trend of increasing width of the distribution with decreasing mean length is emphasised in Figure 8 which shows the relationship between the standard deviation of the length distribution and mean track length in the four selected wells. We have used these data to define an Otway Basin "reference trend" (Green et al. 1988), which will be discussed below.

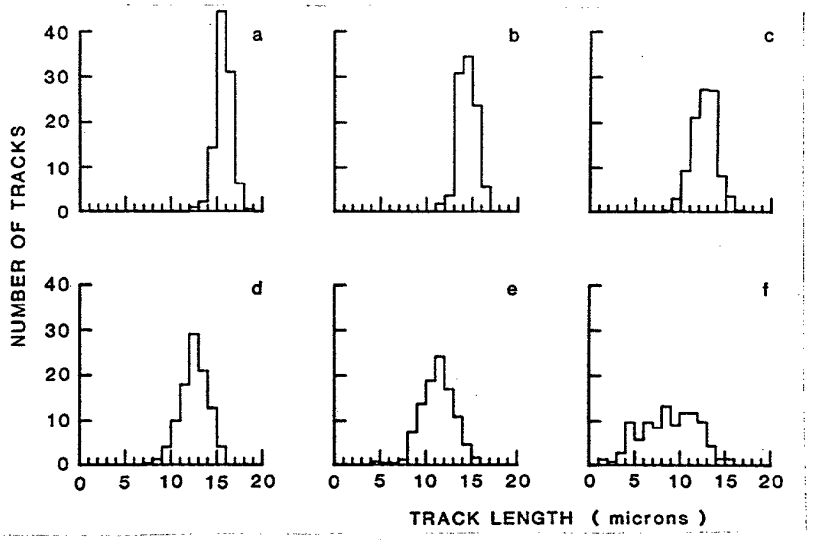

Fig. 16 Distributions of confined fission-track lengths in Otway Group apatites. These are composite distributions (normalised to a total of 100 tracks) produced by summing results from samples in all four wells within the specified temperature limits. Within these limits all samples have essentially similar distributions. Both the mean track length and the form of the track length distribution are highly sensitive indicators of temperature. The flat distribution from lengths of ~1 µm up to ~16 µm shown in F is particularly diagnostic of temperatures in the range 102-110°C.

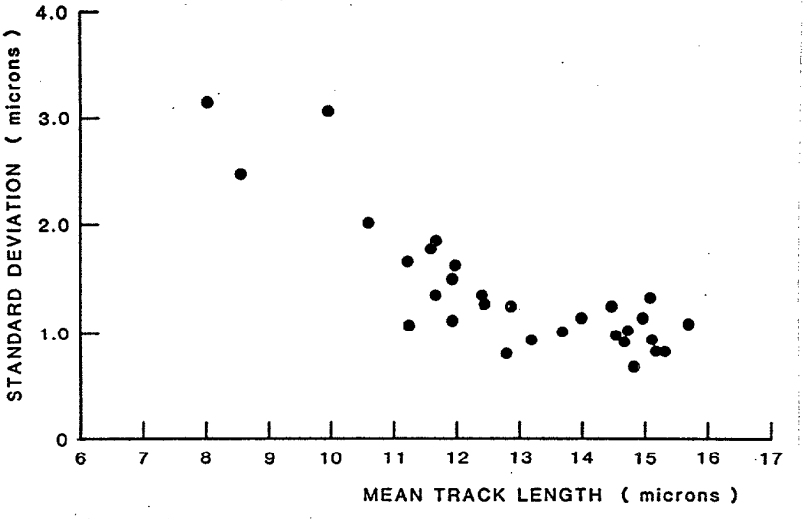

Fig. 17 Relationship between standard deviation of the confined track length distribution and mean track length in subsurface Otway Group apatites from four selected wells. The increase in standard deviation as mean length decreases emphasises the increasing spread of lengths in more annealed samples as shown in Fig. 16.

The increase in the spread of track lengths with increasing temperature is generally more pronounced in these subsurface samples than for the laboratory annealing case and arises from three dominant causes. The first source of broadening of the track length distribution is the anisotropy of the annealing process in apatite as observed in laboratory annealing (Green *et al.* 1986). A second source comes from the variation in annealing properties of individual apatite grains of different composition discussed below. Thus, shorter tracks are contributed from grains more susceptible to annealing, while in more resistant grains, tracks are longer. The third cause of the increasing spread in lengths arises because of the continuous production of tracks with time. Some tracks will have been in existence throughout the whole thermal history, whereas some will have formed only recently.

Predictions of the behaviour of individual fission tracks during annealing, based on the annealing model described above, suggest that for thermal histories in which temperatures are constant, or slowly rising with time, the lengths of individual tracks produced at different times converge to approximately the same length. However, tracks may take approximately 10 Ma to reach this length, and thus some tracks, formed within the last few million years, will be longer than those formed previously.

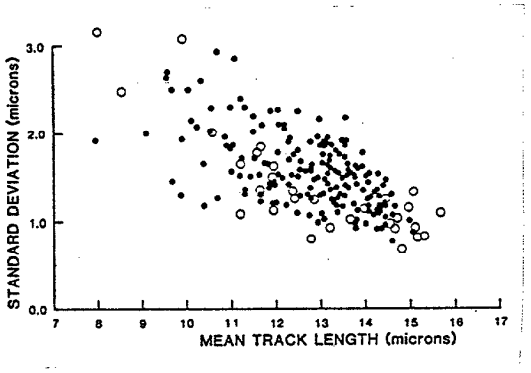

Fig. 18 Relationship between standard deviation of the confined track length distribution and mean track length observed in apatites from over 20 sedimentary basins, including both surface and sub-surface samples. Data from the Otway Basin reference trend (open circles) again show a broadening of the distribution as the mean length decreases, although this trend is distinct from that shown in Fig. 15 for outcropping basement rocks.

In addition to these Otway Basin results, we have compiled a large body of track length data from over 20 sedimentary basins, including both outcrop and subsurface samples. Figure 18 shows the relationship between

standard deviation and mean length for this extensive data set, with the Otway Basin reference trend shown as open circles. It is clear that this sedimentary basin data has a distinctly different trend to that of the outcropping crystalline basement rocks shown in Fig. 15, extending to lower values of mean length, down to about 8 μm in samples where down-hole annealing is particularly pronounced. The larger data set in Fig. 18 occupies a wider field than that defined by the reference wells alone. Data from a particular well or region often define specific sub-trends within this plot, and can provide some initial insight into the thermal history. Examples of individual sub-trends have been discussed in more detail by Gleadow et al (1986b).

Track length data tend to fall on the reference trend for those samples minimally disturbed, but as maximum paleotemperatures increase (i.e. as mean track length decreases) the influence of the thermally shortened tracks draws the data above the reference trend. The region in Fig. 18 above the reference trend seems to be occupied only by samples which have been subject to significantly higher temperatures than those now pertaining.

Interpretation of confined track length distributions

These observations on naturally annealed apatites show that the confined track length distribution of spontaneous fission tracks in any given sample contains a great deal of information about its thermal history at the temperatures typically encountered in the upper few kilometres of the Earth's crust. This information provides a basis for interpreting any apatite fission-track age. For instance, a *volcanic*-type distribution immediately identifies a sample which has cooled extremely rapidly, as for example in a volcanic rock or high level intrusive. Such a distribution could also be found in basement terrains which have undergone a single-stage rapid uplift, followed by equally rapid erosion, as long as temperatures have remained relatively low since. Only apatites with such track length distributions will have fission track ages which can be interpreted in terms of single well-defined events. The reason for the small but consistent difference in mean length between *induced* and *undisturbed volcanic* type distributions is that a small degree of annealing occurs in apatite even at ambient surface temperatures over geological time (Green 1980). In sedimentary basin applications any apatite fission track ages interpreted as being of stratigraphic significance, due to volcanism contemporaneous with sedimentation, must also have an *undisturbed volcanic* type length distribution.

Outcropping rocks in shield areas and crystalline rocks in fold belts which have not been thermally disturbed since cooling to temperatures at which fission tracks are retained, have confined track length distributions similar to the *undisturbed basement* type. Such distributions reflect the more or less continuous uplift and cooling of such regions, albeit at very low rates in some cases, and contain tracks produced at all temperatures

from about 130°C to present day ambient temperatures. As we have discussed in more detail elsewhere (Gleadow, *et al.*, 1986a), it is the uniformity of cooling, rather than its rate, that is important in defining the form of this distribution. Essentially similar distributions may result from very slow cooling rates in ancient shield areas and extremely rapid, but continuous, cooling in young fold belts such as the Alps (Hurford, 1986). The aparent apatite ages in these two extreme cases would, of course, be very different.

Departures from this simple pattern are of great significance and reveal details of the thermal history which are not otherwise accessible. The most obvious examples of this are *bimodal* distributions as discussed above. In such cases it should be possible to extract a great deal of useful information about the thermal history once all the relevant controlling factors are understood (e.g. Laslett *et al.* 1982). Clearly bimodal distributions, however, are at one end of a spectrum of possibilities where a track length distribution represents the combination of two components, one being tracks partially shortened by elevated temperatures, the other being tracks formed after subsequent cooling. It is only when the temperature is sufficient to shorten tracks to a mean of about 9 or 10μm that the two peaks will be well resolved. When the shortened component has a mean length greater than 10μm, this peak will merge with the longer component to give a unimodal distribution with an intermediate mean but a greater standard deviation than would be obtained from a simple cooling history. When the mean length of the annealed component is below 9μm the track length distribution lacks a well defined peak (Gleadow *et al.*, 1986a) and when added to the longer component, may resemble a tail to shorter lengths. The relative proportions of the two components of bimodal distributions is also important in resolving two clear peaks. These will be related to the timing and magnitude of the thermal event. So the conditions for obtaining clearly bimodal distributions are quite strict. In the majority of cases we will instead see a broad, unimodal distribution of the *mixed* type (Fig. 6b), with a shape characteristic of the particular thermal history.

In any of these cases, it is important to realise that the apparent fission track age obtained on these apatites is a composite age and does not relate to a single event. Only by investigating the details of the confined track length distribution can an apatite fission track age be confidently interpreted. An age alone can generally be interpreted in a number of ways, but the confined track length distribution allows firm constraints to be placed on the meaning of the observed age.

Effects of apatite composition

At a number of points in the preseding discussion we have mentioned the effects of compositional variation between different apatites on their annealing properties. We will now consider this factor in more detail by

examining the natural annealing of fission tracks in individual apatite grains over geological time. Fig. 19 shows distributions of fission track ages for single grains of apatite derived from two samples of the volcanogenic Otway Group (Gleadow and Duddy, 1981). The sample in Fig. 19a has an *undisturbed volcanic* type of length distribution and has never been deeply buried since deposition during the early Cretaceous. All individual grains give ages indistinguishable from the pooled age of 120 Ma, which is interpreted to closely approximate the depositional age.

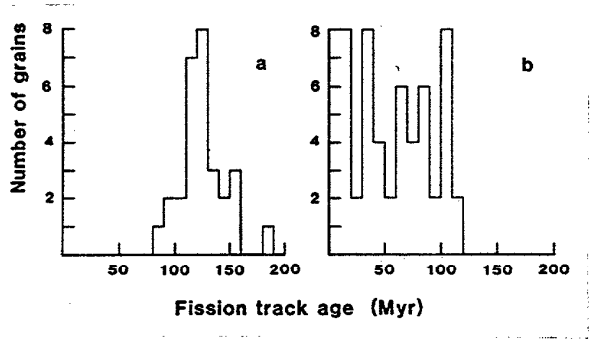

Fig. 19 Distribution of single apatite grain ages in two samples of Otway Group sandstone. (a) shows results for a near surface sample which has never been deeply buried and all grains are consistent with a single pooled age. (b) shows the highly variable single grain ages in a sample now at 92°C in the Flaxmans-1 well, illustrating the varying response of individual crystals to burial annealing.

However the sample in Fig. 19b is taken from the Flaxmans-1 borehole at a present day temperature of 92°C. This sample has been progressively buried to its present depth over the last 120 Ma (Gleadow and Duddy, 1981) and the pooled fission track age of the apatite grains has been reduced to 53 ± 2 Ma by natural annealing. However, the individual apatite grains in this sample show a range of ages from zero up to the depositional age of 120 Ma. Different apatite grains have responded to temperature in different degrees so that while some grains are totally annealed others show little or no annealing. Clearly the individual grains possess different annealing properties since all grains within the same sample must have experienced the same thermal history.

Electron microprobe analyses of these apatites have given the first clear evidence that this variability in annealing properties is compositionally controlled. Analyses of individual apatite grains were carried out on the University of Melbourne JEOL JXA-5A microprobe using a well-certified sample of Durango apatite as standard to minimise matrix effects. The apatite compositions are predominantly fluorapatite with varying subordinate amounts of chlor- and hydroxyapatite. Fig. 20 shows apparent fission track age of individual apatite grains plotted against the

number of chlorine atoms per $Ca_{10}(PO_4)_6(OH,F,Cl)_2$ molecule. It can be seen that those apatites richest in chlorine have ages close to the depositional age and are more resistant to annealing while grains composed dominantly of fluorapatite have been totally annealed, giving zero apparent ages.

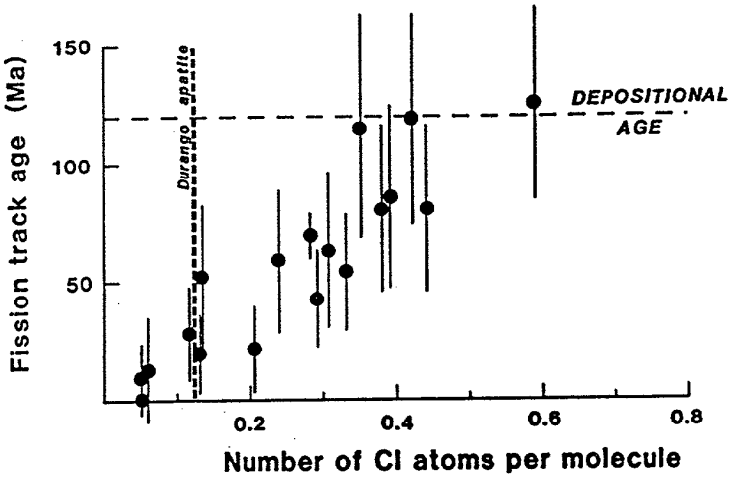

Fig. 20 Relationship between apparent fission track age and composition, in terms of the proportion of chlorine present, in individual apatite grains from a sample of Otway Group sandstone taken from a depth of 2585m in the Flaxmans-1 well (at a present day temperature of 92°C). This relationship suggests that chlorapatite is more resistant to anneaing than fluorapatite. The composition of Durango apatite is also shown, for reference.

These results show that the annealing properties of a single apatite crystal strongly depend on the chemical composition of that crystal, and particularly on the Cl/F ratio. This has also been borne out by preliminary investigation of a sample of almost pure chlorapatite from Snarum, Norway, in which fossil fission tracks have lengths of ~15 μm, and are retained well above 370°C for 1 hour annealing. For comparison, this treatment is sufficient to remove *all* tracks in Durango apatite (used in the laboratory annealing experiments) the composition of which is indicated in Fig. 13, as predominantly fluorapatite.

This observsation that different apatite compositions have different annealing properties, presumably due to some compositional control on activation energy, has important implications for modelling the fission track parameters observed in natural apatites. For example, it is possible that at least part of the fanning observed in the Arrhenius plot for apatite may be due, not as simply to an activation energy which changes with the degree of annealing, but to the superposition of a series of narrow Arrhenius plots corresponding to the range of compositions present. This idea has been developed further in the paper by Green et al. (1985). It seems reasonable to extend the general conclusion of compositional control on

annealing to other minerals since compositional variation is by no means restricted to apatite.

In order to obtain the maximum temperature resolution from apatite analysis it will be necessary to fully quantify the effects of this compositional control on apatite annealing. This is currently being persued as part of our continuing research program. However, it appears that in most cases this will be a second-order effect as the range of apatite compositions in many samples is not great, and generally close to that of the Durango apatite upon which our annealing model is based.

REFERENCES CITED IN PART 2

Bhandari, N., Bhat, S.C., Lal, D., Rajagoplan G., Tamhane A.S. and Venkatavaradan V.S., 1971. Fission fragment tracks in apatite: Recordable track lengths, *Earth Planet. Sci. Lett.* 13, 191-199.

Burchart, J., Butkiewicz, T., Dakowski, M. and Galazka-Friedman, J., 1979. Fission track retention in minerals as a function of heating time during isothermal experiments - a discussion. *Nucl. Tracks* 3, 109-117.

Castaño, J.R. and Sparks, D.M., 1974. Interpretation of vitrinite reflectance measurements in sedimentary rocks and determination of burial history using vitrinite reflectance and authigenic minerals. *Geol. Soc. Amer. Spec. Pap.* 153, 31-52.

Chaillou D. and Chambaudet A., 1981. Isothermal plateau method for apatite fission track dating. *Nucl. Tracks* 5, 181-186.

Dartyge, E., Durand, J.P., Langevin, Y. and Maurette, M., 1978. A new method of investigating the past activity of ancient solar flare cosmic rays over a time scale of a few billion years. *Proc. Lunar Planet. Sci. Conf.* 9th, 2375-2398.

Dartyge, E., Durand, J.P., Langevin, Y. and Maurette, M., 1981. A New model of nuclear particle tracks in dielectric minerals. *Phys. Rev.* B. 23, 5213-5229.

Duddy, I. R., Gleadow, A. J. W., and Keene, J. B., 1984. Fission track dating of apatite and sphene from Paleogene sediments of deep sea drilling project leg 81, site 555, *In* Roberts, D. G., Schnitker, D., et al., eds., *Initial Reports of theDeep Sea Drilling Project,* 81: Washington, United States Government Printing Office, p. 725-729.

Epstein, A.G., Epstein, J.B. and Harris, L.D., 1977. Conodont Colour Alteration - an index to organic metamorphism. U.S. Geol. Surv. Prof. Paper 995., 26p.

Fleischer, R.L., Price, P.B. and Walker, R.M., 1965. Effects of temperature, pressure and ionisation on the formation and stability of fission tracks. *J. Geophys Res.* 70, 1497-1502.

Fleischer, R.L., Price, P.B. and Walker, R.M., 1975. *Nuclear tracks in solids.* University of California Press, Berkeley.

Gleadow, A.J.W., 1981. Fission track dating methods: what are the real alternatives. *Nucl. Tracks* 5, 3-14.

Gleadow, A.J.W. and Duddy, I.R., 1981. A natural long term annealing experiment for apatite. *Nucl. Tracks* 5, 169-174.

Gleadow, A.J.W. and Harrison T.M., 1988. Thermochronology: quantitative constraints on basin modelling and hydrocarbon maturation. *in* K. Sinding-Larsen (ed) *Extensional basin modelling and paleotemperature reconstruction*. International Union of geoogical Sciences (in press).

Gleadow, A.J.W. and Lovering, J.F., 1974. The effect of weathering on fission track dating. *Earth Planet. Sci. Lett.* 22, 163-168.

Gleadow, A.J.W., Duddy, I.R. and Lovering, J.F., 1983. Fission track analysis: a new tool for the evaluation of thermal histories and hydrocarbon potential. *Aust. Petrol. Explor. Assoc. J.* 23, 9-102.

Gleadow, A.J.W., Duddy, I.R., Green P.F. and Hegarty, K.A., 1986a. Fission track lengths in the apatite annealing zone and the interpretation of mixed ages. *Earth Planet. Sci. Lett.* 78, 245-254.

Gleadow, A.J.W., Duddy, I.R., Green, P.F. and Lovering, J.F., 1986b. Confined fission track lengths in apatite - a diagnostic tool for thermal history analysis. *Contr. Miner. Petrol.* 94, 405-415.

Green, P.F., 1980. On the cause of the shortening of spontaneous fission tracks in certain minerals. *Nucl. Tracks* 4, 91-100.

Green, P.F., 1981. "Track-in-Track" length measurements in annealed apatites. *Nucl. Tracks* 5, 121-128.

Green, P.F., Duddy, I.R., Gleadow, A.J.W., Tingate, P.R. and Laslett, G.M., 1985. Fission track annealing in apatite: track length measurements and the form of the Arrhenius plot. *Nucl. Tracks* 10, 323-328.

Green, P.F., Duddy, I.R., Gleadow, A.J.W. and Laslett, G.M., 1986. Thermal annealing of fission tracks in apatite: 1- A qualitative description. *Isot Geosci.* 59, 237-253..

Green, P.F., Duddy, I.R., Gleadow, A.J.W. and Lovering, J. F., 1988. Apatite fission track analysis as a paleotemperature indicator for hydrocarbon exploration. *In* N.D Naeser, (ed.) *Thermal histories of sedimentary basins*. Springer-Verlag (in press).

Green, P.F. and Durrani, S.A., 1977. Annealing studies of tracks in crystals. *Nucl. Tracks* 1, 33-39.

Harris, A.G., 1979. Conodont colour alteration, an organo- mineral metamorphic index, and its application to Appalachian basin geology. *In* SEPM Spec. Publ. 26, 3-16.

Harrision, T.M., 1985. A reassessment of fission track annealing behaviour in apatite. *Nucl. Tracks* 10, 329-334.

Hurford, A.J., 1986. Cooling and uplift patterns in the Lepontine Alps, south central Switzerland and an age of vertical movement on the Insubric fault line, *Contrib. Mineral. Petrol.* 92 413-427.

Hurford, A.J. and Green, P.F., 1983. The zeta calibration of fission track dating. *Isot. Geosci.* 1, 285-317.

Hurford, A.J., Fitch, F.J. and Clarke, A., 1984. Resolution of the age structure of the detrital zircon populations of two Lower Cretaceous sandstones from the Weald of England by fission track dating. *Geol. Mag.* 121, 269-277.

Lal, D., Rajan, R.S., Tamhane, A.S., 1969. Chemical composition of nuclei of Z>22 in cosmic rays using meteoritic minerals as detectors. *Nature* 221, 33-37.

Laslett, G.M., Kendall, W.S., Gleadow, A.J.W. and Duddy, I.R. 1982. Bias in measurement of fission-track length distributions. *Nucl. Tracks* 6, 79-85.

Laslett, G.M., Gleadow, A.J.W. and Duddy, I.R., 1984. The relationship between fission track length and density in apatite. *Nucl. Tracks* 9, 29-38.

Laslett, G.M., Green, P.F., Duddy, I.R. and Gleadow, A.J.W., 1987. Thermal annealing of fission tracks in apatite: II - A quantitative analysis. *Isot. Geosci.* 65, 1-13.

Märk, E., Pahl, M., Purtscheller, F. and Märk, T.D., 1973. Thermische Ausheilung von Uran - Spaltspuren in Apatiten, Alterskorrecturen und Beitrage zur Geothermochronologie. *Tschermaks Miner. Petrol. Mitt.* 20, 131-154.

Naeser, C.W., 1979. Thermal history of sedimentary basins in fission track dating of subsurface rocks. *In* SEPM Special Publication No. 26, 109-112.

Naeser, C.W., 1981. The fading of fission tracks in the geologic environment - data from deep drill holes. *Nucl. Tracks* 5, 248-250.

Naeser, C.W. and Faul, H., 1969. Fission track annealing in apatite and sphene. *J. Geophys. Res.* 74, 705-710.

Wagner , G.A.,1968. Fission track dating of apatites. *Earth Planet. Sci. Lett.* 4, 411-415.

Wagner, G.A., 1981. Fission track ages and their geological significance. *Nucl. Tracks* 5, 15-26.

Wagner, G.A.and Storzer, D., 1972. Fission track length reductions in minerals and the thermal history of rocks, *Trans. Amer. Nucl. Soc.*15, 127-128.

Waples, D.W., 1980. Time and temperature in petroleum formation: application of Lopatin's method to petroleum exploration. *Amer. Assoc. Petrol. Geol. Bull.* 64, 916-926.

Young, E.J., Myers, A.T., Munson, E.L. and Conklin, N.M., 1969. Mineralogy and geochemistry of fluorapatite from Cerro de Mercado, Durango, Mexico. U.S. Geol. Survey Prof. Paper 650-D, D84-D93.

Zimmerman, R.A. and Gaines, A.M., 1978. A new approach to the study of fission track fading. U.S. Geol. Surv. Open-File Report 78-701, 467-468.

PART 3:

FISSION TRACK THERMAL HISTORY ANALYSIS - COOPER-EROMANGA BASIN

INTRODUCTION

The Eromanga-Cooper Basin of South Australia and Queensland (Fig 1.) is a large and complex intracratonic basin containing up to 1500 m of Permo-Triassic sediments overlain by up to 3200 m of younger Mesozoic and Tertiary sediments (Kanstler et al., 1983). General usage refers the older sequence to the Cooper Basin and the Jurassic and Cretaceous rocks to the Eromanga Basin. The basins comprise Australia's most productive onshore petroleum province with the undoubted potential for continuing commercial hydrocarbon discoveries. Detailed reviews of the history of exploration and an overview of exploration and potential are given by Sprigg (1986) and Armstrong and Barr (1986).

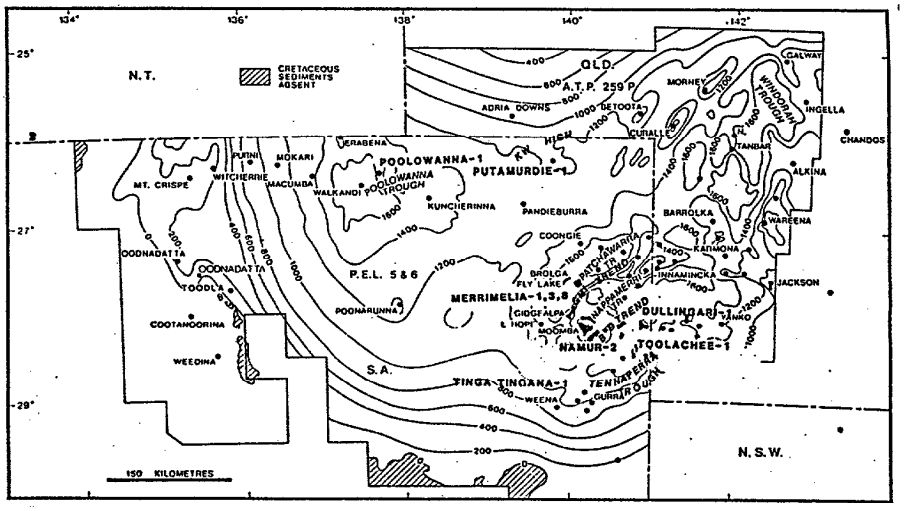

Fig. 1 Regional locality map for the southwestern Eromanga Basin showing well locations and major structural features. Contours show subsea depths (m) to approximate top of the Cadna-Owie Formation (from Moore and Pitt, 1984).

Previous thermal history studies have used various models based on organic parameters, with a significant shift in emphasis from a Karweil -

Bostick model in early studies to a Lopatin-Waples model in more recent published work. As discussed below, these two models have quite different assumed time dependences and as such, the predictions of ***timimg of hydrocarbon maturation*** based on each are incompatible. This has led to a situation where early studies (e.g. Kanstler et al., 1978) indicated that a significant recent (2-5 Ma) rise in geothermal gradient was necessary to explain observed maturation levels in many areas of the basin (e.g. Nappamerri Trough , Fig. 1)., while later studies based on Lopatin techniques either confirmed this conclusion (e.g. Pitt, 1982; 1986) or suggested that maturation levels where consistent with present geothermal gradients acting throughout burial (e.g. Kanstler et.al, 1986).

Here we report an initial study using Apatite Fission Track Analysis (AFTA) for thermal history assessment. Details of the technique are oulined below are discussed in more detail in Gleadow et al., (1983) and in Chapters 1 to 6 in this report. Samples from 17 exploration wells (Table 1) from the Eromanga-Cooper Basin (including Pedirka and Warburton Basin sequences; Fig 2) are discussed in terms of their apatite fission track parameters and interpreted thermal histories.

STRUCTURAL SETTING AND STRATIGRAPHY

The presence of a number of narrow fault-bounded anticlinal horsts provided the basis for subdivision of the Eromanga-Cooper Basin into a number of depositional troughs. The major structural features are shown on Fig. 1. Structural development is characterized by major growth faulting during the Permian (e.g. Mount , 1981), draping and differential compaction controlling Jurassic structures, culminating in broad folding due to left-lateral wrench faulting in the Late Oligocene and Miocene (Senior and Habermehl, 1980).

A generalized stratigraphical column, with significant hydrocarbon occurrences marked, (from Kanstler et al., 1983) is given in Fig. 2. A number of publications deal with the stratigraphy of the area and the reader is referred to Gravestock et al., (1986) for details. Two main periods of burial are indicated one commencing in the early Permian and extending to the mid-Triassic in which up to 1500 m of glacial and fluvial coal measure sediments were deposited, although thickness throughout the Permian basins is very variable. This Cooper Basin depositional phase was followed by uplift and erosion in the late Triassic in most areas of the basin with up to 500 m of section removed in the south-east (Kanstler et al., 1983). In the early Jurassic subsidence was again initiated, this time over a much broader region than encompassed by the Permian basins, resulting in the accumulation of some 1000 m of coal measures sediments. The rate of subsidence increased markedly in the Early Cretaceous with deposition of over 2000 m of fluvial and shallow marine sediments, including approximately 1000m of Winton Fm. in the Albian and Cenomanian (?).

Table 1: Sample details and apatite yields - Eromanga-Cooper Basin

Sample number	Depth (m)	Sample type	Formation/Age	Apatite yield
Dullingari-1				
8622-42	428	core 1	Winton Fm.- E. Cretaceous (?)	Excellent
8622-43	1068	core 3	Allaru Mudstone- E. Cretaceous	Excellent
8622-44	1209	core 4	Wallumbilla Fm. - E. Cretaceous	Excellent
8622-45	1376	core 6	Cadna-owie - E. Cretaceous	Excellent
8622-46	1511	core 7	Murta - E. Cretaceous	Fair
8622-47	1677	core 8	Namur - L. Jurassic	Poor
8622-48	1775	core 10	Birkhead Fm.- Mid. Jurassic	Excellent
8622-49	1916	core 12	Nappamerri Fm. - Triassic	Good
8622-50	2105	core 16	Toolachee Fm. -	None
8622-51	2594	core 23	Patchawarra Fm. -	None
8622-52	2744	core 25	Dullingari	Good
8622-53	2948	core 28	Dullingari	Good
Toolachee-1				
8622-61	303	cuttings	Winton Fm.- E. Cretaceous (?)	Excellent
8622-64	776	cuttings	Allaru Mudstone- E. Cretaceous	Excellent
8622-67	1242	cuttings	Wallumbilla Fm. - E. Cretaceous	Excellent
8622-68	1388	cuttings	Murta - E. Cretaceous	Excellent
8622-69	1507	cuttings	Namur - L. Jurassic	Excellent
8622-36	1849	core 1	Toolachee Fm.	Insufficient
8622-70	1852	cuttings	Toolachee Fm.	Good
8622-37	2105	core 3	Patchawarra Fm.	None
8622-38	2119	core 4	Patchawarra Fm.	None
Tinga Tingana-1				
8622-54	1732	core 4	Tirrawarra Fm. - E. Permian	Excellent
8622-55	2096	core 6	"Interface sequence" - E.Permian	Excellent
Poolowanna-1				
8622-33	2356	core 1	Algebuckina Sandstone	Excellent
8622-34	2354	core 1	Algebuckina Sandstone	Excellent
8622-35	3073	core 5	Ordovician Basement ?	Excellent
Putamurdie-1				
8622-39	1771	core 6	Hutton ?- Early Jurassic	Poor
8622-40	1877	core 8	Nappamerri Fm - Triassic	Good
Merrimelia-1				
8622-56	2421	core 4	Patchawarra Fm - Permian	None
8622-57	2444	core 5	Patchawarra Fm - Permian	None
8622-58	2592	core 8	Tirrawarra Sandstone - Permian	Excellent
8622-59	2946	core 12	Merrimelia Fm. - Permian	Excellent

Sample number	Depth (m)	Sample type*	Formation/Age yield	Apatite
Merrimelia-3				
8622-41	2293	core 5	Permian	Excellent
Merrimelia-6				
R23144	1610	core 3	Namur Sand.- L. Jurassic	None
Merrimelia-8				
R23138	1877	core 3	Hutton Sandstone - E. Jurassic	Excellent
Strzelecki-3				
R23134	1687-1710	core 1&2	Hutton Sandstone - E. Jurassic	None
Namur-2				
R23148	1655-1673	core 1&2	Murta/Namur Sand. - E. Jurassic	Excellent
Burley-2				
8642-168	553	cuttings	Winton Fm. - E. Cret. ?	Excellent
8642-169	754	cuttings	Winton Fm. - E. Cret. ?	Excellent
8642-170	1056	cuttings	Allaru Mudstone. - E. Cret. ?	Excellent
8642-171	1266	cuttings	Wallumbilla Fm. - E. Cret. ?	Excellent
8642-172	1748	cuttings	Murta Member - E. Cret. ?	Excellent
8642-171	1977	cuttings	Namur Sandstone - E. Cret. ?	Good
8642-23	2803	core 1	Toolachee Fm. - Triassic	Good
8642-24	3109	core 3	Epsilon - E. Permian	Good
8642-25	3109	core 4	Patchawarra - E. Permian	Good
Tirrawarra-1				
8642-152	384-430	cuttings	Winton Fm. - E. Cret. ?	Excellent
8642-156	1586	cuttings	Wallumbilla Fm. - E. Cret.	Excellent
8642-157	1669	cuttings	Cadna-owie Fm. - E. Cret.	Excellent
8642-158	1827	cuttings	Murta Member ? - E. Cret.	Excellent
8642-160	2010	cuttings	Birkhead Fm. - Mid. Jurassic	Excellent
McLeod-1				
8642-26	3584	core 1	Tirrawarra Sand. - E. Permian	None
8642-27	3746	core 3	Granitic Basement	Good
Kirby-1				
8642-28	3584	core 2		Excellent
Big Lake-27				
8642-30	1979	core 1		Excellent
8642-31	2706	core 4		None
8642-32	2898	core 8		None
Big Lake-35				
8642-29	2933	core 2		None

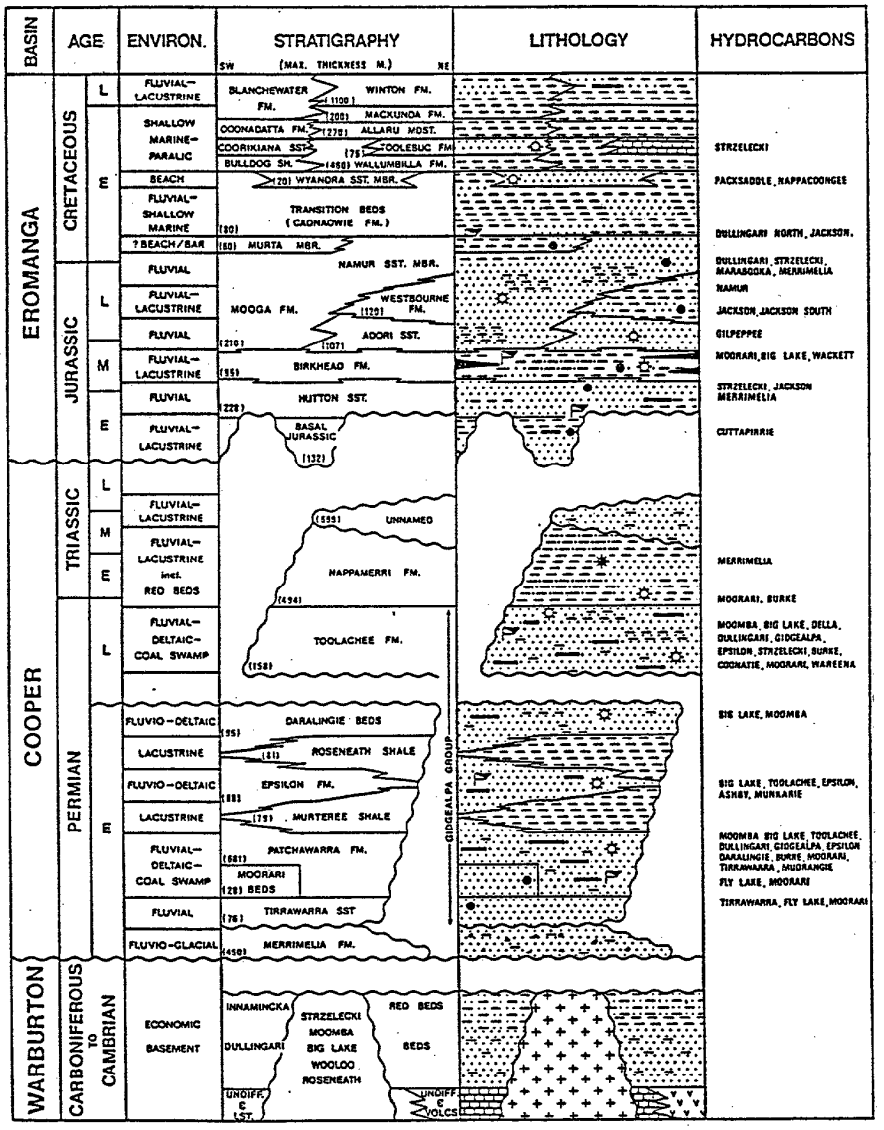

Fig. 2 Generalised stratigraphic column for the Eromanga-Cooper basin sequence.

The generalized burial history of the Central Nappamerri Trough is illustrated in Fig. 3 (from Moore and Pitt, 1984.) There are some changes in stratigraphical nomenclature and distribution of the major Formations across the basin area, the major variations shown in Fig. 4.

PREVIOUS THERMAL HISTORY STUDIES

The Eromanga-Cooper Basin comprises Australia's most productive onshore petroleum province and has been the subject of a number of

studies concerning the assessment of thermal history and organic maturation over about the last 10 years (eg. Kanstler et al., 1978; 1982; 1983;1986; Poll, 1981; Pitt, 1982; 1986; Moore, 1986; Passmore and Boreham, 1986). These studies have used organic parameters, primarily the reflectance of the coal maceral vitrinite, to assess the basins' thermal history and the timing of hydrocarbon generation.

Early studies (e.g. Kanstler et al., 1978) used a vitrinite/coalification model based on work of Karweil (1956) as modified by Bostick (1973). This model related temperature and time to coal rank and vitrinite reflectance (Vr) enabling one parameter to be calculated knowing the other two, and among the commonly used maturation models has the greatest time dependence (Fig. 5). In use (e.g. Kanstler et al., 1978) it is usual to calculate a temperature knowing the stratigraphic age of the rock and the measured Vr. This is referred to as the Tiso (or isothermal model temperature). A second temperature can also be calculated (Tgrad) which is based on the assumption that the measured Vr resulted from a uniformly rising temperature (ie. continuous burial) since deposition. These model temperatures are then compared with the actual down-hole temperature to assess the time scale of heating (see for example Kanstler et al., 1978).

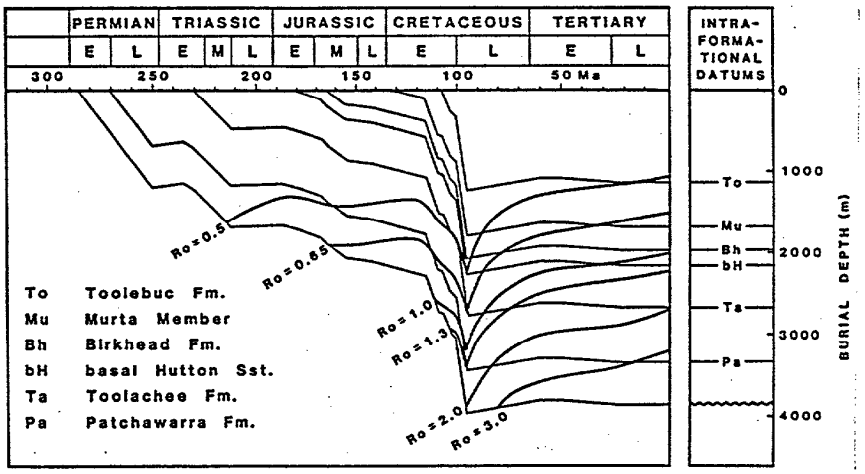

Fig 3 Generalised burial and maturation history of the Central Nappamerri Trough, based on data from Kirby-1 (from Moore and Pitt, 1984).

Pitt (1982; 1986) and Kanstler et al. (1982; 1983; 1986) used a Lopatin-Waples model (Lopatin, 1971; Waples (1980) to calculated an arbitrary time-temperature index (TTI) which was calibrated to vitrinite reflectance using "known" thermal histories in a large number of world-wide exploration wells (Waples, 1980). The technique depends upon two assumptions: 1. Maturation varies exponentially with temperature; 2. Maturation varies

linearly with time, encompassing the "rule of thumb" concept that the reaction rate for maturation will double for each 10°C rise in temperature. The time dependence of this model, and thus its ability to predict variation of organic maturation with time depends fundamentally on the initial assumptions and cannot be construed as a soundly-based model. In use, the accumulated TTI is calculated for a given horizon (source rock) using the known burial history and thermal gradient and is related Vr via a calibration scale. This calculated Vr is then compared with the measured Vr , and changes made to the thermal history so that a satisfactory prediction is obtained. Predictions published for the Eromanga-Cooper Basin are often made using a proprietary calibration (e.g. Kanstler et al., 1983) or with a reaction factor different from "2" (e.g. Pitt, 1986). Details of the calculation of TTI and its use can be found in Pitt (1982;1986).

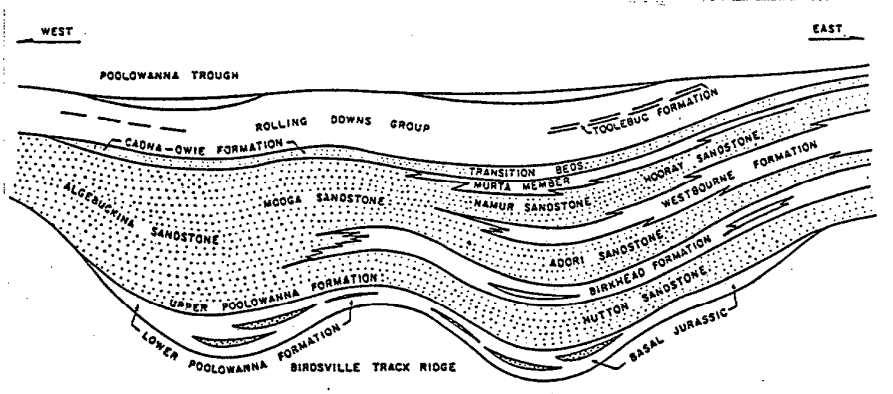

Fig. 4 Stratigraphical nomenclature and major formations across the Eromanga Basin (from Sprigg, 1986).

GEOTHERMAL GRADIENTS

It is clear from data presented by Kanstler et al. (1978), Middleton (1979), Schwebel et al. (1980) and Pitt (1982;1986) that a larger than "normal" range of geothermal gradients are present in the Eromanga-Cooper Basin . Gradients range from around 30 to over 60°C/km over the Basin area. Kanstler et al. (1986) provide a good summary of the thermal gradient distribution. In brief, gradients in excess of 50°C/km in and near the Nappamerri and Tennaperra Troughs with lower gradients around 30-40°C/km in the Patchawarra Trough and Pedirka Basins. High values are exemplified by gradients in the Strzelecki field near 60°C/km with lower values around 35°C/km in Beanbush-1 from the Patchawarra Trough (Pitt, 1982). A list of thermal gradients derived from a large number of petroleum exploration wells is provided by Pitt (1982).

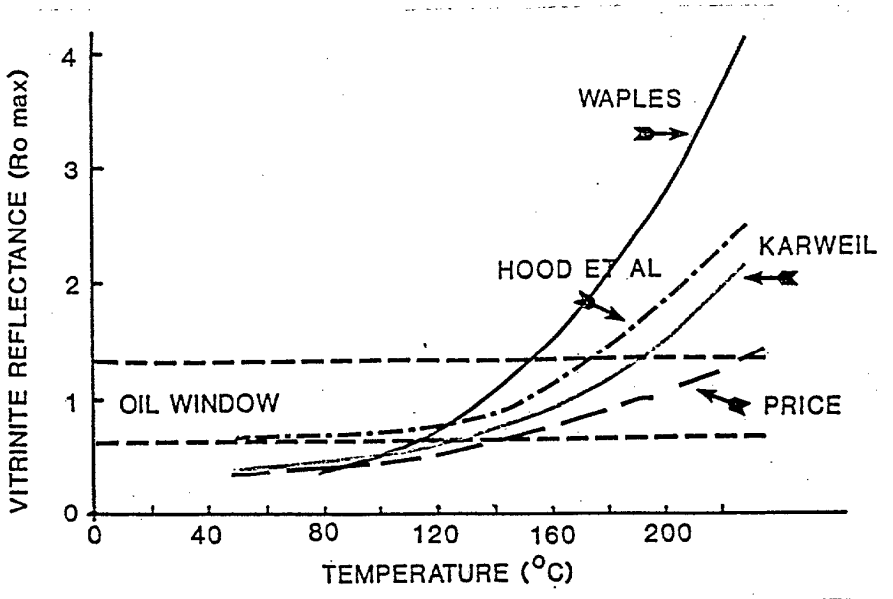

Fig. 5 Comparison of vitrinite reflectance obtained from a number of theoretical models. Calculation based on heating time of 10 Ma at each temperature. At ~150°C the results largely span the conventional range of the oil window of 0.6-1.3 R_o. Note: Karweil model as modified by Bostick (1973), Waples (1980) version of Lopatin (1971), Hood et al. (1975) model of LOM to Vr and Price (1983).

APATITE FISSION TRACK THERMAL HISTORY ANALYSIS

Sample Preparation and apatite yields

Samples for this study were drawn from conventional core, unwashed and washed cuttings. Core samples were washed and dried, reduced in size using a jaw crusher where necessary and then ground in a rotary disc mill to provide material with a diameter up to a maximum of ~500 microns. Both washed and unwashed cuttings were also washed and dried to remove any drilling mud before grinding. The crushed and sized material was then washed to remove material finer than about 50 microns, dried and processed by conventional heavy liquid and magnetic separation techniques to recover any uranium-bearing heavy minerals. Apatite suitable for analysis was recovered from 46 of the 58 samples from the South Australian Eromanga - Cooper Basin sequence (Table 1). In general terms, the Mesozoic sequence has abundant apatite with the lowest or more erratic yields coming from more quartz-rich units such as the Hutton and Namur sandstones (Table 1). A much smaller number of samples have been processed from the Permian sequences, but a broad brush assessment of apatite yields indicates that recovery of apatite from

sandstones throughout the sequence will not be a problem in applying the fission track technique.

Techniques

Fission track age and length measurements were made using techniques outlined by Gleadow et al. (1983). Apatites were mounted in epoxy resin on glass slides, polished and etched for 20 sec in 5M HNO_3 at 20°C to reveal the fossil fission tracks. The apatite mounts were processed by the external detector method (Gleadow, 1981) which, apart from its greater inherent precision, has the advantage of allowing ages to be determined on single grains. Wherever possible, tracks were counted over 20 grains in each mount. In those samples where this number was not present, all available grains were counted, the actual number depending on the availability of suitably etched and oriented apatites. The number of tracks used for each track density and length measurement is shown in Table 2.

For track length studies, the full length of 'confined' fission tracks were measured. Confined tracks are those which do not intersect the polished surface but lie totally below it, having been etched from other tracks or fractures. Lengths were measured on 100 horizontal confined tracks wherever possible, although the number of suitable tracks may be fewer than this in some samples.

Neutron irradiations were carried out in a well thermalised flux (X-7 facility) in the Australian Atomic Energy Commission's HIFAR research reactor. Total neutron fluence was monitored by counting tracks in mica external detectors attached to two pieces of the NBS standard glass SRM612 included in the irradiation cannister at each end of the sample stack. No flux gradient is usually found in the irradiation facility used over the length of the sample package and this was confirmed by the track counts over the two dosimeter glasses. The two values have been pooled to give the single value quoted in Table 2.

DATA PRESENTATION

Full analytical data for the fission track ages are given in Table 2 together with the mean track lengths and the standard deviation of the distributions of confined track lengths. Ages were calculated using the standard fission track age equation (Hurford and Green, 1982) and errors are quoted at the level of one standard deviation throughout. All constants used in derivation of the results are shown at the bottom of Table 2 using the nomenclature of Hurford and Green (1982). The Zeta calibration factor has been determined empirically by direct comparison

Table 2: Fission track analytical Results - Eromanga-Cooper Basin

Sample number	Depth (m)	Number of grains	Standard track density ($x10^6 cm^{-2}$)	Fossil track density ($x10^6 cm^{-2}$)	Induced track density ($x10^6 cm^{-2}$)	Correlation coefficient	Chi square probability	Age (Ma)	Uranium (ppm)	Mean track length (µm)	Std. Dev. (µm)
Dullingari-1											
8642-42	428	33	1.177 (6094)	0.363 (405)	0.704 (785)	0.941	60%	107 ± 6.7	8	14.50 ± 0.09 (100)	0.87
8642-43	1068	20	1.177 (6094)	0.502 (327)	0.774 (634)	0.961	40%	107 ± 7.411		14.10 ± 0.14 (100)	1.41
8642-44	1209	19	1.177 (6094)	0.619 (174)	1.077 (303)	0.983	99%	119 ± 7.412		12.57 ± 0.22 (33)	1.24
8642-45	1376	20	1.177 (6094)	0.375 (279)	0.685 (509)	0.930	40%	114 ± 8.6	8	12.89 ± 0.13 (100)	1.33
8642-46	1511	13	1.177 (6094)	0.452 (87)	1.144 (220)	0.898	<1%	164 ± 36	13	14.68 ± 0.55 (10)	1.72
8642-47	1677	5	1.177 (6094)	0.106 (327)	0.474 (157)	0.398	8%	46.4 ± 8.75		5.7 (1)	-
8642-48	1775	26	1.177 (6094)	0.174 (296)	0.959 (1632)	0.519	<1%	54.3 ± 8.4	11	10.91 ± 0.26 (51)	1.83
8642-49	1916	21	1.177 (6094)	0.079 (61)	2.041 (634)	0.201	<1%	16.1 ± 5.8	23	6.26 ± 1.00 (7)	2.65
8642-52	2744		All Fission Tracks Annnealed						0		0
8642-53	2948		All Fission Tracks Annnealed						0		0
Toolachee-1											
8642-61	303	20	1.396 (5971)	0.212 (247)	0.530 (617)	0.890	60%	98.4 ± 7.55		15.14 ± 0.09 (100)	0.91
8642-64	776	20	1.396 (5971)	0.614 (438)	1.396 (996)	0.961	<1%	165 ± 28	13	14.66 ± 0.14 (100)	1.42
8642-67	1242	22	1.396 (5971)	0.679 (569)	1.275 (1069)	0.909	<1%	123 ± 13	12	13.90 ± 0.10 (99)	1.04
8642-68	1388	21	1.396 (5971)	0.276 (247)	0.460 (412)	0.870	40%	147 ± 12	4	13.92 ± 0.14 (100)	1.42
8642-69	1507	20	1.396 (5971)	0.412 (293)	0.789 (561)	0.942	4%	158 ± 18	8	13.97 ± 0.14 (74)	1.18
8642-70	1852	17	1.396 (5971)	0.176 (106)	0.762 (459)	-0.113	<1%	95 ± 17	7	8.21± 1.71 (9)	5.00
Tinga Tingana-1											
8642-54	1732	23	1.396 (5971)	0.935 (939)	1.612 (1619)	0.800	<1%	133 ± 15	15	11.00 ± 0.16 (100)	1.58
8642-55	2096	21	1.396 (5971)	0.422 (528)	2.006 (2508)	0.392	<1%	119 ± 35	19	9.99 ± 0.25 (100)	2.47
Poolowanna-1											
8642-33	2356	22	1.488 (2547)	0.143 (114)	1.395 (1115)	0.242	<1%	17.6 ± 11	12	9.41 ± 0.49 (25)	2.47
8642-34	2354	20	1.488 (2547)	0.059 (48)	2.583 (2095)	-.054	<1%	10.9 ± 9	23	9.71 ± 1.12 (6)	2.75
8642-35	3073	20	1.488 (2547)	0.023 (10)	2.270 (1006)	-.007	<1%	14.1 ± 8	20	-	-
Putamurdie-1											
8642-40	1877	21	1.177 (6094)	0.083 (20)	2.131 (511)	0.533	<1%	7.1 ± 3.5	24	6.49 ± 0.67 (18)	2.84
Merrimelia-1											
8642-58	2592	3	1.488 (2547)	0.037 (5)	3.309 (453)	1.000	96%	2.9 ± 1.3	30	-	-
8642-59	2946	17	1.488 (2547)	0.019 (5)	1.098 (453)	0.386	<1%	1.6 ± 1.6	10	-	-

Sample number	Depth (m)	Number of grains	Standard track density ($x10^6 cm^{-2}$)	Fossil track density ($x10^6 cm^{-2}$)	Induced track density ($x10^6 cm^{-2}$)	Correlation coefficient	Chi square probability	Age (Ma)	Uranium (ppm)	Mean track length (μm)	Std. Dev. (μm)
Merrimelia-3											
8642-41	2948		All Fission Tracks Annealed						0		0
Merrimelia-8											
R23138	1877	19	1.376 (3014)	0.265 (128)	1.033 (499)	0.737	<1%	89.4 ± 1410		10.02± 0.28 (81)	2.55
Namur-2											
R23148	1664	20	1.376 (3014)	0.060 (51)	2.400 (2049)	-0.001	<1%	14.6 ± 8.8	23	9.31± 1.64 (5)	3.67

Brackets show number of tracks counted or measured. Standard and induced track densities measured on mica external detectors (g=0.5), and fossil track densities on internal mineral surfaces. Ages calculated using ζ=355 for dosimeter glass SRM612 (cf. calibration details in Green, 1985). * Mean age, used where pooled data fail $\chi 2$ test at 5%.

with K-Ar ages for a set of carefully chosen age standards, following the methods outlined by Hurford and Green (1983). The pooled or maximum probability age is determined from the ratio of the two track densities obtained from the pooled data for all grains. Errors for the pooled age were calculated using the 'conventional' technique outlined by Green (1981), based on the total number of tracks counted for each track density measurement.

Two statistical parameters are also summarised in Table 2, which are used to test the variability of apparent ages between single apatite grains. The correlation coefficient indicates the degree of correlation between fossil and induced track densities for all the grains counted. For a population of apatites having a uniform age and a significant spread in uranium concentrations, the correlation coefficient should be close to 1. However, if the uranium concentration is relatively uniform, a low correlation coefficient may be obtained even where the apatite fission track ages are identical. A more useful parameter is the Chi squared statistic which indicates the probability that all the grains counted belong to a single age population. A probability of less than 5% is taken as evidence that the grains represent a mixed age population with real differences between the apparent ages of individual grains. A spread in grain ages can result either from inheritance of detrital grains from mixed source areas, or from partial annealing by heating to above about 90°C.

The usual measurement of combined fission track age, the pooled age, is not strictly valid for samples containing a mixed age population, being biased towards the grains with higher track counts. In such cases the mean grain age provides a useful measure and this parameter has been used as the apparent apatite age where appropriate. The error in the mean grain age is taken as the standard deviation of the mean single grain age.

The variation in both apparent apatite age and mean track length as a function of increasing present corrected down-hole temperature is plotted for three well sequences (Dullingari-1, Toolachee-1 and Tinga-Tingana-1) in Figures 6 to 8. The distribution of single grain ages in each sample is illustrated by a histogram and a smoothed probability function in Figures 9 to 12. Single grain ages are also given with the primary counting results and statistical data in the Appendix. Track length distributions are shown as histograms in Figure 13 to 16. The number of tracks (N) measured is also indicated and the histograms have been normalised to 100 tracks for each sample to facilitate comparison.

PRINCIPLES OF INTERPRETATION

Interpretation of fission track length and age data is based both on observations of the lengths of spontaneous tracks in apatites from a wide variety of geological environments (Part 1; Gleadow et al., 1986b), and also on laboratory study of the response of induced fission tracks to elevated temperatures (Part 1; Green, et al., 1986; Laslett et al, 1987). The basis of the interpretation may be summarised as follows.

In sedimentary rocks which have never been heated above ~50°C since deposition, apatite grains which contained no "inherited" tracks at the time of deposition (e.g. volcanogenic grains, or grains derived from rapidly uplifted basement terrains) have confined track length distributions with mean lengths in the range 14-15 μm, and standard deviations of ~1 μm. In such samples, the apatite fission track age will be equal to the age of deposition, since the technique is calibrated against other isotopic systems using age standards which also have this type of length distribution. Apatites which contain a finite proportion of tracks at the time of deposition will have a fission track age which is older than the depositional age, and the length distribution will be a mixture of inherited tracks, representing the pre-depositional history, and a component similar to that described above, produced after deposition. The actual distribution found in such samples will depend on which of these components is dominant.

In samples which have been subject to temperatures in the range 50 - 130°C after deposition, the length distribution is more complex. The length of each individual track is essentially determined by the maximum temperature that track has experienced. Time differences of an order of magnitude produce changes in fission track parameters that are equivalent to temperature changes of less than 10°C, so temperature is by far the dominant factor in determining the final fission track parameters. In samples for which the present temperature is maximum, all tracks therefore have much the same length resulting in a narrow, roughly symmetric distribution. The degree of shortening will depend on the temperature, with the mean track length falling progressively from ~14μm

at 50°C to zero at around 110 - 130°C, the actual value depending on the time scale of heating, and the composition of the apatites present in the sample. Values quoted here relate to times of the order of 10^7 - 10^8 years, and typical apatite compositions. Shortening of tracks produces an accompanying reduction in the measured or " apparent" fission track age of the apatite. Therefore the age reduction is also highly temperature dependent, with the apparent age falling to zero at around 110 - 130°C, due to total erasure of all tracks.

Complex thermal histories produce correspondingly complex length distributions and apparent "ages". Samples which have cooled from a thermal maximum (with peak temperature between ~50 and 130°C) at some time in the past contain two populations of tracks. Those formed prior to the thermal maximum will all be shortened to the same degree (the precise value depending on the peak temperature) while those formed during and after cooling will be longer due to the lower prevailing temperatures. The length distribution in such samples will be broader than in the simple case, and the apparent age will be a reflection of the final length distribution. In some cases this kind of history produces a characteristic bimodal distribution of confined track lengths. If cooling is sufficiently rapid, and the final temperature is low enough (<~50°C), tracks formed subsequently will have lengths of 14-15μm, and will contribute an age component corresponding to the age of the cooling "event". In such samples, analysis of the length distribution can, in favourable circumstances, allow the timing of this cooling event to be determined. If maximum temperatures exceed ~110 - 130°C, all pre-existing tracks will be erased, and all tracks now present will have formed during and subsequent to cooling. The apparent age in such samples therefore relates directly to the time of cooling.

Based on our laboratory annealing experiments on Durango apatite (Part 1), for each sample we can define a temperature , T_l, at which the measured mean track lengths would be observed if the sample had resided at that temperature for a certain interval of time (Table 3). We can also estimate a value of T_l from our observations of annealing in the Otway Basin (Part 1) , where a greater range of apatite composition is present. Geological observations and laboratory annealing studies in progress have revealed that variation in F and Cl content in apatites have the dominant effect on fission track annealing. Briefly, the more Cl an apatite contains, the greater its ability to retain fission tracks at a given temperature. Thus at present temperatures above ~90°C in the Otway Basin tracks in the most F-rich apatites are totally annealed while those in the most Cl-rich grains (Cl/(Cl+F) ratios up to ~0.5) are only slightly affected (Part 1).

At present, we have no quantitative method of estimating T_l for the Otway-type compositional spread other than for the time-scale of maximum heating of ~20-40 Ma estimated from Otway Basin burial histories for a group of wells defined as the Otway Basin Reference wells.

Table 3: Thermal history assessment - Eromanga-Cooper Basin

Sample Number	Present Temperature (°C)	T_l Otway (°C)	T_l Durango (°C)	Mean Track Length (μm)	Strat. Age (Ma)	Corrected Age (Ma)	Max. Temp. (°C)	Time at Max. Temp. (Ma)
Dullingari-1								
8622-42	41	<50	50	14.50±0.09	90-100	111	present	<40
8622-43	73	55	55	14.10±0.14	100-110	114	present	1-10
8622-44	80	-	-	12.57±0.22	110-120	-	-	-
8622-45	89	76	76	12.89±0.13	120-130	133	present	1-10
8622-46	93	-	-	14.68±0.55	130-140	-	-	-
8622-47	99	-	-	5.7	140-160	-	-	-
8622-48	102	95-100	96	10.91±0.26	160-180	75	>102	>1 ?
8622-49	107	-	-	6.26±1.00	240-245	-	-	-
8622-52	135	>125	>120	Annealed	258-286	-	-	~1
8622-53	142	>125	>120	Annealed	258-286	-	-	~1
Toolachee-1								
8622-61	36	<50	<40	15.14±0.09	90-100	98	present	<40
8622-64	61	<50	55	14.66±0.14	100-110	169	present	1-2
8622-67	86	60	60	13.90±0.10	110-120	133	present	~1
8622-68	94	60	60	13.92±0.14	130-140	171	present	~1
8622-69	100	60	60	13.97±0.14	140-160	170	present	<1
8622-70	118	-	110-120	8.21±1.71	245-258	-	-	-
Tinga-Tingana-1								
8622-54	98-104	99	95	10.93±0.18	258-286	183	present	~10
8622-55	115-121	105	105	9.99±0.25	258-286	194	present	1-2
Poolowanna-1								
8622-33	118	>110	110-120	9.41±0.48	140-180	-	present	1-10
8622-34	118	>110	110-120	9.71±1.12	140-180	-	present	1-10
8622-35	145	>110	110-120	-#	>400?	-	present	<1
Putamurdie-1								
8622-40	97	>110	110-120	6.49±0.67	>286	-	90-110 +	?
Merrimelia-1								
8622-58	121	>115	115-120	-#	-	-	present	<5
8622-59	135	>115	115-120	-#	-	-	present	<1
Merrimelia-3								
8622-41	105	>125	>120	Annealed	-	-	>120	?
Merrimelia-8								
R23138	96	105	105	10.02±2.55	180-190	-	105	1-2
Namur-2								
R23148	123	110-125	110-120	9.31±1.64	140-160	-	present	~10

*: Note that where no T_l estimates are given, insufficient length measurements were available for analysis.

+: Based on apatite compositional information - see text

#: No lengths measured but the presence of tracks giving an age for single grains provides a measure of annealing.

No rigorous estimate of time spent at maximum temperature for samples with such broad spreads in composition is currently possible and estimates given in Table 3 are based on temperature offsets from the Durango-based kinetic model. Experimental work currently in progress by the FTRG is aimed at quantification of the annealing kinetics such as is now available for Durango apatite (Cl/(Cl+F) ~0.1), for a group of apatites encompassing a range of chemical compositions .

A rudimentary analysis of the length distributions and age data allows the calculation of a "corrected age", which represents an estimate of the time over which tracks have been accumulating. This correction is based on the relationship between fission track length and apparent age observed in laboratory annealing experiments on Durango apatite and on geological observations in the Otway Group of the Otway Basin (Gleadow and Duddy, 1981; unpublished data).

Final interpretation is based on computer modelling of track shortening through likely thermal histories for a monocompositional apatite of average composition (Durango Apatite, Cl/F ~0.1), coupled with our observations of geological annealing of fission tracks in apatite from certain exploration wells in the Otway Basin of southeastern Australia. The computer modelling is based on our understanding of track shortening in laboratory heating experiments (Part 1; Laslett et al, 1987). The predictions of such modelling procedures agree well with our observations of fission track annealing for apatites of the appropriate composition in samples from the Otway Basin. These data have been presented by Gleadow and Duddy (1981), Gleadow et al. (1983) and Green et al. (1986). These, together with related laboratory studies, also afford a means of extending the model predictions to apatites of other compositions, and show how the reduction in mean track length is related to the resulting reduction in fission track age.

FISSION TRACK THERMAL HISTORY ASSESSMENT

The following discussion of exploration wells is divided on the basis of structural setting as shown in Figure 1. The method of interpretation is discussed fully for the Dullingari-1 well, with the other well samples discused in a less detailed fashion.

1. Nappacoongee-Murteree-Dullingari High.

DULLINGARI-1

A total of 12 core samples from Dullingari-1 in the Eromanga-Cooper Basin were processed for U-bearing heavy minerals and of these 10 samples yielded sufficient apatite suitable suitable for fission track analysis. Sample types, depths and stratigraphical information are shown in Table 1,

together with the yield of detrital apatite obtained after mineral separation. In general yields were good to excellent in most of the Permian to Early Cretaceous section, with fair and poor yields from the Early Cretaceous Murta member and the Namur sandstone respectively. No apatite was recovered from the two samples from the Toolachee and Patchawarra Formations in Dullingari-1. The samples cover a present temperature range of 41 to 142°C, derived from the two component geothermal gradient data provided by Pitt (1982) of 49.9°C/km (down to Cadna-Owie level) and 34.2°C/km (section below Cadna-Owie).

Observations.

A number of significant observations emerge from inspection of the data presented in Tables 1 & 2. It is clear that the four shallowest samples give apparent apatite fission track ages that are similar to their stratigraphic ages, with a sharp change in age below sample 8642-46 (Murta Mbr). Further, the two shallowest samples (Winton Fm. and Allaru Mudstone) have track lengths >14 μm , indicating that the age of these samples have significance in terms of an event in time as discussed above. In fact, the coherence of the apatite ages and stratigraphic ages suggests that the apatites in these two formations were derived largely from contemporaneous volcanism. The apatite age of 164±36 Ma for the Murta Mbr. sample is due to a mixture of apatites from a volcanogenic and an older basement source as shown by the single crystal ages distributions (Fig. 9) and the failure of its $P(\chi^2)$ value (Table 2). This mixture of sources is developed further below under the provenance heading.

Samples of Namur Sandstone (8642-47) and below have apparent ages much less than their stratigraphic ages, showing immediately that these samples have been subjected to considerable annealing, implying temperatures of around 70°C or above. It is also clear that none of these five deeper samples has a mean track length of around 14 - 15μm which, as discussed above, means that none of the quoted fission track ages have any significance in terms of "events" taking place at that time, the ages being indicators of degree of annealing. Since these latter samples have undergone appreciable annealing, there is little information available on source regions, and their characteristic fission track parameters (i.e. the parameters that would be observed in these samples now, if no significant post-depositional annealing had occurred). However, as discussed below clues to their provenance is provided by analysis of the chemical composition of the apatites.

The above discontinuity in apatite age and length parameters is also reflected in the values of $P(\chi^2)$, from Table 2, with the upper 4 samples having values much >5%, revealing no significant spread in individual grain ages in these samples, and the length distributions while having mean lengths varying between 14.5 and 12.6 μm, are not particularly broad. Such features are suggestive of samples with relatively simple heating

histories. Three of the four deeper samples for which fission track parameters could be measured fail the test at the 5% level with the other passing at only the 8% level, probably only passing due to the small number of grains (5) available for analysis. Such values are indicative of significant annealing at temperatures in excess of 70°C.

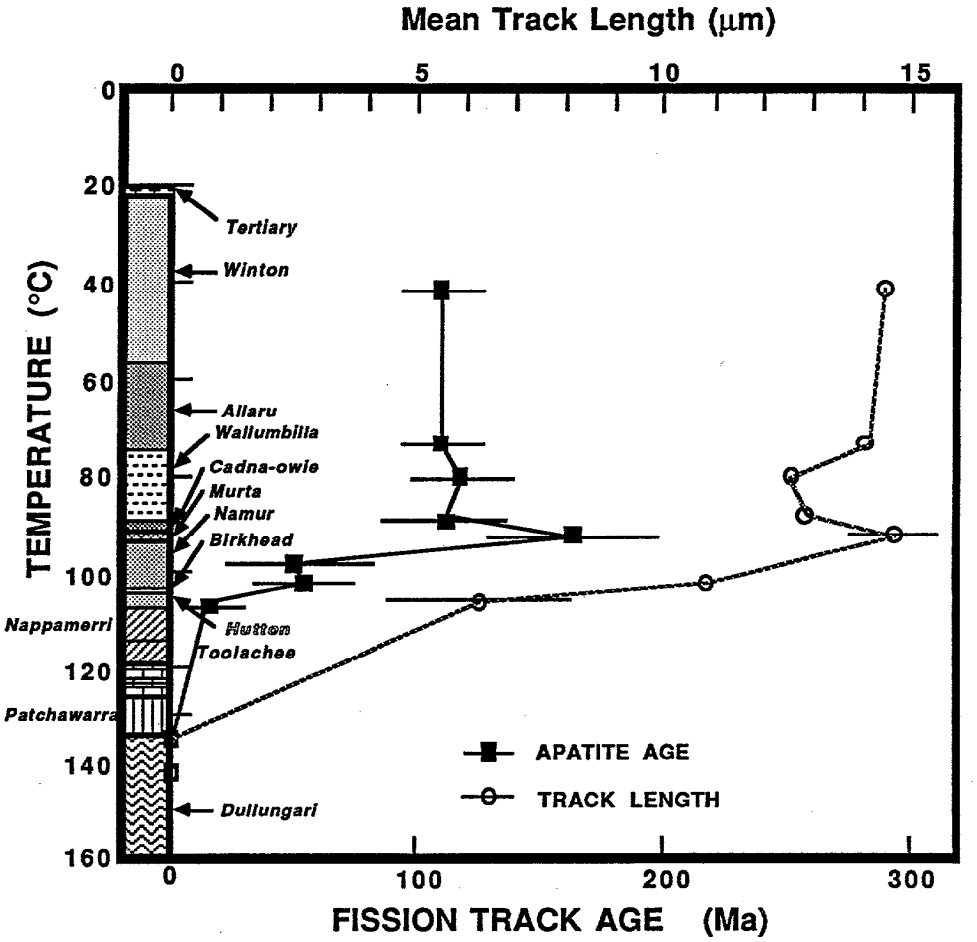

Fig. 6 The variation of apparent fission track age and mean track length with downhole temperature for apatites from Dullingari-1.

The form of the temperature dependence of apparent fission track age and mean confined fission tracks length in Figure 6, show a progressive reduction in age and length with increasing temperature down to the Murta level, with a sudden drop in age and length for samples from the Namur, Birkhead and Nappamerri Fms. This sudden drop is indicative of a fundamental difference in thermal histories for horizons each side of this level. Data for the Birkhead Fm. in particular suggests that the deeper samples have experienced higher temperatures in the past than now operating. All of the samples have strong peaks in their distributions of single grain ages, with the position of this peak shifting to younger ages

with increasing sample temperature (Fig. 9), and only a minor "tail" of grains towards higher ages.

No fission tracks were observed in apatites from the two deepest samples indicating that the present temperatures are sufficiently high for tracks not to be retained for any significant time.

Mean confined track lengths in the samples also show a progressive reduction, from ~14.5μm in the shallowest sample down to zero in the deepest. Standard deviations of the length distributions fall in the range 0.9 - 2.65 μm. although a restricted range of 0.9 to 1.83 is appropriate for samples where sufficient (>50) lengths could be measured. The higher standard deviations are a little broad compared with samples which have undergone relatively simple thermal histories dominated by heating, suggesting that the thermal histories of the samples analysed are more complex. This is borne out by inspection of the confined track length distributions in Fig. 13, which show narrow peaks at long mean lengths typical of volcanogenic source detritus in the shallowest samples and with a typical pattern of a broad peak at longer lengths which is a little skewed towards shorter lengths with increasing sample depth. The position of the longer peak falls with increasing depth and/or temperature. These length patterns are typical of annealed length distributions referred to in Gleadow et al. (1986; & Part 1) and are indicative of increasing downhole temperature.

Estimates of T_l (length estimated temperature: see above) are shown in Table 3, using a time interval of 10 Ma for the Durango-based kinetic model of apatite annealing (Part 1). We also estimate a value of T_l from our observations of annealing in the Otway Basin (Part 1), where a greater range of apatite compositions is present (Cl/(F+Cl) varying from 0 to ~0.5), which has the effect of causing fission tracks to be retained at higher temperatures than that indicated for a more F-rich apatite like Durango (see Green et al., 1985 and above). A time scale of ~20 to 40 Ma is appropriate for the time spent at maximum temperature for the Otway Group Reference Section (Part 1). The Cl/(F+Cl) compositional variation observed for apatites from Dullingari-1 is shown in Fig 17 and discussed in more detail below.

Composition data from various Eromanga-Cooper Basin samples (Fig. 17) suggests that the Otway Based estimates are appropriate for most of the Mesozoic sandstones sampled, while the Durango-based estimates are more appropriate for apatites present in the quartzose sandstones in the Namur and Hutton and for all Permian and older sandstones analysed. Both estimates of T_l are similar illustrating the effect of apatite compositional variation on the time needed for track annealing at a similar temperature. For Dullingari-1 T_l estimates for individual samples tend to be higher than the measured temperatures, but tend to be converging at the highest temperature (Table 3). This suggests that the shallow samples have been at their present temperatures for a shorter time

than used in the Tl calculations. As discussed above, calculation of the time scale of heating (Table 3) are not rigorous for Otway-type compositional spreads so only order of magnitude estimates are given. Nevertheless the data suggests that a given degree of track length reduction Dullingari-1 is displaced towards higher temperatures by 10 to 20°C compared with the Otway Basin Reference Wells (Part 1). This indicates that the present geothermal gradients of 49.9°C/km (down to Cadna-Owie level) and 34.2°C/km (section below Cadna-Owie) (Pitt, 1982) have only increased to these levels in the last 1 to 10 Ma or so, implying a maximum geothermal gradient of ~42°C/km down to Cadna-Owie level prior to this time. It should be emphasised here that as with any technique claiming to assess thermal history, the above analysis depends heavily on the accuracy of the present geothermal gradient.

While the Tl estimate for the Birkhead sample (8642-48) is similar to the present temperature it is clear from the corrected age data (Table 3, Figure 9 and Appendix) that all fission tracks were probably erased in a higher temperature event at some time prior to the recent temperature rise indicated by the shallower data. While the corrected age of ca. 75 Ma is suggestive of temperatures exceeding ~125°C in the late Cretaceous, more samples are required to assess the relevance of this result.

These observations provide the basis for the interpretations of the thermal history for these samples developed below.

Interpretations.

The observations presented above lead to the conclusion that samples above the Murta Mbr. (8642-46) are presently at their maximum temperatures since deposition and that these maximum temperatures have only been acting for less than ~10 Ma. Samples below the Namur on the other hand have probably been subjected to temperatures sufficient to totally anneal all previously formed tracks, during a period of peak temperatures prior to the recent temperature increase, as indicated by the sharp change in apparent apatite age at this level. The nature of this event is not known, but as their are no indications of large amounts (> 1 to 2 km) at this level, the data is most likely the result of thermal perturbations associated with the passage of hot fluids in the Namur/Murta and Hutton/Birkhead aquifer systems. Vitrinite reflectance perturbations at a similar level in some other wells has also been attributed to a similar effect (see for e.g. Kanstler et al., 1986). Future studies aimed at resolution of this phenomenon will require precise temperature data for aquifer fluids and adjacent aquicludes, possibly by use of specific detailed temperature surveys.

Corrected age estimates are shown for each sample in Table 3, and while it must be emphasised that these estimates are very crude, they indicate that the Winton, Alluru, Wallumbilla, and Cadna-Owie units contain apatites derived largely from contemporaneous volcanism and

that only a minor amount of annealing has occurred in these samples since deposition.

Corrected ages and compostional data for the Murta suggest a mixed contemporaneous volcanic and older "granitic" basement source, with tracks still being retained in some grains from prior to deposition, thus confirming that present temperatures are now at a maximum for this unit. Insufficient track lengths could be measured to calculate a corrected age for the Namur sample but the similarity in single crystal age histograms for it and the underlying Birkhead sample (8642-48) suggests that they share a common history (Even with due consideration for the more F-rich apatites occurring in the Namur - see Fig. 17 and below). The Birkhead Fm. corrected age of ~ 75 Ma is less than half of the stratigraphic age (Table 3) with only one single crystal age (Appendix) approaching the depositional age (with large error) and indicates that temperatures close to or greater than ~120°C were experienced by this unit in the past.

Thus in Dullingari-1 the apatite fission track data provides evidence for general elevation in the geothermal gradient in the last 1 to 5 Ma and for the presence of higher temperatures, probably close to ~120°C, in the Birkhead-Namur section . It seems likely that the annealing is due to the passage of hot fluids in the aquifer system.

2. Tennaperra Trough - Toolachee Trend.

TOOLACHEE-1

Six cuttings samples, from the Winton, Allaru, Wallumbilla, Murta, Namur and Toolachee units were analysed from Toolachee-1, all of which provided sufficient apatite for analysis (Table 1). The samples covered a present downhole temperature range from 36 to 118°C. A present geothermal gradient of 53°C/km was used, recalculated from Middleton (1979) using a surface temperature of 20°C.

Observations and Interpretations

A detailed discussion is not presented for this well, and the reader is referred to the analysis presented above for Dullingari-1 for a fuller example of the method of analysis. Fission track age and length data is presented in Table 2 and the Appendix. The variation in fission track parameters with corrected downhole temperature is illustrated in Fig.7, and the apatite single crystal and length distribution data is presented in Figs. 10 and 14 respectively. Variation of apatite single crystal age for several of the samples is provided in Fig. 17.

The compositional data presented in Fig.17 for the Wallumbilla, Murta, Mooga (Namur ?) and Toolachee indicates that, as for Dullingari-1 the apatites present are largely derived from a volcanogenic source and that an Otway-based annealing model is appropriate. It is clear from petrographic observations, however, that rounded "basement" derived

grains are present throughout much of the section below the Winton Fm (8642-61). This is also reflected in the single crystal fission track data (Fig. 16 and Appendix) and in the corrected ages shown in Table 3 which tend to exceed the stratigraphic ages.

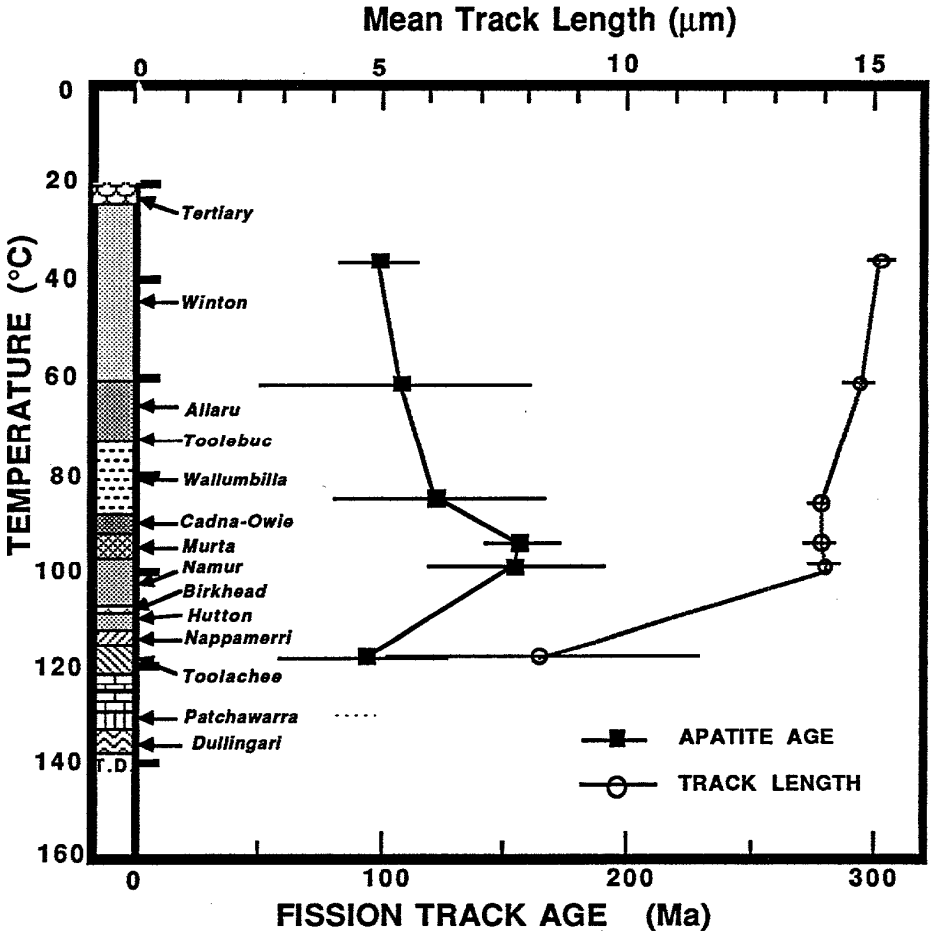

Fig. 7 The variation of apparent fission track age and mean track length with downhole temperature for apatites from Toolachee-1.

The T_l estimates indicate that the mean fission track lengths for all samples (except the deepest sample, 8642-70, which had insufficient lengths for analysis) are grossly out of equilibrium with the present temperatures for the Otway Reference time-scale of 20 -40 Ma. In fact the data indicates that the present high temperatures can only have been acting for about the last 1 Ma (Table 3). A thermal gradient of ~27°C/km is indicated (using 8642-69 as the point of calculation) prior to the recent elevation in gradients, although the range of present temperature (86 to 100) over which little change in track length occurs may suggest that the system does not possess a presently uniform thermal gradient. Even allowing for some error in the present thermal gradient it is unlikely that

any thermal gradient measured presently in the Eromanga Basin could explain the data without significant recent heating.

TINGA TINGANA-1

Two core samples from the basal Permian glacial sequence were separated from this well and both yielded excellent apatite for analysis (Table 1). A thermal gradient of 45°C/km was calculated from the available log data. This gradient is essentially same as that used by Kanstler et al. (1982, their Fig. 3) and is almost identical to nearby wells in the Tennaperra Trough given in Pitt (1982).

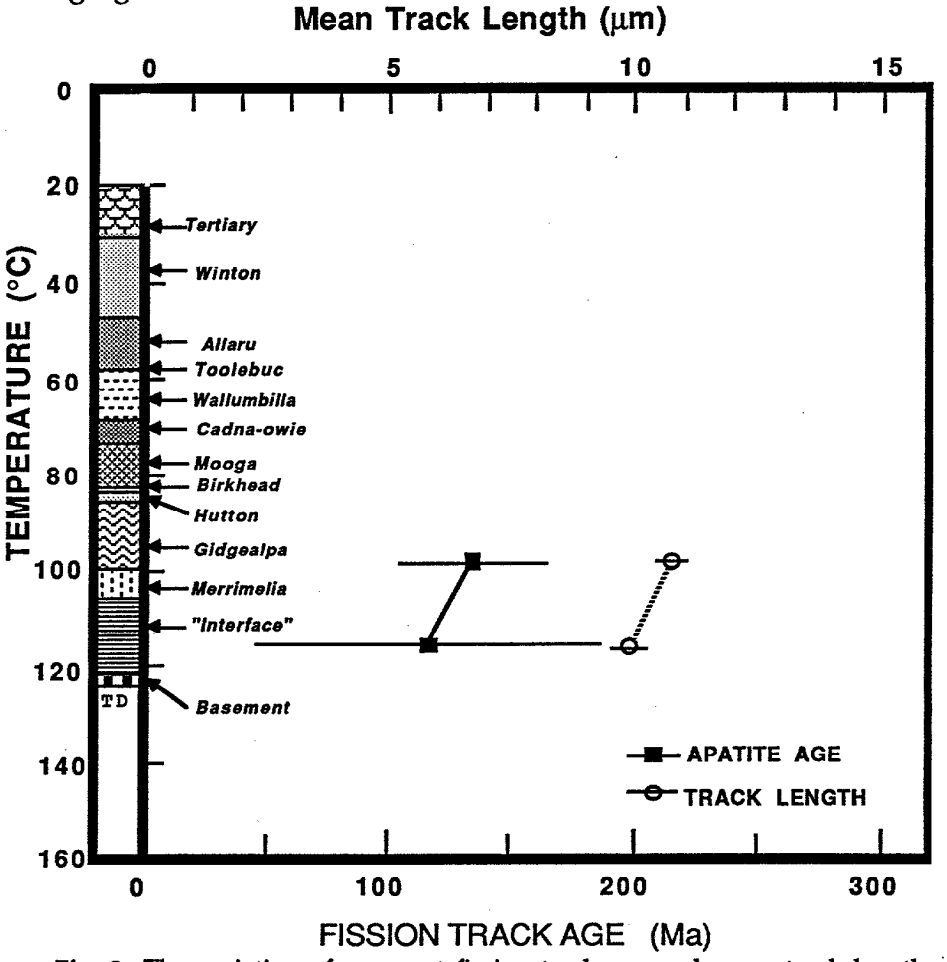

Fig. 8 The variation of apparent fission track age and mean track length with downhole temperature for apatites from Tinga Tingana-1.

Observations and Interpretations

All primary data is presented in Tables 1 &2 and the Appendix and displayed in graphical form in Figs. 8, 11 & 15. Apatite composition data for both samples is shown in Fig 17 and demonstrates that the Durango-based kinetic model is appropriate for these samples. The thermal history

assessment presented in Table 3, shows that the samples are consistent with a recent temperature rise in the last 1 to 10 Ma. The data for the two samples is a little disparate and further samples form this well are needed to confirm the generality of the recent heating argument.

It is also evident in Table 3 that the corrected ages fall considerably short of the stratigraphic ages, and well short of the likely source ages of the detrital apatites. Although the age correction procedures are not rigorous, this suggests the possibility that these samples have lost all or most of their tracks at sometime in the past at temperatures in excess of ~120°C (depending of course on the length of time spent). This is supported by the single crystal age data shown in Figs. 11 and 17, particularly for 8642-54, where only one single approaches the depositional age and there are no crystals that have lost all of their tracks at the presently operating temperatures.

3. Poolowanna Trough

POOLOWANNA-1

Three core samples were processed from this well and all provided excellent apatite yields (Table 1). Two sample came from the the same core near the base of the Jurassic Algebuckina Sandstone and one came from the underlying pre-Permian (Ordovician?) basement. A dog-leg thermal gradient of 43.3°C/km and 38°C/km was used (Pitt ,1982).

Observations and Interpretations

All primary data is presented in Tables 1 &2 and the Appendix and displayed in graphical form in Figs. 11 & 15. Apatite composition data for the three samples is not presented in this report but it shows that the Durango-based kinetic model is appropriate for these samples. Although all sample are close to being totally annealed the age data provides a basis for the thermal assessment in Table 3. This data demonstrates that samples in Poolowanna-1 can only have been at present temperatures for approximately the last 1 to 10 Ma. The deepest sample (8642-35) from the pre-Permian basement still contains F-rich apatites (unpublished) retaining fission tracks even though the present temperature is ~145°C.

4. Kopperomanna-Warbreccan High

PUTAMURDIE-1

Only one of the two core samples analysed from Putamurdie-1 contained apatite (Table 1), it coming from the Triassic Nappamerri Fm. An average thermal gradient of 41.2°C/km was used (Pitt ,1982).

Observations and Interpretations

All primary data is presented in Tables 1 &2 and the Appendix and displayed in graphical form in Figs. 11 & 15. Apatite composition data for the sample is presented in Fig. 17 and it shows that the Durango-based kinetic model is appropriate as a maximum temperature model for this sample as all grains are more F-rich the an the Durango apatite.

This sample is almost totally annealed at the present temperature of 97°C, and considering the apatite compositions present, this temperature would appear to be sufficient to account for the observed annealing (Table 3). Few fission tracks remain in the apatites and insufficient lengths were measured for any estimate of corrected age to be made. Samples from lower present day temperatures in this this well are required to control the time scale of heating.

5. Gidgealpa - Merrimelia - Innamincka Trend

MERRIMELIA-1, 3 & 8

Two of the four core samples analysed from Merrimelia-1, one core sample from Merrimelia-3 and one from Merrimelia-8 contained excellent apatite suitable for analysis (Table 1). A single sample from the Namur sandstone in Merrimelia-6 did not yield (Table 1). A dog-leg thermal gradient of 43.4°C/km and 32.2°C/km was used for Merrimelia-1 (Pitt ,1982), a dog-leg thermal gradient of 38.9°C/km and 32.2°C/km was used for Merrimelia-3 (Pitt ,1982) and a gradient of 40.4°C/km was calculated from log data for Merrimelia-8.

Observations and Interpretations

All primary data is presented in Tables 1 &2 and the Appendix and displayed in graphical form in Figs. 11,12, 15 & 16. Apatite composition data for these samples are not yet available but based on the data set from other wells presented in Fig. 17 we assume that the Durango-based kinetic model is appropriate for all of these samples

All fission tracks in the sample from 105°C in Merrimelia-3 are totally annealed. While the Durango based T_1 estimate for a 10 Ma timescale would suggest temperatures of approx. 120°C are required to this, it is possible that more F-rich compositions would be totally annealed at this temperature. Thus no information on time scale of heating is available.

Both samples from Merrimelia-1 are almost totally annealed at present temperatures of 121 and 135°C (Tables 2 & 3). The presence of tracks in one grain in each of these samples (Appendix) at temperatures above that which should be required for total erasure, does provide evidence for a recent elevation in temperature. It is emphasised however, that such data needs to backed up by sample from higher in the well before it can be generally accepted.

The Merrimelia-8 sample from the Hutton sandstone does provide sufficient data for estimates of T_1 to be made (Table 3) and these suggest that the present temperature of 96°C has been acting for about 1-2 Ma. More information on the source ages of apatites in the Hutton to interpret the corrected age data but it falls only marginally short of the depositional age, and considering the errors involved in the correction procedure for lengths around 10 μm, no conclusion can be drawn concerning possible aquifer heating effects as discussed for Dullingari-1.

5. Moomba Trough

NAMUR-2

A single sample of Murta-Namur sandstone yielded an excellent quantity of apatite for analysis (Table 1). An average gradient of 61.9°C/km was calculated from log data for Namur-2.

Observations and Interpretations

All primary data is presented in Tables 1 &2 and the Appendix and displayed in graphical form in Figs. 12 & 16. Apatite composition data for this samples not yet available and based on the data set from other wells presented in Fig. 17 it is possible that the Namur/Murta sample analyses may have either a Durango or Otway-type compositional spread.

Insufficient lengths were available for rigorous analysis at the degree of annealing shown by the sample and it is only possible to give an order of magnitude estimate of the timescale of heating. The estimate of 10 Ma given in Table 3 is appropriate for the Otway -type spread but if, as is likely from petrographic observations of this sample, a more restricted F-rich apatite population is present, then a more recent rise in temperature cannot be excluded.

TIMING OF HYDROCARBON MATURATION

Poll (1981) argued from the point of view of Eromanga Basin Burial histories that hydrocarbon migration (and generation) most likely occurred in the late Cretaceous or early Tertiary as a result of the increase in temperature that would have been associated with the rapid deposition on the Cretaceous Winton Fm. From Karweil/Bostick-based coalification studies Kanstler et al. (1978) concluded that the present temperatures in many areas of the basin were far too high to have acted for any significant length of time. The further postulated an "early" thermal event in parts of the Nappamerri Trough , widespread moderate gradients in the Mesozoic and Mid-Tertiary and a recent (2 -5 Ma) elevation to present values. This view was supported by Pitt (1982, 1986) using Lopatin/Waples-based techniques. Using similar Lopatin/Waples-based techniques Kanstler et al.

(1986) have recently claimed successful modelling of vitrinite reflectance for Nappamerri Trough wells using the present thermal gradient throughout the history. That this can occur is due largely to the unfounded assumptions on which the organic-based thermal modelling techniques are based (see above).

The importance of understanding the thermal history of the Eromanga-Cooper basin cannot be under estimated. If temperatures have increased only recently then generation from source rocks presently at much higher temperatures than is implied by the data in Chapter 2 (Fig. 2, p.26) will be possible., which will have obvious implications for exploration models. Indeed, a recent rise in temperature of 20°C in 1 Ma is of similar magnitude to depositing 1 km of Pleistocene sediment, and in thermal history terms, is similar to the thermal environments encountered in areas like the Gulf Coast, North Sea, Indonesia etc. where maximum hydrocarbon generation can be from source rocks near 150°C.

CONCLUSIONS AND CONCLUDING REMARKS

Recent elevation of geothermal gradients

The data presented above is generally indicative of a basin-wide increase in thermal gradients in at least the last 10 Ma and possibly as precent as the last 1-2 Ma. Such a rise is not predictable from the form of the burial histories for the basin (e.g. Fig. 3), which show no significant burial since the Early Tertiary and a late Tertiary that is generally characterised by minor uplift. The use of the fission track data in situations where recent heating occurs depends fundamentally of an accurate knowledge of the present temperatures at which the samples analysed were taken from, and an understanding of the annealing kinetics and composition of the apatites analysed. At this stage we have an the required kinetic description for a single apatite composition (Durango) and understand the relative importance of varying composition, as expressed by the ratio of Cl/(Cl+F). It is also reasonable to assume that the presently high and variable geothermal gradients found in the Eromanga basin are real, and that based on world wide data, these gradients are highly unusual, and may be unlikely to be a long-lived phenomenon.

The cause of the high geothermal gradients has been ascribed variously to the presence of a K and U-rich granites underlying some areas (Middleton, 1979) and differences in the bulk conductivity of the sequence, particularly the thermal blanketing effect of the Cretaceous "mudstone" sequence Kanstler et al. (1986), and also to effects due to the presence of the artesian aquifer system. It is clear from the fission track data however, that a very recent rise in thermal gradient has occurred in several areas of the basin and this effect is not compatible with proximity to basement of thermal conductivity arguments which are only relevant to the long term background heat flow conditions. The fact that the recent rise in gradients

is also apparent in rocks far removed from the aquifer system (e.g. Basement in Poolowanna-1) suggests that the recent rise in gradients is due to a fundamental change in the deep seated thermal regime.

As originally discussed by Kanstler et al.(1978) a recent rapid rise in temperature would be presumed to give rise to enhanced generation in source rocks although perhaps only limited migration and this may be the reason for the common occurrence of Eromanga Basin hydrocarbon traps not being filled to spill point. The apatite fission track data tends to support the original contentions of Kanstler et al (1978) and not the most recent interpretation provided by his (with different authors) Waples/Lopatin-based modelling (Kanstler et al., 1986). The Melbourne University Fission Track Research Group is currently involved in a more extensive Eromanga-Basin sampling programme under the terms of NERDDC Grant 86/6144, in both South Australia and Queensland, which aims to provide more extensive data on the importance of the recent heating event revealed in the present study.

Apatite composition

The effect of composition on the annealing of fission tracks in apatite was discussed in Chapter 4 in terms of the variation in fluorine and chlorine content in the apatite crystal lattice. The effect on annealing was first noticed in samples of volcanogenic sandstones in the Otway Group of Victoria (Gleadow and Duddy, 1981) and was finally ascribed to primary F - Cl variation by Green et al., (Chapter 4). Further data have since been accumulated by workers in the Melbourne University Fission Track Research Group, confirming the generality of the effect, and is reported here for the Eromanga Basin samples.

Plots of apatite single crystal age versus the ratio of F to (F+Cl) in those individual crystals are presented in Figure 17 for samples from Dullingari-1, Toolachee-1, Tinga-Tingana-1 and Putamurdie-1.

Three main conclusions arise from this data:

1. Apatites from contemporaneous volcanogenic source rocks (as indicated by the apatite age data) display a range of Cl/(F+Cl) values, confirming the generality on the concept developed from the Otway Group and also seen in volcanogenic sandstones from the Late Permian coal measure sequences of the Bowen Basin (Marshallsea, unpublished data).

2. Apatites from "Granitic" basement sources are generally F-rich (as typified by data from the Namur and Nappamerri units in Dullingari-1 and the Permian glacial units in Tinga Tingana-1.

3. During annealing at elevated temperatures, fission tracks in the most F-rich apatites are more readily annealed in a progressive and predictable matter. This is illustrated well by the Birkhead sample

presently at ~102°C in Dullingari 1 (Fig. 17) which shows a good relationship between the most F-rich apatites which are virtually totally annealed and the most Cl-rich grains which still retain a large amount of age.

The available data provides a basis for future application of the fission track annealing model described in the preceding chapters to samples from the Eromanga-Cooper samples. The Durango-based model is more appropriate for apatites present in the quartzose sandstones in the Namur and Hutton and for all Permian and older sandstones analysed while the Otway-based model is appropriate for the wide spread in apatite compositions observed in the Winton, Allaru, Wallumbilla, Cadna-Owie, Murta, Birkhead (and possibly Hutton due to the transitional relationship with the "dirty" (ie. volcanogenic) Birkhead lithologies), and Toolachee units.

Provenance

The apatite fission track and chemical compositional data indicates that sandstone lithologies in the South Australian portion of the Eromanga Basin are the result of interplay between two major sources of detritus:

- a **contemporaneous volcanogenic source** which is reflected in the occurrence of dirty, less desirable reservoirs such as the Birkhead, Murta and early Cretaceous units.
- a **pre-existing basement source** which is reflected in the occurrence of relatively clean quartzose sandstones typified by the Hutton and Namur units.

The replacement in the middle Jurassic of the clean Hutton lithologies with the volcanogenic Birkhead sandstones is a transitional event and suggests that the influx volcanogenic detritus floods in and swamps detritus from basin margin sources (presumably Broken Hill and Arunta blocks to the south and west). The Birkhead Fm. correlates in time with the obviously volcanogenic Walloon Coal Measures in eastern Queensland (e.g. Exon, 1976) and it seems reasonable that the South Australian unit represents the distal fluvial deposits of volcanoes located in an arc corresponding approximately with the present eastern continental margin. The Birkhead Fm. is not recognized across the Birdsville Track Ridge which may either be the result of the ridge forming a barrier to the westward progression of the volcanogenic detritus or to the dilution of the volcanogenic detritus in areas close to major basin margin inputs. Further fission track work in the Algebuckina Sandstone of the Poolowanna Trough may clarify this aspect.

Waning of the mid-Jurassic volcanic episode allowed the re-establishment of the dominance of the basement derived detritus with the

deposition of the quartzose Namur and equivalent reservoirs over much of the basin. Resurgence of volcanism in the earliest Cretaceous resulted in the quartzose units being again supplanted by the dirty volcanogenic sandstones, this time of the Murta and Cadna-Owie units.

The early Cretaceous deposition was dominated by contemporaneous volcanism with deposition of a thick sequence of dirty volcanogenic sediments over the entire Eromanga Basin of South Australia and Queensland. As in the Otway, Gippsland and Bass Basins of southeastern Australia contemporaneous volcanism (Duddy, 1983) was associated with rapid subsidence of the depositional troughs and the accumulation of thick sequences with poor to non-existent reservoir potential.

REFERENCES CITED IN PART 3

Armstrong J.D. and Barr T.M. 1982, The Eromanga Basin: An overview of Exploration and potential; in Gravestock, D.I., Moore, P.S. and Pitt, G.M. (editors), *Contributions to the Geology and Hydrocarbon Potential of the Eromanga Basin*, Geol. Soc. Aust. Special Publ. No 12, 25-38.

Bostick N.H. 1973, Time as a factor in thermal metamorphism of phytoclasts (coaly particles). *Compte Rendue 7th Congres Int. Strat . et Geolo. Carbonif., Krefeld, 1971, 2, 183-193.*

Duddy I.R. 1983, The Geology, Petrology and Geochemistry of the Otway Formation volcanogenic sediments. *PhD. Thesis, University of Melbourne (unpublished).*

Exon N.F. 1976, Geology of the Surat Basin in Queensland. *Bureau of Mineral Resources, Australia, Bulletin, 166.*

Gleadow A.J.W. 1981, Fission track dating methods; what are the real alternatives? *Nuclear Tracks 5*, 3-14.

Gleadow A.J.W. and Duddy I.R. 1981, A natural long-term track annealing experiment for apatite. *Nuclear Tracks 5*, 169-174.

Gleadow A.J.W., Duddy, I.R. and Lovering J.F. 1983, Fission track analysis; a new tool for the evaluation of thermal histories and hydrocarbon potential. *APEA J.* 23, 93-102.

Gleadow A.J.W., Duddy, I.R., Green, P.F.,and Hegarty K.A. 1986, "Fission track lengths in the apatite annealing zone and the interpretation of mixed ages. *Earth and Planetary Science Letters, 78, 245-254.*

Gleadow, A.J.W., Duddy, I.R., Green, P.F. and Lovering, J.F., 1986b. Confined fission track lengths in apatite - a diagnostic tool for thermal history analysis. *Contr. Miner. Petrol.* 94, 405-415.

Gravestock D.I., Moore P.S. and Pitt G.M. (editors), Contributions to the Geology and Hydrocarbon Potential of the Eromanga Basin, *Geol. Soc. Aust. Special Publ. No 12, 384 pp.*

Green P.F. 1981, A new look at statistics in fission track dating. *Nuclear Tracks 5*, 77-86.

Green P.F. 1985, "A comparison of zeta calibration baselines in zircon, sphene and apatite". *Chem. Geol. (Isot. Geol. Sect.)* 58. 1-22.

Green,P.F., Duddy I.R., Gleadow A.J.W., Laslett G.M. and Tingate P.R. 1986, "Thermal annealing of fission tracks in apatite: I - a qualitative description" *Isotope Geoscience.* 59, 237-253.

Green, P.F., Duddy, I.R., Gleadow, A.J.W. and Lovering, J. F., 1988. Apatite fission track analysis as a paleotemperature indicator for hydrocarbon exploration. *In* N.D Naeser, (ed.) *Thermal histories of sedimentary basins.* Springer-Verlag (in press).

Hood a. Gutjahr C.C.M. and Heacock, R.L., 1975, Organic metamorphism and the generation of petroleum *Am. Assoc. Pet. Geol. Bull. 59, 986-996.*

Hurford A.J. and Green P.F. 1982, A user's guide to fission track dating calibration. *Earth Planet. Sci Lett. 59,* 343 -354.

Hurford A.J. and Green P.F. 1983, The zeta age calibration of fission track dating. *Isotope Geoscience 1,* 285-317.

Kanstler A.J., Cook, A.C. and Zwigulis, M. 1982, Maturation patterns in the Eromanga Basin. *in* Moore, P.S. and Mount, T.J. (compliers) *Eromanga Basin Symposium, Summary Papers.* Geol .Soc. Aust. & Pet. Explor.Soc. Aust., Adelaide, 284-295.

Kanstler A.J., Cook, A.C. and Zwigulis, M. 1986, Organic maturation in the Eromanga Basin. *Geological Society of Australia Special Publication No. 12, 305-322.*

Kanstler A.J., Prudence, T.J.C., Cook, A.C. and Zwigulis, M. 1983, Hydrocarbon habitat of the Cooper/Eromanga Basin. *APEA J. 23 (1), 75-92.*

Kanstler A.J., Smith G.C. and Cook, A.C. 1978, Lateral and vertical rank variation: implications for hydrocarbon exploration. *APEA J. 18(1), 143-156.*

Karweil J., 1956, Die metamorphose der Kohlen vom Standpunkt der physikalischen Chemie. *Zeltschrift Deutschen Geologischen Gesellschaft, 107, 132-139.*

Laslett, G.M., Green, P.F., Duddy, I.R. and Gleadow, A.J.W., 1987. Thermal annealing of fission tracks in apatite: II - A quantitative analysis. *Isot. Geosci.* 65, 1-13.

Lopatin N.V. 1971, Temperature and geologic time as factors in coalification. *Akad. Nauk SSSR Izv. Ser. Geol., 3, 95-106.* (Russian). English Translation, N.H. Bostick, Illinois State Geol. Surv. 1972.

Moore P.S. 1986, Jurassic and Triassic stratigraphy and hydrocarbon potential of the Poolowanna Trough (Simpson Desert region) northern South Australia. *in* Gravestock, D.I., Moore, P.S. and Pitt, G.M. (editors), *Contributions to the Geology and Hydrocarbon Potential of the Eromanga Basin,* Geol. Soc. Aust. Special Publ. No 12, 39-51.

Moore P.S. and Pitt G.M. 1982, Cretaceous of the southwestern Eromanga Basin: stratigraphy, facies variations and petroleum potential; *in* Moore, P.S. and Mount , T.J. (compliers) *Eromanga Basin Symposium, Summary Papers.* Geol .Soc. Aust. & Pet. Explor.Soc. Aust., Adelaide, 127-144.

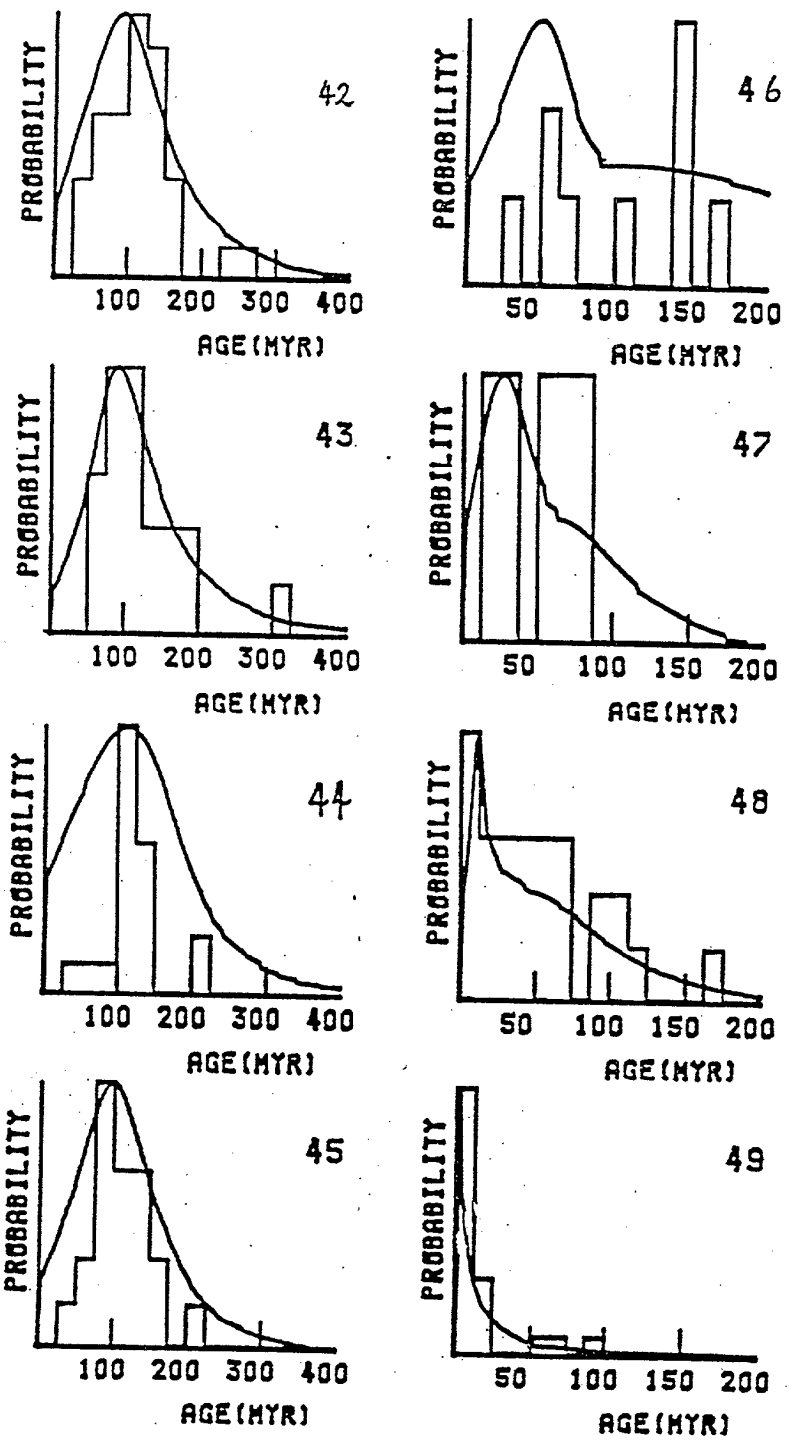

Fig. 9 Single grain age distributions and smoothed probability distributions for samples from Dullingari-1. Sample numbers are prefixed 8622-.

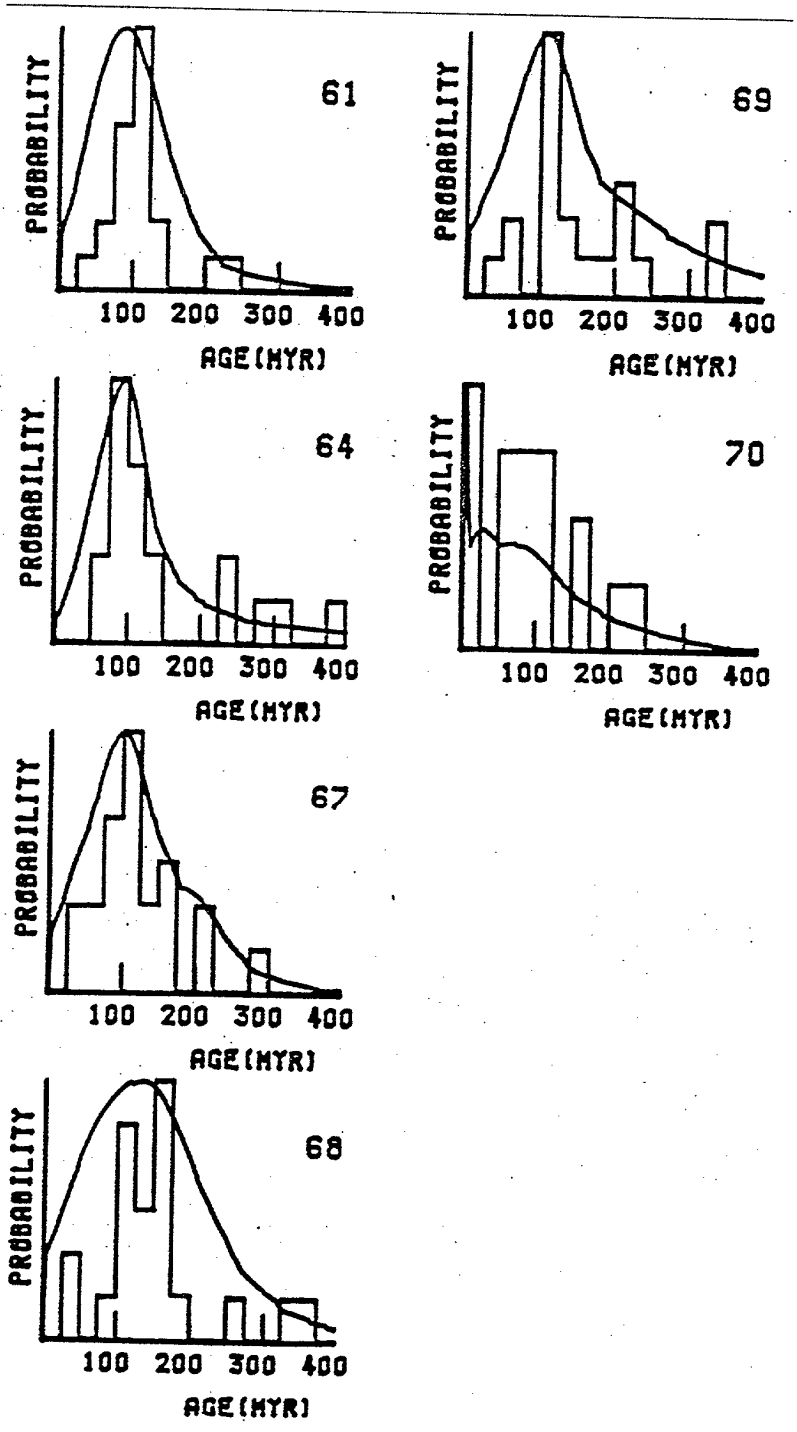

Fig. 10 Single grain age distributions and smoothed probability function for samples from Toolachi-1. Sample numbers are prefixed 8622-.

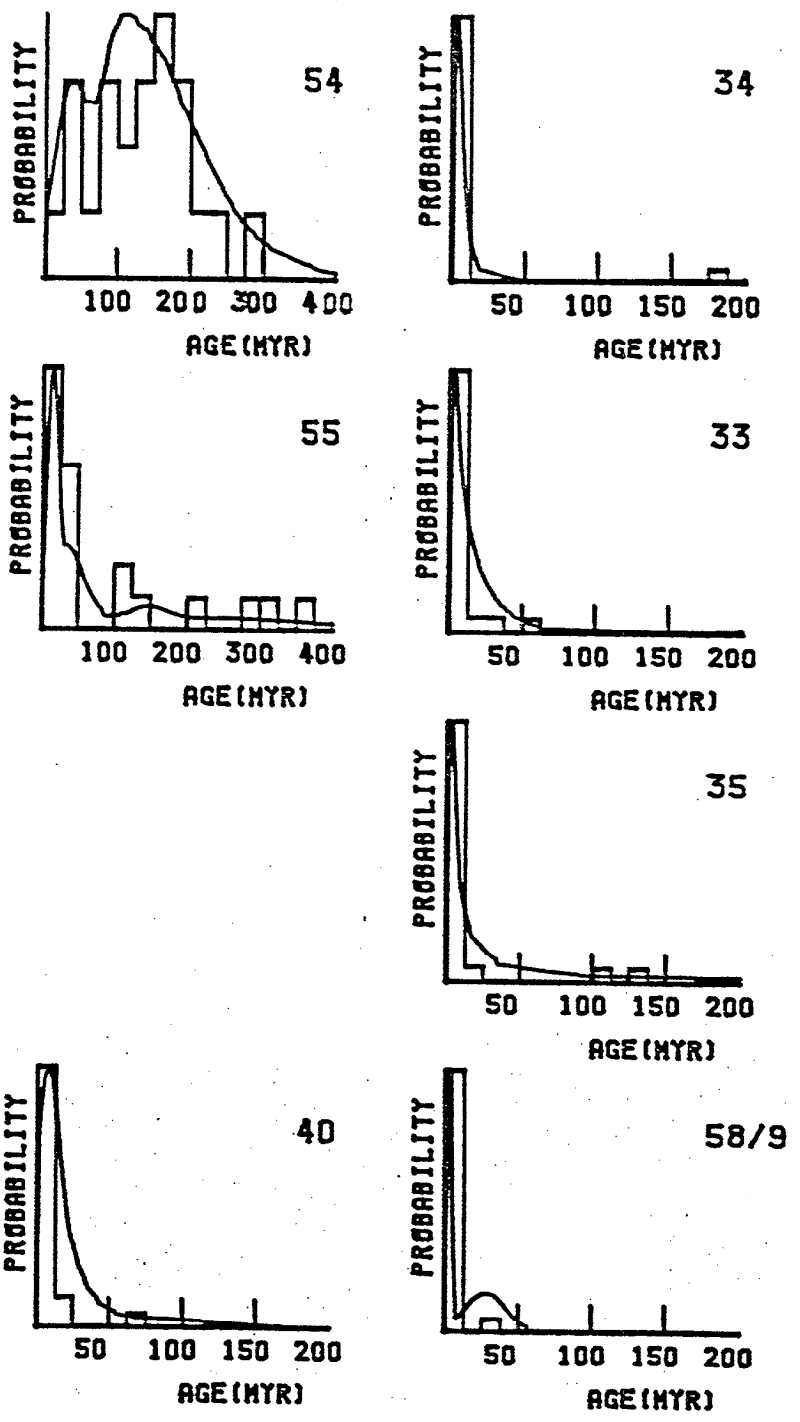

Fig. 11 Single grain age distributions and smoothed probability distributions for samples from Tinga Tingara-1 (54,55), Poolawanna-1 (33-35), Putamurdie-1 (40) and Merrimelia-1 (58/9). Sample numbers are prefixed 8622-.

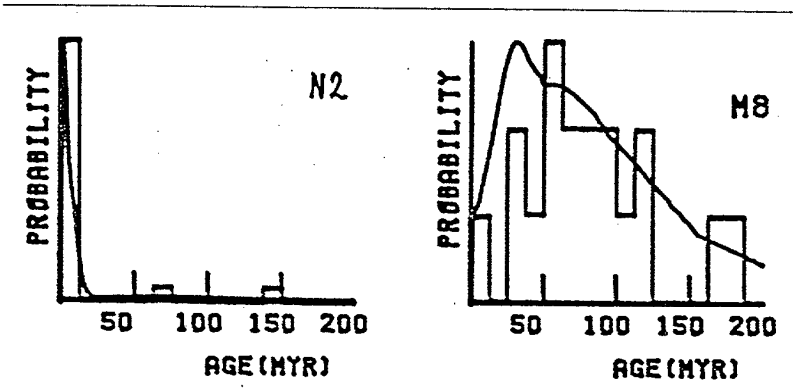

Fig. 12 Single grain age distributions and smoothed probability function for samples from Namur-2 (N2) and Merrimelia-8 (M8). Sample numbers are prefixed by 8622-.

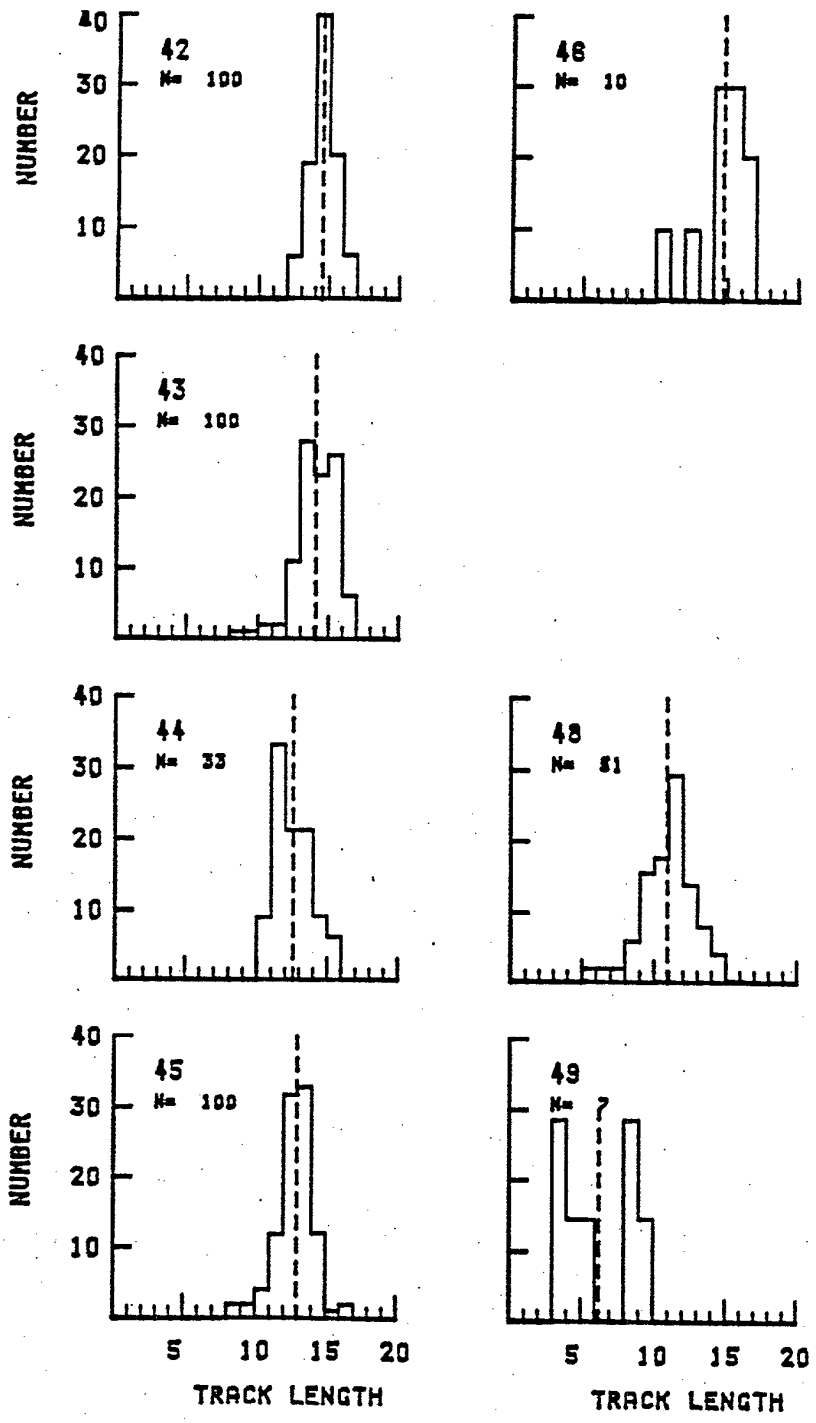

Fig. 13 Confined fission track length distributions for samples from Dullingari-1. Sample numbers are prefixed 8622-.

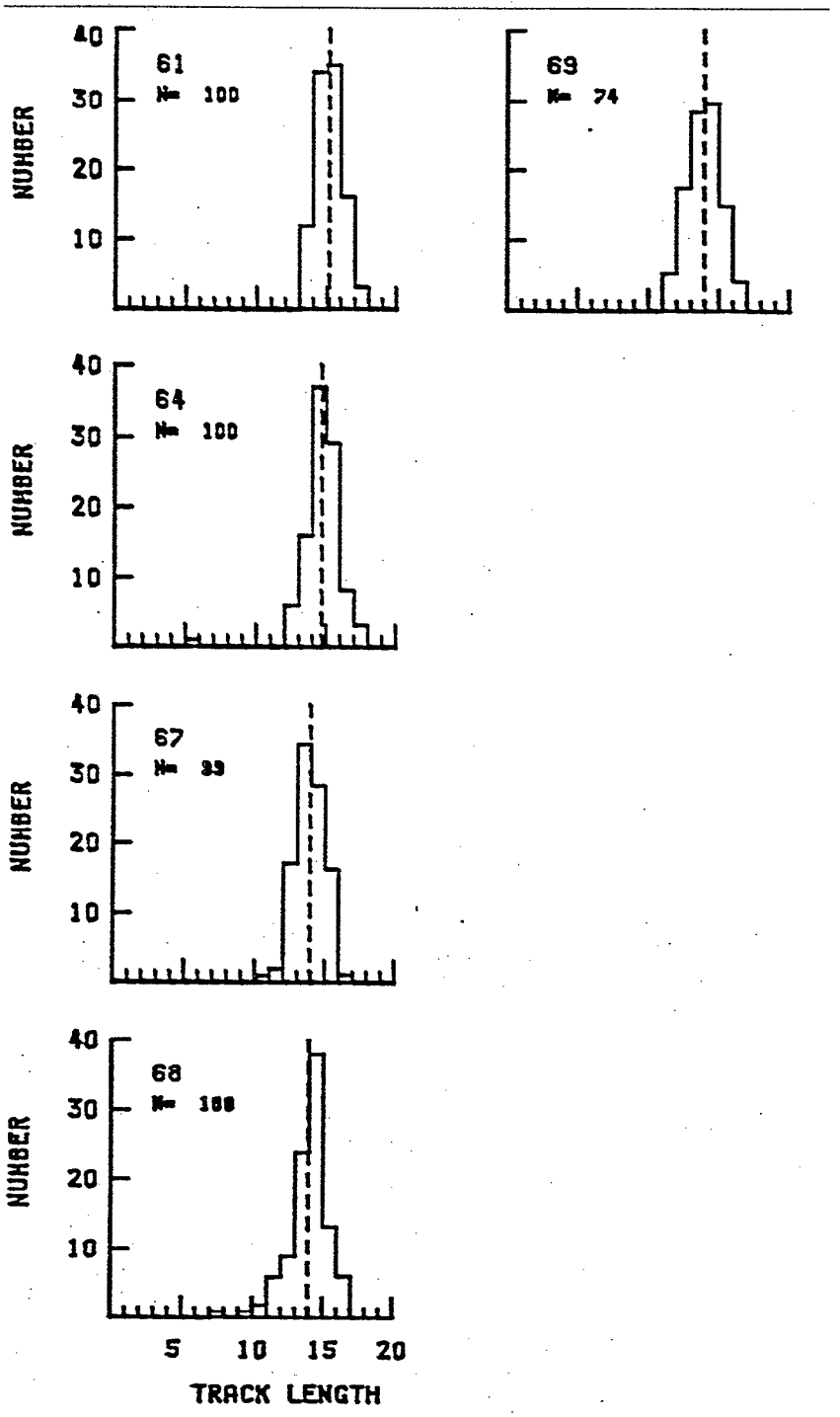

Fig. 14 Confined fission track length distributions for samples from Toolachi-1. Sample numbers are prefixed 8622-.

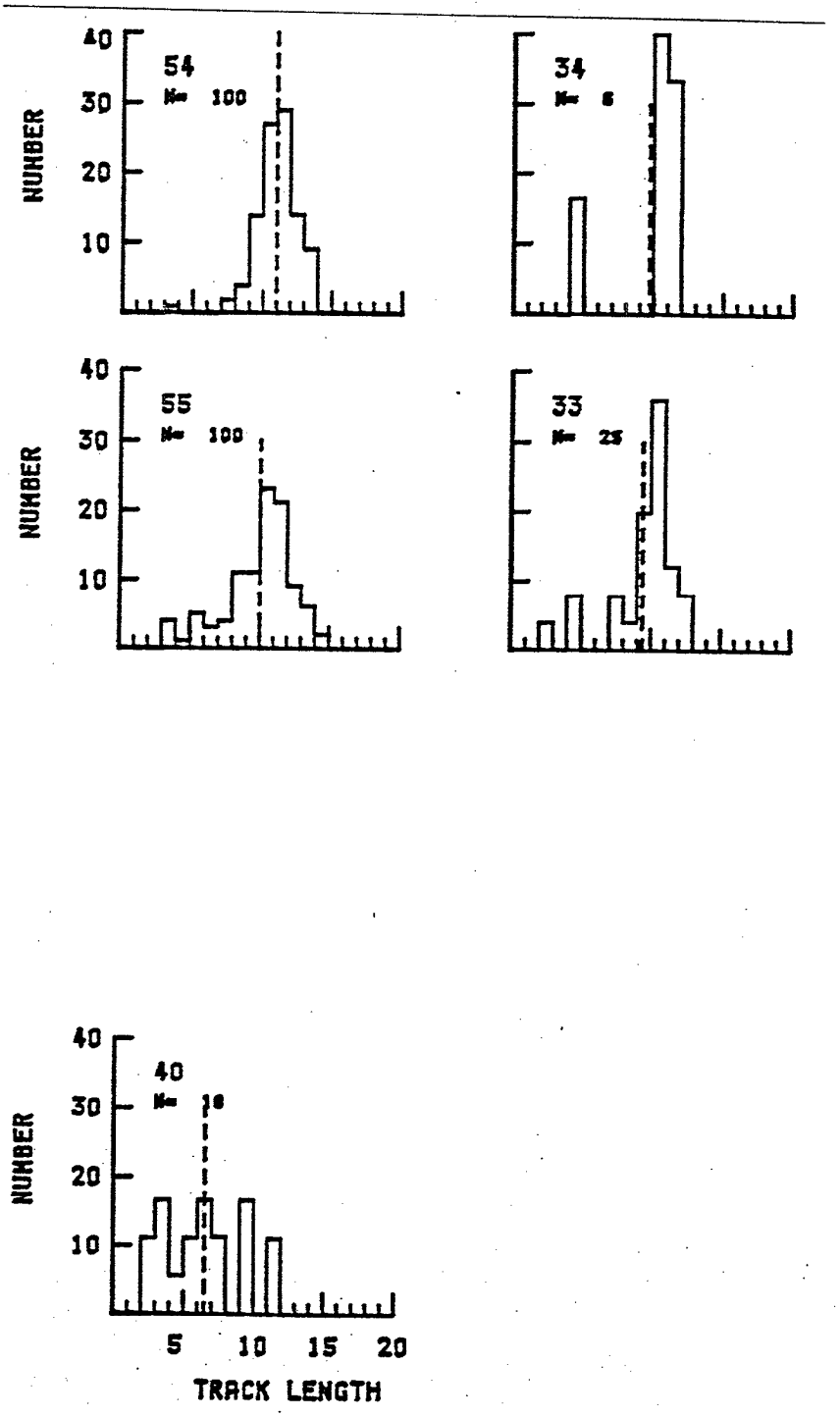

Fig. 15 Confined fission track length distributions for samples from Tinga Tingana-1 (54, 55), Poolowanna-1 (33, 34), and Putamurdie-1 (40). Numbers are prefixed 8622-.

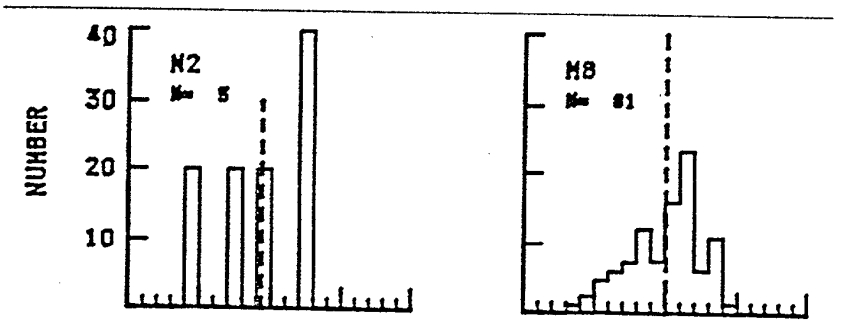

Fig. 16 Confined fission track length distributions for samples from Namur-2 (N2) and Merrimelia-8 (M8). Sample numbers are prefixed 8622-.

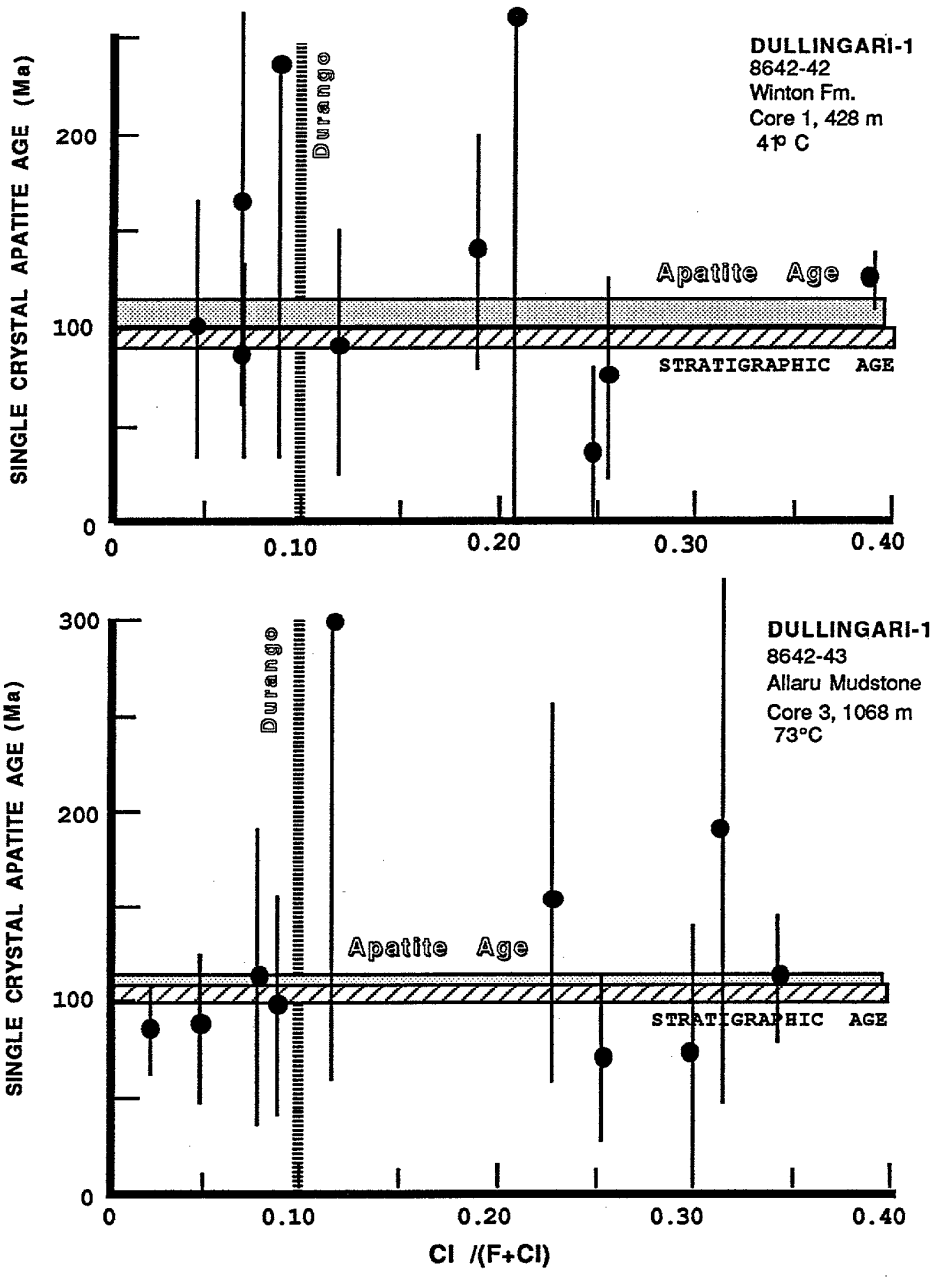

Fig. 17 Variation in the apparent fission track age of individual apatite grains with chemical composition of the same crystals.

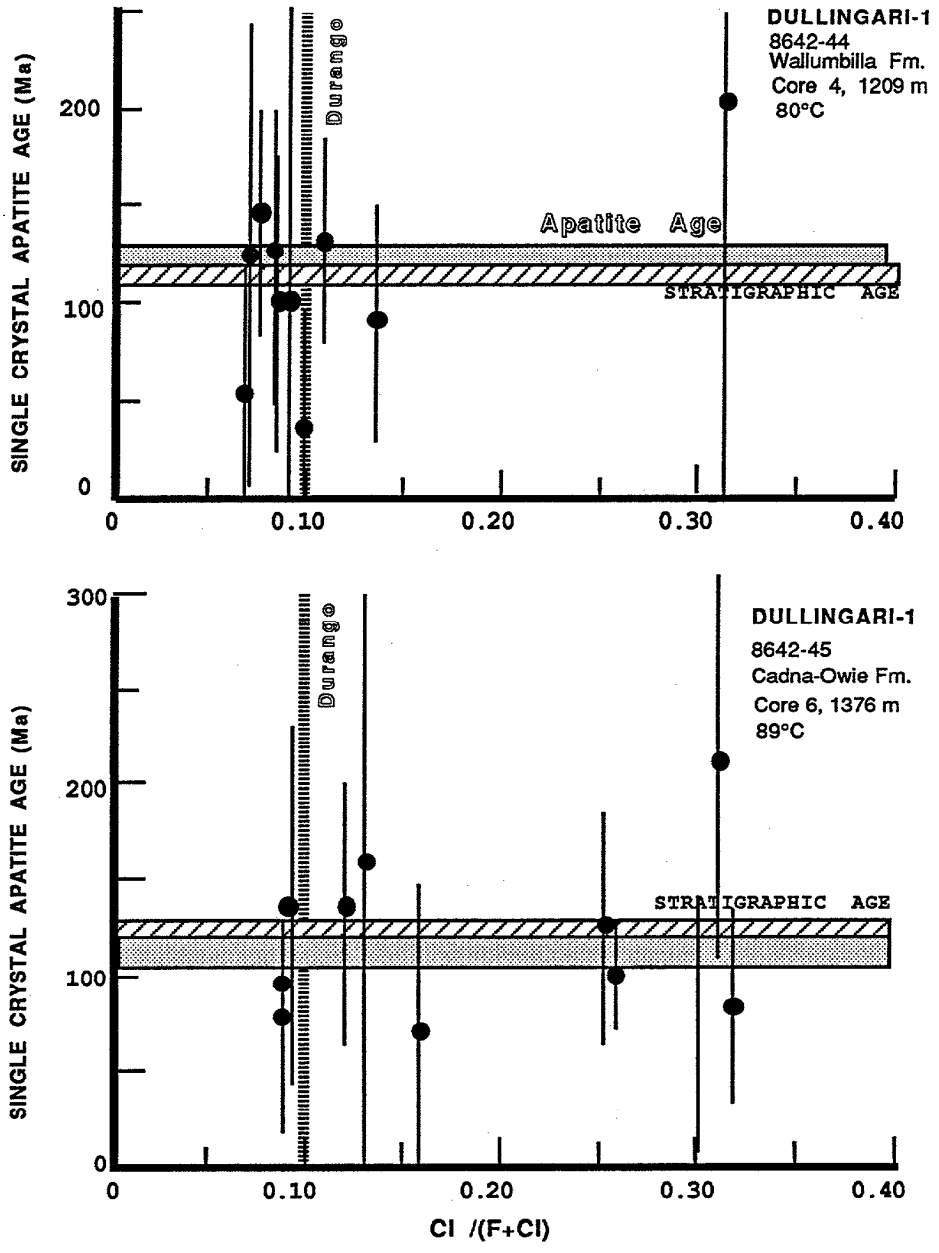

Fig. 17 Variaton in the apparent fission track age of individual apatite grains with chemical composition of the same crystals.

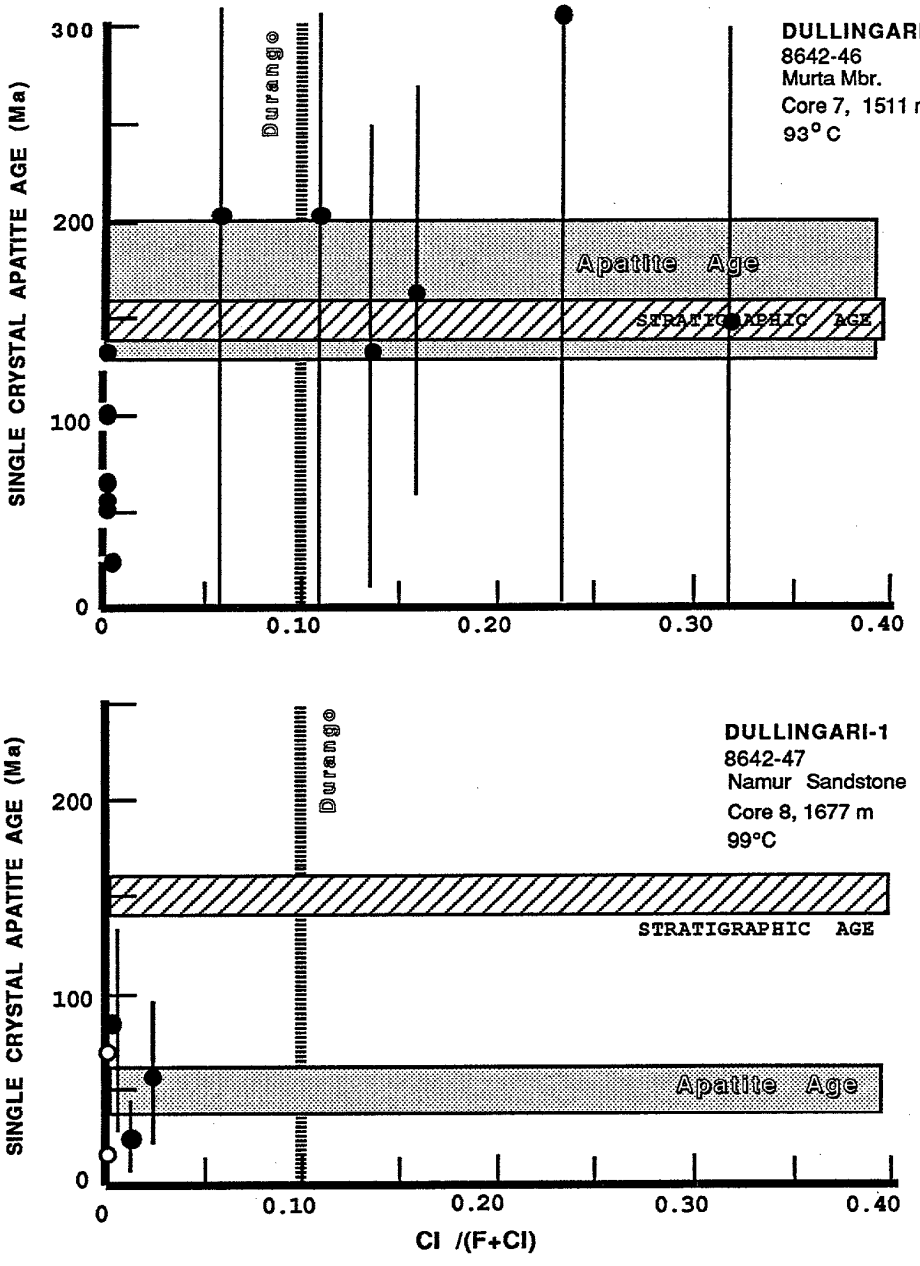

Fig . 17 Variation in the apparent fission track age of individual apatite grains with chemical composition of the same crystals.

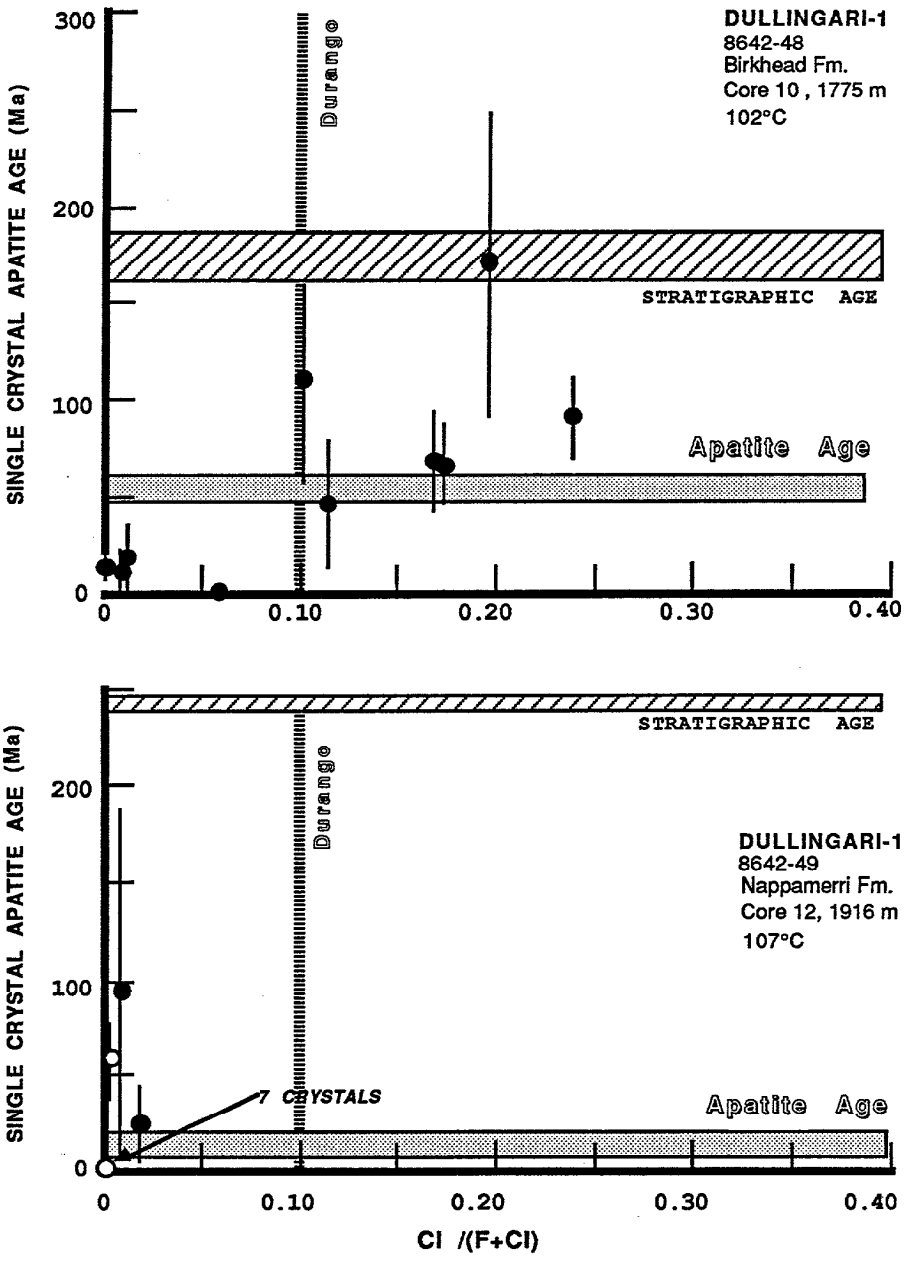

Fig. 17 Variation in the apparent fission track age of individual apatite grains with chemical composition of the same crystals.

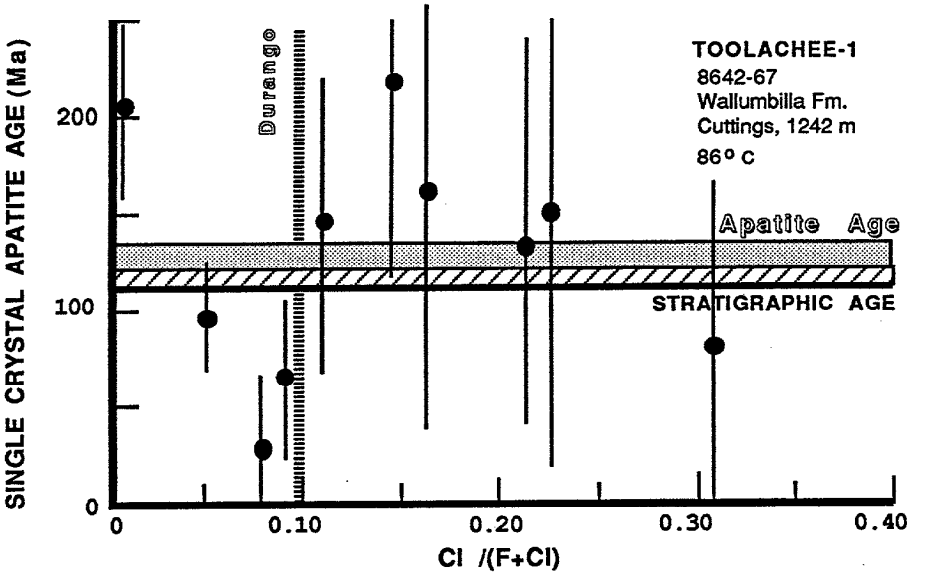
SINGLE CRYSTAL APATITE AGE (Ma)
200
100
0
Durango
TOOLACHEE-1
8642-67
Wallumbilla Fm.
Cuttings, 1242 m
86° C
Apatite Age
STRATIGRAPHIC AGE
0
0.10
0.20
0.30
0.40
Cl /(F+Cl)

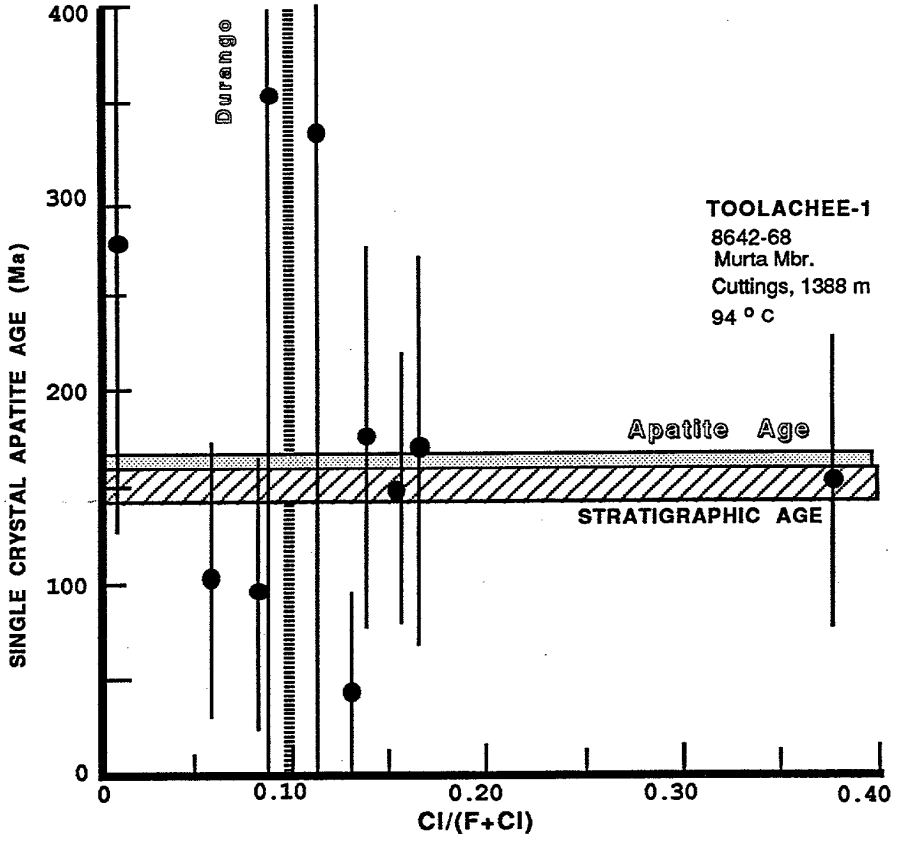
SINGLE CRYSTAL APATITE AGE (Ma)
400
300
200
100
0
Durango
TOOLACHEE-1
8642-68
Murta Mbr.
Cuttings, 1388 m
94 ° C
Apatite Age
STRATIGRAPHIC AGE
0
0.10
0.20
0.30
0.40
Cl/(F+Cl)

Fig. 17 Variation in the apparent fission track age of individual apatite grains with chemical composition of the same crystals.

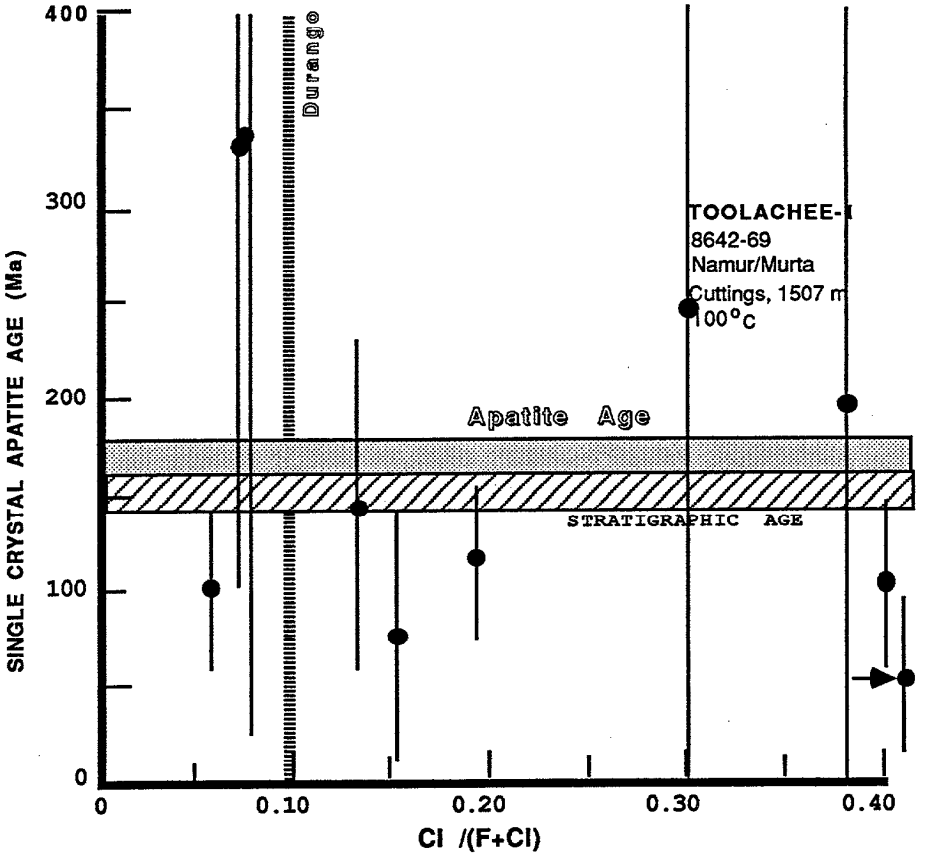

Fig. 17 Variation in the apparent fission track age of individual apatite grains with chemical composition of the same crystals.

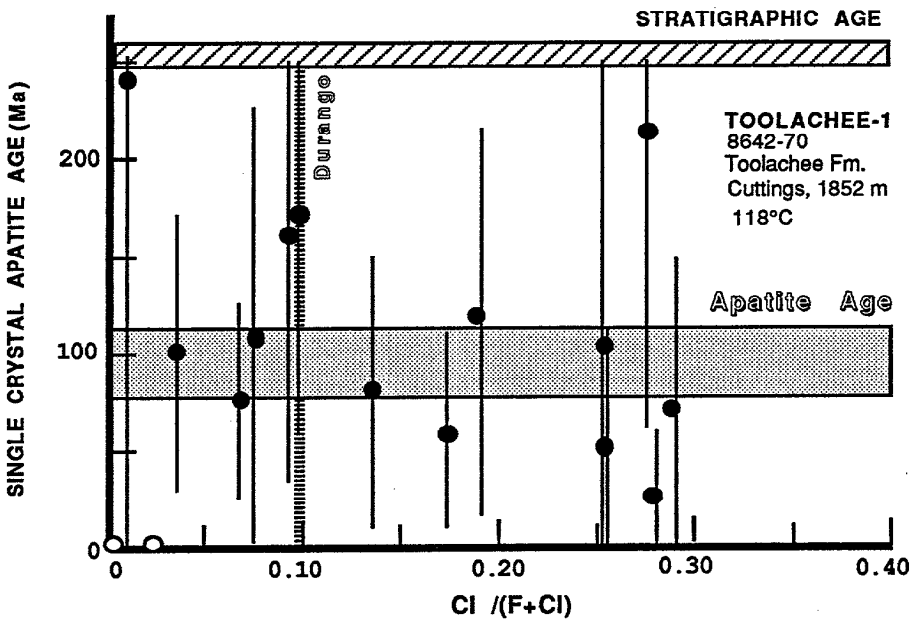

Fig. 17 Variation in the apparent fission track age of individual apatite grains with chemical composition of the same crystals.

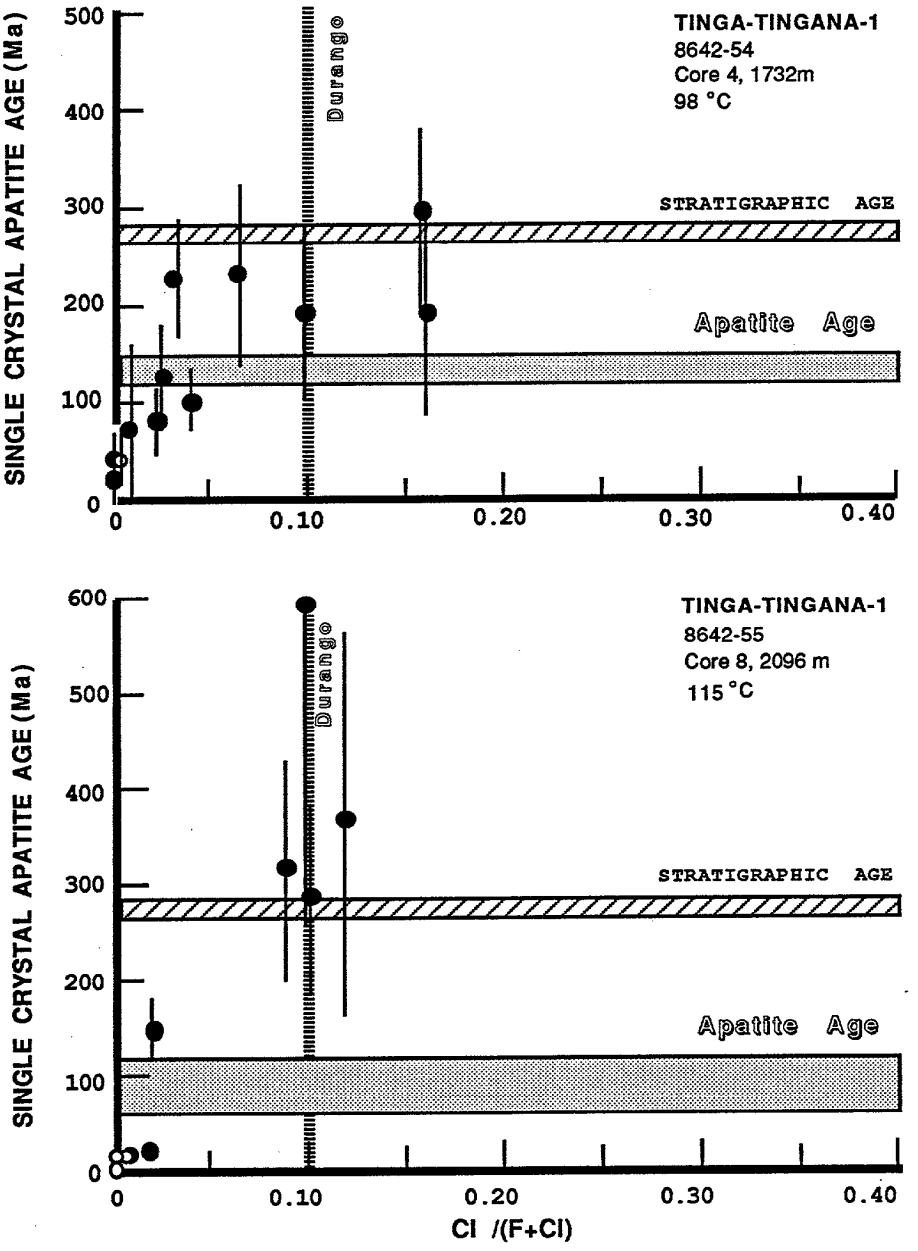

Fig. 17 Variation in the apparent fission track age of individual apatite grains with chemical composition of the same crystals.

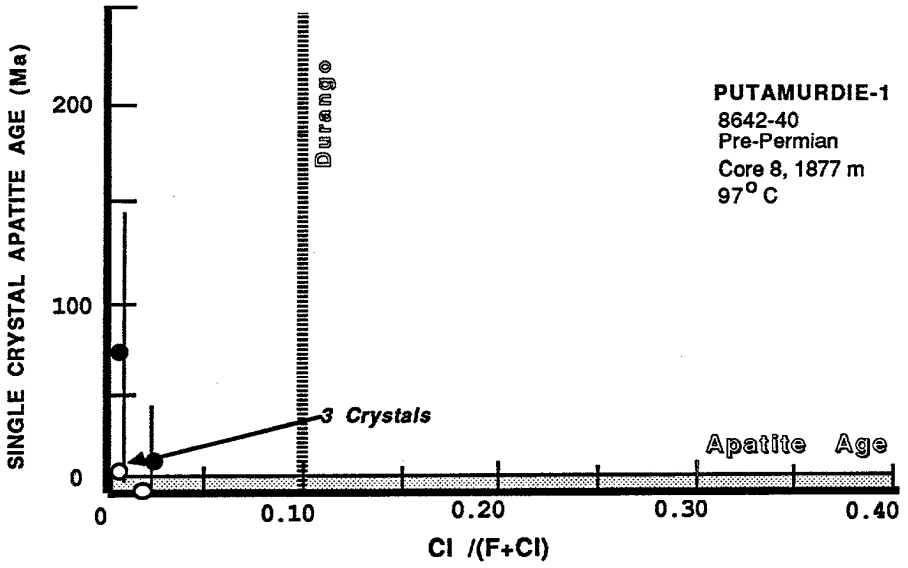

Fig. 17 Variation in the apparent fission track age of individual apatite grains with chemical composition of the same crystals.

APPENDIX

Apatite fission track counting and statistical data Cooper-Eromanga Basin

8642-42 APATITE Dullingari-1,425m
IRRADIATION PT776 SLIDE NUMBER 4
COUNTED BY: IRD

No.	Ns	Ni	Na	RATIO	U(ppm)	RHOs	RHOi	F.T.AGE(Ma)
1	25	50	36	0.500	17.9	8.051E+05	1.610E+06	103.7± 25.5
2	3	17	25	0.176	8.8	1.391E+05	7.883E+05	36.8± 23.0
3	7	22	34	0.318	8.3	2.387E+05	7.501E+05	66.2± 28.7
4	4	14	36	0.286	5.0	1.288E+05	4.508E+05	59.4± 33.7
5	1	5	50	0.200	1.3	2.319E+04	1.159E+05	41.7± 45.6
6	14	21	40	0.667	6.8	4.058E+05	6.086E+05	137.8± 47.6
7	4	3	40	1.333	1.0	1.159E+05	8.695E+04	272.8±208.4
8	6	9	22	0.667	5.3	3.162E+05	4.743E+05	137.8± 72.7
9	14	12	30	1.167	5.2	5.410E+05	4.637E+05	239.3± 94.2
10	4	12	36	0.333	4.3	1.288E+05	3.864E+05	69.3± 40.0
11	7	21	36	0.333	7.5	2.254E+05	6.762E+05	69.3± 30.3
12	7	9	28	0.778	4.1	2.898E+05	3.726E+05	160.5± 80.9
13	5	13	30	0.385	5.6	1.932E+05	5.024E+05	79.9± 42.1
14	10	28	56	0.357	6.4	2.070E+05	5.796E+05	74.2± 27.4
15	7	10	22	0.700	5.9	3.689E+05	5.269E+05	144.7± 71.3
16	4	8	30	0.500	3.4	1.546E+05	3.091E+05	103.7± 63.5
17	20	25	36	0.800	9.0	6.440E+05	8.051E+05	165.1± 49.6
18	5	9	36	0.556	3.2	1.610E+05	2.898E+05	115.1± 64.2
19	6	9	32	0.667	3.6	2.174E+05	3.260E+05	137.8± 72.7
20	14	23	60	0.609	4.9	2.705E+05	4.444E+05	126.0± 42.8
21	17	30	40	0.567	9.7	4.927E+05	8.695E+05	117.4± 35.7
22	41	59	41	0.695	18.6	1.159E+06	1.668E+06	143.6± 29.3
23	19	43	56	0.442	9.9	3.933E+05	8.902E+05	91.7± 25.3
24	3	16	36	0.188	5.7	9.661E+04	5.152E+05	39.1± 24.6
25	19	32	40	0.594	10.3	5.507E+05	9.274E+05	122.9± 35.7
26	5	9	36	0.556	3.2	1.610E+05	2.898E+05	115.1± 64.2
27	13	29	44	0.448	8.5	3.425E+05	7.641E+05	93.0± 31.1
28	55	113	36	0.487	40.5	1.771E+06	3.639E+06	100.9± 16.7
29	16	32	57	0.500	7.2	3.254E+05	6.508E+05	103.7± 31.8
30	22	53	55	0.415	12.4	4.637E+05	1.117E+06	86.2± 21.9
31	6	8	21	0.750	4.9	3.312E+05	4.416E+05	154.9± 83.7
32	11	25	80	0.440	4.0	1.594E+05	3.623E+05	91.3± 33.1
33	11	16	36	0.688	5.7	3.542E+05	5.152E+05	142.1± 55.7
	405	785			7.8	3.631E+05	7.038E+05	

Area of basic unit = 9.026E-07 cm-2
CHI SQUARED = 28.00324 WITH 32 DEGREES OF FREEDOM
P(chi squared) = 66.9 %
CORRELATION COEFFICIENT = 0.941
VARIANCE OF SQR(Ns) = 1.904875
VARIANCE OF SQR(Ni) = 3.359253
Ns/Ni = 0.516 ± 0.032
MEAN RATIO = 0.548 ± 0.043

POOLED AGE = 106.9 ± 6.8 Ma
MEAN AGE = 113.6 ± 9.2 Ma

Ages calculated using a zeta of 355 ± 4 for SRM612 glass
RHO D = 1.177E+06cm-2; ND = 6094

8642-43 APATITE Dullingari-1, 1068.3m

IRRADIATION PT776 SLIDE NUMBER 5
COUNTED BY: IRD

No.	Ns	Ni	Na	RATIO	U(ppm)	RHOs	RHOi	F.T.AGE(Ma)
1	8	23	45	0.348	6.6	2.061E+05	5.925E+05	72.3± 29.7
2	7	9	16	0.778	7.3	5.072E+05	6.521E+05	160.5± 80.9
3	12	8	28	1.500	3.7	4.968E+05	3.312E+05	306.1±139.8
4	10	29	28	0.345	13.4	4.140E+05	1.201E+06	71.7± 26.3
5	12	19	49	0.632	5.0	2.839E+05	4.495E+05	130.7± 48.2
6	18	30	36	0.600	10.7	5.796E+05	9.661E+05	124.2± 37.1
7	6	7	36	0.857	2.5	1.932E+05	2.254E+05	176.7± 98.4
8	13	28	60	0.464	6.0	2.512E+05	5.410E+05	96.3± 32.4
9	12	13	50	0.923	3.4	2.782E+05	3.014E+05	190.1± 76.2
10	56	138	70	0.406	25.4	9.274E+05	2.285E+06	84.3± 13.4
11	25	60	36	0.417	21.5	8.051E+05	1.932E+06	86.5± 20.6
12	20	26	36	0.769	9.3	6.440E+05	8.373E+05	158.8± 47.3
13	13	29	40	0.448	9.4	3.768E+05	8.405E+05	93.0± 31.1
14	8	19	24	0.421	10.2	3.864E+05	9.178E+05	87.4± 36.9
15	6	11	36	0.545	3.9	1.932E+05	3.542E+05	113.0± 57.4
16	18	29	40	0.621	9.4	5.217E+05	8.405E+05	128.4± 38.6
17	6	17	20	0.353	11.0	3.478E+05	9.854E+05	73.3± 34.8
18	64	116	29	0.552	51.6	2.558E+06	4.637E+06	114.3± 17.9
19	6	10	36	0.600	3.6	1.932E+05	3.220E+05	124.2± 64.2
20	7	13	40	0.538	4.2	2.029E+05	3.768E+05	111.6± 52.3
	327	634			10.8	5.021E+05	9.735E+05	

Area of basic unit = 9.026E-07 cm-2

CHI SQUARED = 19.1938 WITH 19 DEGREES OF FREEDOM
P(chi squared) = 44.4 %
CORRELATION COEFFICIENT = 0.961
VARIANCE OF SQR(Ns) = 2.42655
VARIANCE OF SQR(Ni) = 5.942325

Ns/Ni = 0.516 ± 0.035
MEAN RATIO = 0.606 ± 0.060

POOLED AGE = 106.9 ± 7.5 Ma
MEAN AGE = 125.4 ± 12.7 Ma

Ages calculated using a zeta of 355 ± 4 for SRM612 glass
RHO D = 1.177E+06cm-2; ND = 6094

8642-44 APATITE Dullingari-1, 1214.1m

IRRADIATION PT776 SLIDE NUMBER 6
COUNTED BY: IRD

No.	Ns	Ni	Na	RATIO	U(ppm)	RHOs	RHOi	F.T.AGE(Ma)
1	23	38	33	0.605	14.9	8.080E+05	1.335E+06	125.3± 33.2
2	2	4	6	0.500	8.6	3.864E+05	7.729E+05	103.7± 89.8
3	2	11	8	0.182	17.7	2.898E+05	1.594E+06	37.9± 29.1
4	4	8	9	0.500	11.5	5.152E+05	1.030E+06	103.7± 63.5
5	4	6	16	0.667	4.8	2.898E+05	4.347E+05	137.8± 89.0
6	1	1	12	1.000	1.1	9.661E+04	9.661E+04	205.7±290.9
7	4	8	16	0.500	6.4	2.898E+05	5.796E+05	103.7± 63.5
8	3	11	21	0.273	6.8	1.656E+05	6.072E+05	56.7± 37.0
9	4	7	28	0.571	3.2	1.656E+05	2.898E+05	118.3± 74.2
10	2	2	10	1.000	2.6	2.319E+05	2.319E+05	205.7±205.7
11	10	20	15	0.500	17.2	7.729E+05	1.546E+06	103.7± 40.2
12	37	52	9	0.712	74.5	4.766E+06	6.698E+06	147.0± 31.7
13	5	10	12	0.500	10.7	4.830E+05	9.661E+05	103.7± 56.8
14	4	8	24	0.500	4.3	1.932E+05	3.864E+05	103.7± 63.5
15	42	65	50	0.646	16.8	9.738E+05	1.507E+06	133.6± 26.6
16	6	10	20	0.600	6.4	3.478E+05	5.796E+05	124.2± 64.2
17	12	28	9	0.429	40.1	1.546E+06	3.607E+06	89.0± 30.7
18	4	7	12	0.571	7.5	3.864E+05	6.762E+05	118.3± 74.2
19	5	7	16	0.714	5.6	3.623E+05	5.072E+05	147.6± 86.5
	174	303			12.0	6.188E+05	1.077E+06	

Area of basic unit = 9.026E-07 cm-2

CHI SQUARED = 7.026189 WITH 18 DEGREES OF FREEDOM
P(chi squared) = 99.0 %
CORRELATION COEFFICIENT = 0.983
VARIANCE OF SQR(Ns) = 2.391178
VARIANCE OF SQR(Ni) = 3.532487

Ns/Ni = 0.574 ± 0.055
MEAN RATIO = 0.577 ± 0.046

POOLED AGE = 118.9 ± 11.5 Ma
MEAN AGE = 119.6 ± 9.7 Ma

Ages calculated using a zeta of 355 ± 4 for SRM612 glass
RHO D = 1.177E+06cm-2; ND = 6094

8642-45 APATITE Dullingari-1, 1376m

IRRADIATION PT776 SLIDE NUMBER 7
COUNTED BY: IRD

No.	Ns	Ni	Na	RATIO	U(ppm)	RHOs	RHOi	F.T.AGE(Ma)
1	24	37	60	0.649	8.0	4.637E+05	7.149E+05	134.2± 35.2
2	10	21	40	0.476	6.8	2.898E+05	6.086E+05	98.8± 38.0
3	2	8	40	0.250	2.6	5.796E+04	2.319E+05	52.0± 41.1
4	4	7	62	0.571	1.5	7.479E+04	1.309E+05	118.3± 74.2
5	1	6	40	0.167	1.9	2.898E+04	1.739E+05	34.7± 37.5
6	36	35	88	1.029	5.1	4.743E+05	4.611E+05	211.5± 50.3
7	7	9	39	0.778	3.0	2.081E+05	2.675E+05	160.5± 80.9
8	11	15	16	0.733	12.1	7.970E+05	1.087E+06	151.5± 60.2
9	25	41	64	0.610	8.3	4.528E+05	7.427E+05	126.2± 32.1
10	4	12	20	0.333	7.7	2.319E+05	6.956E+05	69.3± 40.0
11	7	18	38	0.389	6.1	2.136E+05	5.491E+05	80.8± 36.0
12	13	20	50	0.650	5.2	3.014E+05	4.637E+05	134.4± 47.9
13	4	8	35	0.500	2.9	1.325E+05	2.650E+05	103.7± 63.5
14	4	11	39	0.364	3.6	1.189E+05	3.270E+05	75.6± 44.1
15	17	28	36	0.607	10.0	5.474E+05	9.017E+05	125.7± 38.7
16	10	25	36	0.400	9.0	3.220E+05	8.051E+05	83.1± 31.1
17	7	14	40	0.500	4.5	2.029E+05	4.058E+05	103.7± 48.0
18	54	112	23	0.482	62.8	2.722E+06	5.645E+06	100.0± 16.7
19	22	40	60	0.550	8.6	4.251E+05	7.729E+05	113.9± 30.3
20	17	42	36	0.405	15.0	5.474E+05	1.352E+06	84.0± 24.2
	279	509			7.6	3.752E+05	6.845E+05	

Area of basic unit = 9.026E-07 cm-2

CHI SQUARED = 16.12288 WITH 19 DEGREES OF FREEDOM
P(chi squared) = 64.9 %
CORRELATION COEFFICIENT = 0.930
VARIANCE OF SQR(Ns) = 2.593589
VARIANCE OF SQR(Ni) = 3.770472

Ns/Ni = 0.548 ± 0.041
MEAN RATIO = 0.522 ± 0.044

POOLED AGE = 113.6 ± 8.7 Ma
MEAN AGE = 108.2 ± 9.3 Ma

Ages calculated using a zeta of 355 ± 4 for SRM612 glass
RHO D = 1.177E+06cm-2; ND = 6094

8642-46 APATITE Dullingari-1, 1511m

IRRADIATION PT776 SLIDE NUMBER 8
COUNTED BY: IRD

No.	Ns	Ni	Na	RATIO	U(ppm)	RHOs	RHOi	F.T.AGE(Ma)
1	29	111	32	0.261	44.7	1.051E+06	4.021E+06	54.4± 11.4
2	16	20	30	0.800	8.6	6.183E+05	7.729E+05	165.1± 55.4
3	5	5	20	1.000	3.2	2.898E+05	2.898E+05	205.7±130.1
4	6	40	6	0.150	86.0	1.159E+06	7.729E+06	31.3± 13.7
5	3	2	15	1.500	1.7	2.319E+05	1.546E+05	306.1±279.5
6	4	6	19	0.667	4.1	2.441E+05	3.661E+05	137.8± 89.0
7	1	3	9	0.333	4.3	1.288E+05	3.864E+05	69.3± 80.0
8	5	7	19	0.714	4.8	3.051E+05	4.271E+05	147.6± 86.5
9	8	12	20	0.667	7.7	4.637E+05	6.956E+05	137.8± 63.0
10	5	2	10	2.500	2.6	5.796E+05	2.319E+05	502.4±420.4
11	1	2	15	0.500	1.7	7.729E+04	1.546E+05	103.7±127.0
12	2	8	16	0.250	6.4	1.449E+05	5.796E+05	52.0± 41.1
13	2	2	12	1.000	2.1	1.932E+05	1.932E+05	205.7±205.7
	87	220			12.7	4.523E+05	1.144E+06	

Area of basic unit = 9.026E-07 cm-2

CHI SQUARED = 29.4675 WITH 12 DEGREES OF FREEDOM
P(chi squared) = 0.3 %
CORRELATION COEFFICIENT = 0.898
VARIANCE OF SQR(Ns) = 1.506985
VARIANCE OF SQR(Ni) = 6.839063

Ns/Ni = 0.395 ± 0.050
MEAN RATIO = 0.796 ± 0.176

POOLED AGE = 82.1 ± 10.5 Ma
MEAN AGE = 164.2 ± 36.4 Ma

Ages calculated using a zeta of 355 ± 4 for SRM612 glass
RHO D = 1.177E+06cm-2; ND = 6094

8642-47 APATITE Dullingari-1, 1677m

IRRADIATION PT776 SLIDE NUMBER 9
COUNTED BY: IRD

No.	Ns	Ni	Na	RATIO	U(ppm)	RHOs	RHOi	F.T.AGE(Ma)
1	4	12	58	0.333	2.7	7.995E+04	2.399E+05	69.3± 40.0
2	7	58	90	0.121	8.3	9.017E+04	7.471E+05	25.2± 10.1
3	10	37	100	0.270	4.8	1.159E+05	4.289E+05	56.2± 20.1
4	12	29	100	0.414	3.7	1.391E+05	3.362E+05	85.9± 29.5
5	2	21	36	0.095	7.5	6.440E+04	6.762E+05	19.9± 14.7
	35	157			5.3	1.057E+05	4.740E+05	

Area of basic unit = 9.026E-07 cm-2

CHI SQUARED = 7.965881 WITH 4 DEGREES OF FREEDOM
P(chi squared) = 9.3 %
CORRELATION COEFFICIENT = 0.398
VARIANCE OF SQR(Ns) = .7028341
VARIANCE OF SQR(Ni) = 2.447128

Ns/Ni = 0.223 ± 0.042
MEAN RATIO = 0.247 ± 0.061

POOLED AGE = 46.4 ± 8.7 Ma
MEAN AGE = 51.3 ± 12.8 Ma

Ages calculated using a zeta of 355 ± 4 for SRM612 glass
RHO D = 1.177E+06cm-2; ND = 6094

8642-48 APATITE Dullingari-1, 1775m

IRRADIATION PT776 SLIDE NUMBER 10
COUNTED BY: IRD

No.	Ns	Ni	Na	RATIO	U(ppm)	RHOs	RHOi	F.T.AGE(Ma)
1	2	7	32	0.286	2.8	7.246E+04	2.536E+05	59.4± 47.7
2	26	31	50	0.839	8.0	6.028E+05	7.188E+05	172.9± 46.1
3	3	15	36	0.200	5.4	9.661E+04	4.830E+05	41.7± 26.4
4	4	80	36	0.050	28.7	1.288E+05	2.576E+06	10.4± 5.4
5	8	45	60	0.178	9.7	1.546E+05	8.695E+05	37.0± 14.2
6	10	44	100	0.227	5.7	1.159E+05	5.101E+05	47.3± 16.6
7	7	48	64	0.146	9.7	1.268E+05	8.695E+05	30.4± 12.3
8	6	18	80	0.333	2.9	8.695E+04	2.608E+05	69.3± 32.7
9	36	82	100	0.439	10.6	4.173E+05	9.506E+05	91.1± 18.3
10	9	18	80	0.500	2.9	1.304E+05	2.608E+05	103.7± 42.4
11	4	17	80	0.235	2.7	5.796E+04	2.463E+05	49.0± 27.2
12	7	29	36	0.241	10.4	2.254E+05	9.339E+05	50.2± 21.2
13	15	48	100	0.312	6.2	1.739E+05	5.565E+05	65.0± 19.3
14	4	85	91	0.047	12.0	5.096E+04	1.083E+06	9.8± 5.0
15	35	640	80	0.055	103.2	5.072E+05	9.274E+06	11.4± 2.0
16	6	36	100	0.167	4.6	6.956E+04	4.173E+05	34.7± 15.3
17	15	32	48	0.469	8.6	3.623E+05	7.729E+05	97.2± 30.5
18	36	109	100	0.330	14.1	4.173E+05	1.264E+06	68.7± 13.2
19	1	20	100	0.050	2.6	1.159E+04	2.319E+05	10.4± 10.7
20	5	17	100	0.294	2.2	5.796E+04	1.971E+05	61.2± 31.1
21	4	50	36	0.080	17.9	1.288E+05	1.610E+06	16.7± 8.7
22	0	17	64	0.000	3.4	0.000E+00	3.079E+05	0.0± 0.0
23	22	37	99	0.595	4.8	2.576E+05	4.333E+05	123.1± 33.2
24	26	48	100	0.542	6.2	3.014E+05	5.565E+05	112.2± 27.4
25	3	39	100	0.077	5.0	3.478E+04	4.521E+05	16.1± 9.6
26	2	20	100	0.100	2.6	2.319E+04	2.319E+05	20.9± 15.5
	296	1632			10.7	1.740E+05	9.594E+05	

Area of basic unit = 9.026E-07 cm-2

CHI SQUARED = 219.0748 WITH 25 DEGREES OF FREEDOM
P(chi squared) = 100.0 %
CORRELATION COEFFICIENT = 0.519
VARIANCE OF SQR(Ns) = 2.656692
VARIANCE OF SQR(Ni) = 17.94358

Ns/Ni = 0.181 ± 0.011
MEAN RATIO = 0.261 ± 0.040

POOLED AGE = 37.8 ± 2.5 Ma
MEAN AGE = 54.4 ± 8.4 Ma

Ages calculated using a zeta of 355 ± 4 for SRM612 glass
RHO D = 1.177E+06cm-2; ND = 6094

8642-49 APATITE Dullingari-1, 1916m

IRRADIATION PT776 SLIDE NUMBER 11
COUNTED BY: IRD

No.	Ns	Ni	Na	RATIO	U(ppm)	RHOs	RHOi	F.T.AGE(Ma)
1	2	129	38	0.016	43.8	6.102E+04	3.935E+06	3.2± 2.3
2	6	55	58	0.109	12.2	1.199E+05	1.099E+06	22.8± 9.8
3	8	17	36	0.471	6.1	2.576E+05	5.474E+05	97.6± 41.9
4	1	19	26	0.053	9.4	4.459E+04	8.472E+05	11.0± 11.3
5	2	25	36	0.080	9.0	6.440E+04	8.051E+05	16.7± 12.3
6	1	50	24	0.020	26.9	4.830E+04	2.415E+06	4.2± 4.2
7	23	82	60	0.280	17.6	4.444E+05	1.584E+06	58.4± 13.8
8	2	140	35	0.014	51.6	6.624E+04	4.637E+06	3.0± 2.1
9	2	56	50	0.036	14.4	4.637E+04	1.298E+06	7.5± 5.4
10	0	1	24	0.000	0.5	0.000E+00	4.830E+04	0.0± 0.0
11	1	16	64	0.062	3.2	1.811E+04	2.898E+05	13.0± 13.5
12	0	1	64	0.000	0.2	0.000E+00	1.811E+04	0.0± 0.0
13	0	73	36	0.000	26.2	0.000E+00	2.351E+06	0.0± 0.0
14	1	50	30	0.020	21.5	3.864E+04	1.932E+06	4.2± 4.2
15	1	16	32	0.062	6.4	3.623E+04	5.796E+05	13.0± 13.5
16	0	20	64	0.000	4.0	0.000E+00	3.623E+05	0.0± 0.0
17	6	720	62	0.008	149.8	1.122E+05	1.346E+07	1.7± 0.7
18	0	32	24	0.000	17.2	0.000E+00	1.546E+06	0.0± 0.0
19	2	6	16	0.333	4.8	1.449E+05	4.347E+05	69.3± 56.6
20	0	8	15	0.000	6.9	0.000E+00	6.183E+05	0.0± 0.0
21	3	58	100	0.052	7.5	3.478E+04	6.724E+05	10.8± 6.4
	61	1574			22.7	7.910E+04	2.041E+06	

Area of basic unit = 9.026E-07 cm-2

CHI SQUARED = 197.4619 WITH 20 DEGREES OF FREEDOM
P(chi squared) = 100.0 %
CORRELATION COEFFICIENT = 0.201
VARIANCE OF SQR(Ns) = 1.399817
VARIANCE OF SQR(Ni) = 29.89709

Ns/Ni = 0.039 ± 0.005
MEAN RATIO = 0.077 ± 0.028

POOLED AGE = 8.1 ± 1.1 Ma
MEAN AGE = 16.1 ± 5.8 Ma

Ages calculated using a zeta of 355 ± 4 for SRM612 glass
RHO D = 1.177E+06cm-2; ND = 6094

8642-61 APATITE Toolachee-1, 303m

IRRADIATION PT784 SLIDE NUMBER 6
COUNTED BY: IRD

No.	Ns	Ni	Na	RATIO	U(ppm)	RHOs	RHOi	F.T.AGE(Ma)
1	4	19	100	0.211	2.1	4.675E+04	2.221E+05	51.9± 28.6
2	5	10	80	0.500	1.4	7.305E+04	1.461E+05	122.7± 67.2
3	15	33	40	0.455	9.0	4.383E+05	9.642E+05	111.6± 34.8
4	21	51	100	0.412	5.6	2.454E+05	5.961E+05	101.2± 26.3
5	10	11	63	0.909	1.9	1.855E+05	2.041E+05	221.4± 96.8
6	11	50	100	0.220	5.5	1.286E+05	5.844E+05	54.3± 18.1
7	22	47	90	0.468	5.7	2.857E+05	6.104E+05	114.9± 29.8
8	6	19	28	0.316	7.4	2.504E+05	7.931E+05	77.8± 36.4
9	8	20	60	0.400	3.7	1.558E+05	3.896E+05	98.3± 41.2
10	4	24	59	0.167	4.5	7.924E+04	4.754E+05	41.2± 22.2
11	4	9	36	0.444	2.7	1.299E+05	2.922E+05	109.2± 65.6
12	22	63	80	0.349	8.6	3.214E+05	9.204E+05	85.9± 21.3
13	28	61	61	0.459	11.0	5.365E+05	1.169E+06	112.7± 25.8
14	3	3	36	1.000	0.9	9.740E+04	9.740E+04	243.1±198.5
15	27	51	80	0.529	7.0	3.945E+05	7.451E+05	129.8± 31.0
16	13	29	60	0.448	5.3	2.532E+05	5.649E+05	110.1± 36.8
17	6	11	59	0.545	2.0	1.189E+05	2.179E+05	133.7± 67.9
18	8	18	64	0.444	3.1	1.461E+05	3.287E+05	109.2± 46.4
19	11	32	64	0.344	5.5	2.009E+05	5.844E+05	84.6± 29.6
20	19	56	100	0.339	6.1	2.221E+05	6.545E+05	83.5± 22.2
	247	617			5.0	2.123E+05	5.302E+05	

Area of basic unit = 9.056E-07 cm-2

CHI SQUARED = 16.80121 WITH 19 DEGREES OF FREEDOM
P(chi squared) = 60.3 %
CORRELATION COEFFICIENT = 0.890
VARIANCE OF SQR(Ns) = 1.324683
VARIANCE OF SQR(Ni) = 3.412928

Ns/Ni = 0.400 ± 0.030
MEAN RATIO = 0.448 ± 0.045

POOLED AGE = 98.4 ± 7.6 Ma
MEAN AGE = 110.0 ± 11.3 Ma

Ages calculated using a zeta of 355 ± 4 for SRM612 glass
RHO D = 1.396E+06cm-2; ND = 5971

8642-64 APATITE Tollachee-1, 776m

IRRADIATION PT784 SLIDE NUMBER 7
COUNTED BY: IRD

No.	Ns	Ni	Na	RATIO	U(ppm)	RHOs	RHOi	F.T.AGE(Ma)
1	5	4	20	1.250	2.2	2.922E+05	2.338E+05	302.5±203.0
2	18	48	48	0.375	11.0	4.383E+05	1.169E+06	92.2± 25.5
3	17	32	30	0.531	11.7	6.623E+05	1.247E+06	130.3± 39.2
4	10	30	47	0.333	7.0	2.487E+05	7.460E+05	82.1± 30.0
5	3	3	40	1.000	0.8	8.766E+04	8.766E+04	243.1±198.5
6	18	40	64	0.450	6.9	3.287E+05	7.305E+05	110.5± 31.4
7	37	110	36	0.336	33.5	1.201E+06	3.571E+06	82.8± 15.8
8	13	8	32	1.625	2.7	4.748E+05	2.922E+05	390.5±175.6
9	112	266	36	0.421	81.1	3.636E+06	8.636E+06	103.5± 11.8
10	30	90	100	0.333	9.9	3.506E+05	1.052E+06	82.1± 17.4
11	6	13	32	0.462	4.5	2.191E+05	4.748E+05	113.3± 56.0
12	11	9	34	1.222	2.9	3.781E+05	3.094E+05	295.9±133.1
13	8	4	36	2.000	1.2	2.597E+05	1.299E+05	477.4±292.4
14	56	125	16	0.448	85.7	4.091E+06	9.131E+06	110.0± 17.8
15	5	16	40	0.312	4.4	1.461E+05	4.675E+05	77.0± 39.5
16	13	33	50	0.394	7.2	3.039E+05	7.714E+05	96.9± 31.8
17	34	35	15	0.971	25.6	2.649E+06	2.727E+06	236.3± 57.0
18	16	71	40	0.225	19.5	4.675E+05	2.075E+06	55.6± 15.4
19	6	24	58	0.250	4.5	1.209E+05	4.836E+05	61.6± 28.2
20	20	35	60	0.571	6.4	3.896E+05	6.818E+05	140.0± 39.3
	438	996			13.1	6.138E+05	1.396E+06	

Area of basic unit = 9.056E-07 cm-2

CHI SQUARED = 52.18875 WITH 19 DEGREES OF FREEDOM
P(chi squared) = 0.0 %
CORRELATION COEFFICIENT = 0.961
VARIANCE OF SQR(Ns) = 4.413682
VARIANCE OF SQR(Ni) = 13.30432

Ns/Ni = 0.440 ± 0.025
MEAN RATIO = 0.676 ± 0.112

POOLED AGE = 108.0 ± 6.5 Ma
MEAN AGE = 165.2 ± 27.5 Ma

Ages calculated using a zeta of 355 ± 4 for SRM612 glass
RHO D = 1.396E+06cm-2; ND = 5971

8642-67 APATITE Toolachee-1, 1242m

IRRADIATION PT784 SLIDE NUMBER 8
COUNTED BY: IRD

No.	Ns	Ni	Na	RATIO	U(ppm)	RHOs	RHOi	F.T.AGE(Ma)
1	8	19	34	0.421	6.1	2.750E+05	6.531E+05	103.5± 43.6
2	13	23	60	0.565	4.2	2.532E+05	4.480E+05	138.5± 48.1
3	13	50	36	0.260	15.2	4.221E+05	1.623E+06	64.1± 20.0
4	163	192	35	0.849	60.2	5.443E+06	6.412E+06	207.0± 22.3
5	22	56	57	0.393	10.8	4.511E+05	1.148E+06	96.6± 24.4
6	22	36	64	0.611	6.2	4.018E+05	6.574E+05	149.6± 40.6
7	6	21	16	0.286	14.4	4.383E+05	1.534E+06	70.4± 32.6
8	8	13	16	0.615	8.9	5.844E+05	9.496E+05	150.7± 67.8
9	15	13	36	1.154	4.0	4.870E+05	4.221E+05	279.7±106.1
10	1	6	60	0.167	1.1	1.948E+04	1.169E+05	41.2± 44.5
11	10	22	36	0.455	6.7	3.247E+05	7.142E+05	111.6± 42.6
12	8	19	60	0.421	3.5	1.558E+05	3.701E+05	103.5± 43.6
13	64	165	40	0.388	45.2	1.870E+06	4.821E+06	95.4± 14.1
14	3	24	40	0.125	6.6	8.766E+04	7.013E+05	30.9± 18.9
15	37	41	20	0.902	22.5	2.162E+06	2.396E+06	219.8± 50.0
16	7	15	40	0.467	4.1	2.045E+05	4.383E+05	114.6± 52.5
17	5	15	50	0.333	3.3	1.169E+05	3.506E+05	82.1± 42.4
18	64	128	36	0.500	39.0	2.078E+06	4.156E+06	122.7± 18.9
19	10	15	100	0.667	1.6	1.169E+05	1.753E+05	163.1± 66.6
20	21	62	40	0.339	17.0	6.136E+05	1.812E+06	83.4± 21.1
21	15	23	64	0.652	3.9	2.739E+05	4.200E+05	159.6± 53.0
22	54	111	40	0.486	30.4	1.578E+06	3.243E+06	119.4± 19.9
	569	1069			12.0	6.786E+05	1.275E+06	

Area of basic unit = 9.056E-07 cm-2

CHI SQUARED = 57.46169 WITH 21 DEGREES OF FREEDOM
P(chi squared) = 0.0 %
CORRELATION COEFFICIENT = 0.909
VARIANCE OF SQR(Ns) = 7.150496
VARIANCE OF SQR(Ni) = 10.19408

Ns/Ni = 0.532 ± 0.028
MEAN RATIO = 0.503 ± 0.052

POOLED AGE = 130.5 ± 7.1 Ma
MEAN AGE = 123.3 ± 12.9 Ma

Ages calculated using a zeta of 355 ± 4 for SRM612 glass
RHO D = 1.396E+06cm-2; ND = 5971

8642-68 APATITE Toolachee-1, 1388m

IRRADIATION PT784 SLIDE NUMBER 9
COUNTED BY: IRD

No.	Ns	Ni	Na	RATIO	U(ppm)	RHOs	RHOi	F.T.AGE(Ma)
1	19	27	64	0.704	4.6	3.470E+05	4.931E+05	172.0± 51.6
2	9	23	64	0.391	3.9	1.644E+05	4.200E+05	96.2± 37.9
3	29	46	100	0.630	5.0	3.389E+05	5.376E+05	154.3± 36.7
4	31	50	60	0.620	9.1	6.039E+05	9.740E+05	151.8± 34.8
5	8	18	24	0.444	8.2	3.896E+05	8.766E+05	109.2± 46.4
6	10	14	36	0.714	4.3	3.247E+05	4.545E+05	174.6± 72.3
7	3	2	30	1.500	0.7	1.169E+05	7.792E+04	361.3±329.9
8	7	15	50	0.467	3.3	1.636E+05	3.506E+05	114.6± 52.5
9	4	22	32	0.182	7.5	1.461E+05	8.035E+05	44.9± 24.4
10	12	17	39	0.706	4.8	3.596E+05	5.095E+05	172.5± 65.1
11	2	10	24	0.200	4.6	9.740E+04	4.870E+05	49.4± 38.2
12	5	9	20	0.556	4.9	2.922E+05	5.259E+05	136.2± 76.0
13	26	23	64	1.130	3.9	4.748E+05	4.200E+05	274.1± 78.6
14	7	5	40	1.400	1.4	2.045E+05	1.461E+05	337.8±197.9
15	9	19	64	0.474	3.3	1.644E+05	3.470E+05	116.3± 47.1
16	9	13	24	0.692	5.9	4.383E+05	6.331E+05	169.3± 73.5
17	24	33	80	0.727	4.5	3.506E+05	4.821E+05	177.7± 47.8
18	11	18	80	0.611	2.5	1.607E+05	2.630E+05	149.6± 57.3
19	12	29	54	0.414	5.9	2.597E+05	6.277E+05	101.7± 35.0
20	2	4	40	0.500	1.1	5.844E+04	1.169E+05	122.7±106.3
21	8	15	58	0.533	2.8	1.612E+05	3.023E+05	130.8± 57.3
	247	412			4.3	2.757E+05	4.599E+05	

Area of basic unit = 9.056E-07 cm-2

CHI SQUARED = 21.02595 WITH 20 DEGREES OF FREEDOM
P(chi squared) = 39.6 %
CORRELATION COEFFICIENT = 0.870
VARIANCE OF SQR(Ns) = 1.514049
VARIANCE OF SQR(Ni) = 2.021524

Ns/Ni = 0.600 ± 0.048
MEAN RATIO = 0.647 ± 0.073

POOLED AGE = 146.8 ± 12.1 Ma
MEAN AGE = 158.4 ± 18.0 Ma

Ages calculated using a zeta of 355 ± 4 for SRM612 glass
RHO D = 1.396E+06cm-2; ND = 5971

8642-69 APATITE Toolachee-1, 1507m

IRRADIATION PT784 SLIDE NUMBER 10
COUNTED BY: IRD

No.	Ns	Ni	Na	RATIO	U(ppm)	RHOs	RHOi	F.T.AGE(Ma)
1	6	9	19	0.667	5.2	3.691E+05	5.536E+05	163.1± 86.0
2	10	12	36	0.833	3.7	3.247E+05	3.896E+05	203.2± 87.1
3	7	31	40	0.226	8.5	2.045E+05	9.058E+05	55.7± 23.3
4	1	7	29	0.143	2.6	4.030E+04	2.821E+05	35.3± 37.7
5	7	23	35	0.304	7.2	2.338E+05	7.680E+05	75.0± 32.4
6	43	92	16	0.467	63.1	3.141E+06	6.720E+06	114.8± 21.3
7	8	9	59	0.889	1.7	1.585E+05	1.783E+05	216.5±105.3
8	19	14	39	1.357	3.9	5.694E+05	4.196E+05	327.8±115.6
9	40	98	42	0.408	25.6	1.113E+06	2.727E+06	100.3± 18.9
10	8	10	20	0.800	5.5	4.675E+05	5.844E+05	195.2± 92.7
11	21	24	25	0.875	10.5	9.818E+05	1.122E+06	213.2± 63.8
12	19	32	60	0.594	5.8	3.701E+05	6.233E+05	145.4± 42.2
13	11	19	58	0.579	3.6	2.217E+05	3.829E+05	141.9± 53.8
14	3	3	35	1.000	0.9	1.002E+05	1.002E+05	243.1±198.5
15	11	8	25	1.375	3.5	5.143E+05	3.740E+05	332.0±154.4
16	4	8	50	0.500	1.8	9.350E+04	1.870E+05	122.7± 75.2
17	45	96	48	0.469	21.9	1.096E+06	2.338E+06	115.1± 20.9
18	18	41	59	0.439	7.6	3.566E+05	8.122E+05	107.9± 30.6
19	5	10	36	0.500	3.0	1.623E+05	3.247E+05	122.7± 67.2
20	7	15	100	0.467	1.6	8.181E+04	1.753E+05	114.6± 52.5
	293	561			7.4	4.121E+05	7.890E+05	

Area of basic unit = 9.056E-07 cm-2

CHI SQUARED = 30.5189 WITH 19 DEGREES OF FREEDOM
P(chi squared) = 4.6 %
CORRELATION COEFFICIENT = 0.942
VARIANCE OF SQR(Ns) = 2.548245
VARIANCE OF SQR(Ni) = 6.071135

Ns/Ni = 0.522 ± 0.038
MEAN RATIO = 0.645 ± 0.075

POOLED AGE = 128.1 ± 9.5 Ma
MEAN AGE = 157.7 ± 18.5 Ma

Ages calculated using a zeta of 355 ± 4 for SRM612 glass
RHO D = 1.396E+06cm-2; ND = 5971

8642-70 APATITE Toolachee-1, 1852m

IRRADIATION PT784 SLIDE NUMBER 11
COUNTED BY: IRD

No.	Ns	Ni	Na	RATIO	U(ppm)	RHOs	RHOi	F.T.AGE(Ma)
1	12	38	32	0.316	13.0	4.383E+05	1.388E+06	77.8± 25.8
2	6	25	37	0.240	7.4	1.895E+05	7.897E+05	59.2± 26.9
3	2	2	16	1.000	1.4	1.461E+05	1.461E+05	243.1±243.1
4	7	21	60	0.333	3.8	1.364E+05	4.091E+05	82.1± 35.8
5	2	158	60	0.013	28.9	3.896E+04	3.078E+06	3.1± 2.2
6	4	9	25	0.444	3.9	1.870E+05	4.208E+05	109.2± 65.6
7	3	14	30	0.214	5.1	1.169E+05	5.454E+05	52.9± 33.6
8	16	23	50	0.696	5.0	3.740E+05	5.376E+05	170.1± 55.4
9	3	40	41	0.075	10.7	8.552E+04	1.140E+06	18.6± 11.1
10	11	27	73	0.407	4.1	1.761E+05	4.323E+05	100.2± 35.9
11	0	14	48	0.000	3.2	0.000E+00	3.409E+05	0.0± 0.0
12	8	17	35	0.471	5.3	2.671E+05	5.677E+05	115.5± 49.6
13	14	16	12	0.875	14.6	1.364E+06	1.558E+06	213.2± 78.1
14	2	5	16	0.400	3.4	1.461E+05	3.652E+05	98.3± 82.3
15	2	21	60	0.095	3.8	3.896E+04	4.091E+05	23.6± 17.4
16	4	14	24	0.286	6.4	1.948E+05	6.818E+05	70.4± 39.9
17	10	15	80	0.667	2.1	1.461E+05	2.191E+05	163.1± 66.6
	106	459			7.2	1.772E+05	7.675E+05	

Area of basic unit = 9.056E-07 cm-2

CHI SQUARED = 87.75456 WITH 16 DEGREES OF FREEDOM
P(chi squared) = 0.0 %
CORRELATION COEFFICIENT = -0.113
VARIANCE OF SQR(Ns) = 1.11045
VARIANCE OF SQR(Ni) = 5.691938

Ns/Ni = 0.231 ± 0.025
MEAN RATIO = 0.384 ± 0.070

POOLED AGE = 57.0 ± 6.2 Ma
MEAN AGE = 94.5 ± 17.3 Ma

Ages calculated using a zeta of 355 ± 4 for SRM612 glass
RHO D = 1.396E+06cm-2; ND = 5971

8642-54 APATITE Tinga Tingana-1, 1732m

IRRADIATION PT784 SLIDE NUMBER 4
COUNTED BY: IRD

No.	Ns	Ni	Na	RATIO	U(ppm)	RHOs	RHOi	F.T.AGE(Ma)
1	39	76	36	0.513	23.2	1.266E+06	2.467E+06	125.9± 24.9
2	22	33	89	0.667	4.1	2.889E+05	4.334E+05	163.1± 45.0
3	82	153	64	0.536	26.2	1.497E+06	2.794E+06	131.4± 18.1
4	83	112	40	0.741	30.7	2.425E+06	3.273E+06	181.0± 26.4
5	6	19	30	0.316	6.9	2.338E+05	7.402E+05	77.8± 36.4
6	3	11	50	0.273	2.4	7.013E+04	2.571E+05	67.2± 43.8
7	11	75	25	0.147	32.9	5.143E+05	3.506E+06	36.2± 11.7
8	43	62	64	0.694	10.6	7.853E+05	1.132E+06	169.6± 33.8
9	72	115	44	0.626	28.7	1.913E+06	3.055E+06	153.3± 23.2
10	33	73	63	0.452	12.7	6.122E+05	1.354E+06	111.0± 23.4
11	3	5	45	0.600	1.2	7.792E+04	1.299E+05	147.0±107.4
12	2	24	34	0.083	7.7	6.875E+04	8.250E+05	20.6± 15.2
13	10	63	100	0.159	6.9	1.169E+05	7.363E+05	39.2± 13.4
14	66	161	44	0.410	40.1	1.753E+06	4.277E+06	100.8± 14.8
15	47	139	61	0.338	25.0	9.005E+05	2.663E+06	83.2± 14.1
16	117	128	33	0.914	42.5	4.144E+06	4.533E+06	222.6± 28.7
17	101	85	15	1.188	62.2	7.870E+06	6.623E+06	287.9± 42.7
18	20	25	40	0.800	6.9	5.844E+05	7.305E+05	195.2± 58.7
19	1	5	36	0.200	1.5	3.247E+04	1.623E+05	49.4± 54.1
20	28	30	72	0.933	4.6	4.545E+05	4.870E+05	227.2± 59.8
21	69	86	36	0.802	26.2	2.240E+06	2.792E+06	195.8± 31.8
22	16	43	63	0.372	7.5	2.968E+05	7.977E+05	91.5± 26.8
23	65	96	90	0.677	11.7	8.441E+05	1.247E+06	165.6± 26.8
	939	1619			15.1	9.348E+05	1.612E+06	

Area of basic unit = 9.056E-07 cm-2

CHI SQUARED = 123.4113 WITH 22 DEGREES OF FREEDOM
P(chi squared) = 0.0 %
CORRELATION COEFFICIENT = 0.800
VARIANCE OF SQR(Ns) = 8.93541
VARIANCE OF SQR(Ni) = 10.04322

Ns/Ni = 0.580 ± 0.024
MEAN RATIO = 0.541 ± 0.060

POOLED AGE = 142.1 ± 6.3 Ma
MEAN AGE = 132.6 ± 14.8 Ma

Ages calculated using a zeta of 355 ± 4 for SRM612 glass
RHO D = 1.396E+06cm-2; ND = 5971

8642-55 APATITE Tinga Tingana-1, 2096m

IRRADIATION PT784 SLIDE NUMBER 5
COUNTED BY: IRD

No.	Ns	Ni	Na	RATIO	U(ppm)	RHOs	RHOi	F.T.AGE(Ma)
1	42	17	100	2.471	1.9	4.909E+05	1.987E+05	584.7±168.4
2	4	110	98	0.036	12.3	4.770E+04	1.312E+06	9.0± 4.6
3	21	104	36	0.202	31.7	6.818E+05	3.376E+06	49.8± 12.0
4	1	15	36	0.067	4.6	3.247E+04	4.870E+05	16.5± 17.0
5	15	78	60	0.192	14.3	2.922E+05	1.519E+06	47.5± 13.4
6	11	24	24	0.458	11.0	5.357E+05	1.169E+06	112.6± 41.0
7	67	750	100	0.089	82.3	7.831E+05	8.766E+06	22.1± 2.8
8	0	4	64	0.000	0.7	0.000E+00	7.305E+04	0.0± 0.0
9	35	23	64	1.522	3.9	6.392E+05	4.200E+05	366.4± 98.5
10	5	11	100	0.455	1.2	5.844E+04	1.286E+05	111.6± 60.2
11	121	203	64	0.596	34.8	2.210E+06	3.707E+06	146.0± 17.0
12	1	18	36	0.056	5.5	3.247E+04	5.844E+05	13.7± 14.1
13	44	33	100	1.333	3.6	5.143E+05	3.857E+05	322.1± 74.4
14	10	86	60	0.116	15.7	1.948E+05	1.675E+06	28.7± 9.6
15	27	500	48	0.054	114.3	6.574E+05	1.217E+07	13.4± 2.7
16	12	196	100	0.061	21.5	1.403E+05	2.291E+06	15.2± 4.5
17	53	45	99	1.178	5.0	6.257E+05	5.313E+05	285.4± 58.1
18	11	189	100	0.058	20.7	1.286E+05	2.209E+06	14.4± 4.5
19	4	30	36	0.133	9.1	1.299E+05	9.740E+05	32.9± 17.5
20	6	30	36	0.200	9.1	1.948E+05	9.740E+05	49.4± 22.1
21	38	42	100	0.905	4.6	4.441E+05	4.909E+05	220.3± 49.5
	528	2508			18.8	4.224E+05	2.006E+06	

Area of basic unit = 8.556E-07 cm-2

CHI SQUARED = 683.1558 WITH 20 DEGREES OF FREEDOM
P(chi squared) = 0 %
CORRELATION COEFFICIENT = 0.392
VARIANCE OF SQR(Ns) = 7.43146
VARIANCE OF SQR(Ni) = 41.54103

Ns/Ni = 0.211 ± 0.010
MEAN RATIO = 0.485 ± 0.142

POOLED AGE = 51.9 ± 2.6 Ma
MEAN AGE = 119.0 ± 34.8 Ma

Ages calculated using a zeta of 355 ± 4 for SRM612 glass
RHO D = 1.396E+06cm-2; ND = 5971

8642-33 APATITE Poolawanna-1, 2356m

IRRADIATION PT785 SLIDE NUMBER 1
COUNTED BY: IRD

No.	Ns	Ni	Na	RATIO	U(ppm)	RHOs	RHOi	F.T.AGE(Ma)
1	0	28	58	0.000	5.0	0.000E+00	5.642E+05	0.0± 0.0
2	0	5	24	0.000	2.1	0.000E+00	2.435E+05	0.0± 0.0
3	1	141	24	0.007	60.4	4.870E+04	6.867E+06	1.9± 1.9
4	0	2	16	0.000	1.3	0.000E+00	1.461E+05	0.0± 0.0
5	2	54	100	0.037	5.6	2.338E+04	6.311E+05	9.8± 7.0
6	4	78	15	0.051	53.5	3.117E+05	6.078E+06	13.5± 6.9
7	3	213	24	0.014	91.3	1.461E+05	1.037E+07	3.7± 2.2
8	0	16	59	0.000	2.8	0.000E+00	3.170E+05	0.0± 0.0
9	0	39	60	0.000	6.7	0.000E+00	7.597E+05	0.0± 0.0
10	0	8	50	0.000	1.6	0.000E+00	1.870E+05	0.0± 0.0
11	1	25	24	0.040	10.7	4.870E+04	1.217E+06	10.6± 10.8
12	0	6	32	0.000	1.9	0.000E+00	2.191E+05	0.0± 0.0
13	1	76	32	0.013	24.4	3.652E+04	2.776E+06	3.5± 3.5
14	16	123	24	0.130	52.7	7.792E+05	5.990E+06	34.3± 9.1
15	0	1	24	0.000	0.4	0.000E+00	4.870E+04	0.0± 0.0
16	0	2	40	0.000	0.5	0.000E+00	5.844E+04	0.0± 0.0
17	0	3	60	0.000	0.5	0.000E+00	5.844E+04	0.0± 0.0
18	2	44	80	0.045	5.7	2.922E+04	6.428E+05	12.0± 8.7
19	0	2	36	0.000	0.6	0.000E+00	6.493E+04	0.0± 0.0
20	2	10	62	0.200	1.7	3.770E+04	1.885E+05	52.6± 40.8
21	5	153	60	0.033	26.2	9.740E+04	2.980E+06	8.6± 3.9
22	77	86	30	0.895	29.5	3.000E+06	3.350E+06	232.3± 36.8
	114	1115			12.3	1.427E+05	1.395E+06	

Area of basic unit = 8.556E-07 cm-2

CHI SQUARED = 339.6945 WITH 21 DEGREES OF FREEDOM
P(chi squared) = 0 %
CORRELATION COEFFICIENT = 0.242
VARIANCE OF SQR(Ns) = 3.966974
VARIANCE OF SQR(Ni) = 17.11983

Ns/Ni = 0.102 ± 0.010
MEAN RATIO = 0.067 ± 0.041

POOLED AGE = 27.0 ± 2.7 Ma
MEAN AGE = 17.6 ± 10.8 Ma

Ages calculated using a zeta of 355 ± 4 for SRM612 glass
RHO D = 1.488E+06cm-2; ND = 2547

8642-34 APATITE Poolawanna-1, 2354m

IRRADIATION PT785 SLIDE NUMBER 2
COUNTED BY: IRD

No.	Ns	Ni	Na	RATIO	U(ppm)	RHOs	RHOi	F.T.AGE(Ma)
1	3	177	36	0.017	50.6	9.740E+04	5.746E+06	4.5± 2.6
2	2	101	40	0.020	26.0	5.844E+04	2.951E+06	5.2± 3.7
3	0	35	20	0.000	18.0	0.000E+00	2.045E+06	0.0± 0.0
4	1	23	80	0.043	3.0	1.461E+04	3.360E+05	11.5± 11.7
5	0	60	100	0.000	6.2	0.000E+00	7.013E+05	0.0± 0.0
6	36	51	20	0.706	26.2	2.104E+06	2.980E+06	183.8± 40.2
7	0	71	24	0.000	30.4	0.000E+00	3.458E+06	0.0± 0.0
8	0	27	40	0.000	6.9	0.000E+00	7.889E+05	0.0± 0.0
9	0	49	96	0.000	5.3	0.000E+00	5.966E+05	0.0± 0.0
10	1	54	64	0.019	8.7	1.826E+04	9.862E+05	4.9± 4.9
11	0	15	32	0.000	4.8	0.000E+00	5.479E+05	0.0± 0.0
12	0	1	36	0.000	0.3	0.000E+00	3.247E+04	0.0± 0.0
13	0	38	36	0.000	10.9	0.000E+00	1.234E+06	0.0± 0.0
14	2	210	36	0.010	60.0	6.493E+04	6.818E+06	2.5± 1.8
15	0	86	36	0.000	24.6	0.000E+00	2.792E+06	0.0± 0.0
16	0	750	100	0.000	77.1	0.000E+00	8.766E+06	0.0± 0.0
17	3	210	30	0.014	72.0	1.169E+05	8.181E+06	3.8± 2.2
18	0	11	36	0.000	3.1	0.000E+00	3.571E+05	0.0± 0.0
19	0	94	36	0.000	26.9	0.000E+00	3.052E+06	0.0± 0.0
20	0	32	50	0.000	6.6	0.000E+00	7.480E+05	0.0± 0.0
	48	2095			22.7	5.918E+04	2.583E+06	

Area of basic unit = 8.556E-07 cm-2

CHI SQUARED = 640.7885 WITH 19 DEGREES OF FREEDOM
P(chi squared) = 100.0 %
CORRELATION COEFFICIENT = -0.054
VARIANCE OF SQR(Ns) = 1.988746
VARIANCE OF SQR(Ni) = 32.16334

Ns/Ni = 0.023 ± 0.003
MEAN RATIO = 0.041 ± 0.035

POOLED AGE = 6.1 ± 0.9 Ma
MEAN AGE = 10.9 ± 9.3 Ma

Ages calculated using a zeta of 355 ± 4 for SRM612 glass
RHO D = 1.488E+06cm-2; ND = 2547

8642-35 APATITE Poolawanna-1, 3073m

IRRADIATION PT785 SLIDE NUMBER 3
COUNTED BY: IRD8

No.	Ns	Ni	Na	RATIO	U(ppm)	RHOs	RHOi	F.T.AGE(Ma)
1	0	42	28	0.000	15.4	0.000E+00	1.753E+06	0.0± 0.0
2	1	30	18	0.033	17.1	6.493E+04	1.948E+06	8.8± 8.9
3	1	12	36	0.083	3.4	3.247E+04	3.896E+05	22.0± 22.9
4	0	149	30	0.000	51.1	0.000E+00	5.805E+06	0.0± 0.0
5	3	7	9	0.429	8.0	3.896E+05	9.090E+05	112.2± 77.5
6	0	6	16	0.000	3.9	0.000E+00	4.383E+05	0.0± 0.0
7	0	13	16	0.000	8.4	0.000E+00	9.496E+05	0.0± 0.0
8	2	180	15	0.011	123.4	1.558E+05	1.403E+07	2.9± 2.1
9	1	65	16	0.015	41.8	7.305E+04	4.748E+06	4.1± 4.1
10	0	45	36	0.000	12.9	0.000E+00	1.461E+06	0.0± 0.0
11	0	22	30	0.000	7.5	0.000E+00	8.571E+05	0.0± 0.0
12	0	14	40	0.000	3.6	0.000E+00	4.091E+05	0.0± 0.0
13	2	4	40	0.500	1.0	5.844E+04	1.169E+05	130.8±113.3
14	0	46	20	0.000	23.7	0.000E+00	2.688E+06	0.0± 0.0
15	0	3	32	0.000	1.0	0.000E+00	1.096E+05	0.0± 0.0
16	0	3	18	0.000	1.7	0.000E+00	1.948E+05	0.0± 0.0
17	0	34	30	0.000	11.7	0.000E+00	1.325E+06	0.0± 0.0
18	0	117	16	0.000	75.2	0.000E+00	8.547E+06	0.0± 0.0
19	0	10	36	0.000	2.9	0.000E+00	3.247E+05	0.0± 0.0
20	0	204	36	0.000	58.3	0.000E+00	6.623E+06	0.0± 0.0
	10	1006			20.0	2.256E+04	2.270E+06	

Area of basic unit = 9.056E-07 cm-2

CHI SQUARED = 165.6691 WITH 19 DEGREES OF FREEDOM
P(chi squared) = 0.0 %
CORRELATION COEFFICIENT = -0.007
VARIANCE OF SQR(Ns) = .3758925
VARIANCE OF SQR(Ni) = 15.50129

Ns/Ni = 0.010 ± 0.003
MEAN RATIO = 0.054 ± 0.032

POOLED AGE = 2.6 ± 0.8 Ma
MEAN AGE = 14.1 ± 8.4 Ma

Ages calculated using a zeta of 355 ± 4 for SRM612 glass
RHO D = 1.488E+06cm-2; ND = 2547

8642-40 APATITE Putamurdi-1, 1877m

IRRADIATION PT776 SLIDE NUMBER 3
COUNTED BY: IRD

No.	Ns	Ni	Na	RATIO	U(ppm)	RHOs	RHOi	F.T.AGE(Ma)
1	0	10	16	0.000	8.1	0.000E+00	7.246E+05	0.0± 0.0
2	1	20	9	0.050	28.7	1.288E+05	2.576E+06	10.4± 10.7
3	0	8	12	0.000	8.6	0.000E+00	7.729E+05	0.0± 0.0
4	0	17	12	0.000	18.3	0.000E+00	1.642E+06	0.0± 0.0
5	1	38	20	0.026	24.5	5.796E+04	2.203E+06	5.5± 5.6
6	5	116	15	0.043	99.7	3.864E+05	8.965E+06	9.0± 4.1
7	2	24	15	0.083	20.6	1.546E+05	1.855E+06	17.4± 12.8
8	2	24	15	0.083	20.6	1.546E+05	1.855E+06	17.4± 12.8
9	0	32	10	0.000	41.3	0.000E+00	3.710E+06	0.0± 0.0
10	0	20	9	0.000	28.7	0.000E+00	2.576E+06	0.0± 0.0
11	0	12	9	0.000	17.2	0.000E+00	1.546E+06	0.0± 0.0
12	2	37	20	0.054	23.9	1.159E+05	2.145E+06	11.3± 8.2
13	1	13	9	0.077	18.6	1.288E+05	1.675E+06	16.1± 16.7
14	7	20	12	0.350	21.5	6.762E+05	1.932E+06	72.7± 32.0
15	0	24	12	0.000	25.8	0.000E+00	2.319E+06	0.0± 0.0
16	0	11	9	0.000	15.8	0.000E+00	1.417E+06	0.0± 0.0
17	0	8	9	0.000	11.5	0.000E+00	1.030E+06	0.0± 0.0
18	0	35	10	0.000	45.1	0.000E+00	4.058E+06	0.0± 0.0
19	0	13	35	0.000	4.8	0.000E+00	4.306E+05	0.0± 0.0
20	0	22	12	0.000	23.6	0.000E+00	2.125E+06	0.0± 0.0
21	1	29	15	0.034	24.9	7.729E+04	2.241E+06	7.2± 7.3
	22	533			24.1	8.949E+04	2.168E+06	

Area of basic unit = 9.026E-07 cm-2

CHI SQUARED = 45.64509 WITH 20 DEGREES OF FREEDOM
P(chi squared) = 0.0 %
CORRELATION COEFFICIENT = 0.518
VARIANCE OF SQR(Ns) = .6898776
VARIANCE OF SQR(Ni) = 2.976742

Ns/Ni = 0.041 ± 0.009
MEAN RATIO = 0.038 ± 0.017

POOLED AGE = 8.6 ± 1.9 Ma
MEAN AGE = 8.0 ± 3.5 Ma

Ages calculated using a zeta of 355 ± 4 for SRM612 glass
RHO D = 1.177E+06cm-2; ND = 6094

8642-58 APATITE Merrimelia-1, 2592m

IRRADIATION PT785 SLIDE NUMBER 4
COUNTED BY: IRD

No.	Ns	Ni	Na	RATIO	U(ppm)	RHOs	RHOi	F.T.AGE(Ma)
1	5	445	100	0.011	45.8	5.844E+04	5.201E+06	3.0± 1.3
2	0	4	36	0.000	1.1	0.000E+00	1.299E+05	0.0± 0.0
3	0	4	24	0.000	1.7	0.000E+00	1.948E+05	0.0± 0.0
	5	453			29.1	3.652E+04	3.309E+06	

Area of basic unit = 9.056E-07 cm-2

CHI SQUARED = .08987 WITH 2 DEGREES OF FREEDOM
P(chi squared) = 95.6 %
CORRELATION COEFFICIENT = 1.000
VARIANCE OF SQR(Ns) = 1.666667
VARIANCE OF SQR(Ni) = 121.54

Ns/Ni = 0.011 ± 0.005
MEAN RATIO = 0.004 ± 0.004

POOLED AGE = 2.9 ± 1.3 Ma
MEAN AGE = 1.0 ± 1.0 Ma

Ages calculated using a zeta of 355 ± 4 for SRM612 glass
RHO D = 1.488E+06cm-2; ND = 2547

8642-58/59 APATITE Merrimelia-1, 2592/ 2946m

IRRADIATION PT785 SLIDE NUMBER 4
COUNTED BY: IRD

No.	Ns	Ni	Na	RATIO	U(ppm)	RHOs	RHOi	F.T.AGE(Ma)
1	5	445	100	0.011	45.8	5.844E+04	5.201E+06	3.0± 1.3
2	0	4	36	0.000	1.1	0.000E+00	1.299E+05	0.0± 0.0
3	0	4	24	0.000	1.7	0.000E+00	1.948E+05	0.0± 0.0
4	9	85	16	0.106	54.6	6.574E+05	6.209E+06	27.9± 9.8
5	0	30	16	0.000	19.3	0.000E+00	2.191E+06	0.0± 0.0
6	0	149	35	0.000	43.8	0.000E+00	4.976E+06	0.0± 0.0
7	0	4	16	0.000	2.6	0.000E+00	2.922E+05	0.0± 0.0
8	0	21	16	0.000	13.5	0.000E+00	1.534E+06	0.0± 0.0
9	0	7	36	0.000	2.0	0.000E+00	2.273E+05	0.0± 0.0
10	0	6	39	0.000	1.6	0.000E+00	1.798E+05	0.0± 0.0
11	0	31	16	0.000	19.9	0.000E+00	2.264E+06	0.0± 0.0
12	0	9	64	0.000	1.4	0.000E+00	1.644E+05	0.0± 0.0
13	0	29	9	0.000	33.1	0.000E+00	3.766E+06	0.0± 0.0
14	0	17	30	0.000	5.8	0.000E+00	6.623E+05	0.0± 0.0
15	0	4	36	0.000	1.1	0.000E+00	1.299E+05	0.0± 0.0
16	0	12	33	0.000	3.7	0.000E+00	4.250E+05	0.0± 0.0
17	0	27	16	0.000	17.4	0.000E+00	1.972E+06	0.0± 0.0
18	0	45	70	0.000	6.6	0.000E+00	7.514E+05	0.0± 0.0
19	0	8	36	0.000	2.3	0.000E+00	2.597E+05	0.0± 0.0
20	0	31	64	0.000	5.0	0.000E+00	5.661E+05	0.0± 0.0
	14	968			14.1	2.311E+04	1.598E+06	

Area of basic unit = 9.056E-07 cm-2

CHI SQUARED = 51.06712 WITH 19 DEGREES OF FREEDOM
P(chi squared) = 0.0 %
CORRELATION COEFFICIENT = 0.543
VARIANCE OF SQR(Ns) = .6646937
VARIANCE OF SQR(Ni) = 20.52665

Ns/Ni = 0.014 ± 0.004
MEAN RATIO = 0.006 ± 0.005

POOLED AGE = 3.8 ± 1.0 Ma
MEAN AGE = 1.5 ± 1.4 Ma

Ages calculated using a zeta of 355 ± 4 for SRM612 glass
RHO D = 1.488E+06cm-2; ND = 2547

R23138 APATITE Merrimelia-8, 1877m

IRRADIATION PT588 SLIDE NUMBER 2
COUNTED BY: IRD

No.	Ns	Ni	Na	RATIO	U(ppm)	RHOs	RHOi	F.T.AGE(Ma)
1	10	20	22	0.500	9.9	5.154E+05	1.031E+06	120.2± 46.6
2	9	13	36	0.692	3.9	2.835E+05	4.095E+05	165.8± 72.0
3	5	21	40	0.238	5.7	1.417E+05	5.953E+05	57.5± 28.6
4	8	45	34	0.178	14.4	2.668E+05	1.501E+06	43.0± 16.5
5	6	18	24	0.333	8.1	2.835E+05	8.504E+05	80.4± 37.9
6	15	37	36	0.405	11.2	4.725E+05	1.165E+06	97.6± 30.0
7	18	159	12	0.113	144.0	1.701E+06	1.502E+07	27.4± 6.8
8	9	12	20	0.750	6.5	5.103E+05	6.803E+05	179.5± 79.2
9	7	18	20	0.389	9.8	3.969E+05	1.021E+06	93.7± 41.8
10	5	22	40	0.227	6.0	1.417E+05	6.237E+05	54.9± 27.2
11	7	25	15	0.280	18.1	5.292E+05	1.890E+06	67.6± 28.9
12	3	10	35	0.300	3.1	9.719E+04	3.240E+05	72.4± 47.7
13	4	9	60	0.444	1.6	7.559E+04	1.701E+05	107.0± 64.3
14	2	2	40	1.000	0.5	5.670E+04	5.670E+04	238.2±238.2
15	2	4	16	0.500	2.7	1.417E+05	2.835E+05	120.2±104.1
16	12	38	30	0.316	13.8	4.536E+05	1.436E+06	76.2± 25.3
17	3	14	14	0.214	10.9	2.430E+05	1.134E+06	51.8± 33.0
18	3	24	24	0.125	10.9	1.417E+05	1.134E+06	30.3± 18.5
19	0	8	30	0.000	2.9	0.000E+00	3.024E+05	0.0± 0.0
	128	499			9.9	2.649E+05	1.033E+06	

Area of basic unit = 9.019E-07 cm-2

CHI SQUARED = 38.88509 WITH 18 DEGREES OF FREEDOM
P(chi squared) = 0.3 %
CORRELATION COEFFICIENT = 0.737
VARIANCE OF SQR(Ns) = .9754795
VARIANCE OF SQR(Ni) = 5.636152

Ns/Ni = 0.257 ± 0.025
MEAN RATIO = 0.369 ± 0.056

POOLED AGE = 61.9 ± 6.3 Ma
MEAN AGE = 88.9 ± 13.6 Ma

Ages calculated using a zeta of 355 ± 4 for SRM612 glass
RHO D = 1.367E+06cm-2; ND = 3014

R23148 APATITE Namur-2, 1658m

IRRADIATION PT588 SLIDE NUMBER 1
COUNTED BY: IRD

No.	Ns	Ni	Na	RATIO	U(ppm)	RHOs	RHOi	F.T.AGE(Ma)
1	0	400	24	0.000	181.1	0.000E+00	1.890E+07	0.0± 0.0
2	1	104	29	0.010	39.0	3.910E+04	4.066E+06	2.3± 2.3
3	9	230	33	0.039	75.7	3.092E+05	7.903E+06	9.5± 3.2
4	1	116	47	0.009	26.8	2.413E+04	2.799E+06	2.1± 2.1
5	9	29	21	0.310	15.0	4.860E+05	1.566E+06	74.9± 28.6
6	0	100	100	0.000	10.9	0.000E+00	1.134E+06	0.0± 0.0
7	0	121	60	0.000	21.9	0.000E+00	2.287E+06	0.0± 0.0
8	0	48	60	0.000	8.7	0.000E+00	9.071E+05	0.0± 0.0
9	1	69	50	0.014	15.0	2.268E+04	1.565E+06	3.5± 3.5
10	0	30	36	0.000	9.1	0.000E+00	9.449E+05	0.0± 0.0
11	15	22	26	0.682	9.2	6.542E+05	9.595E+05	163.4± 54.8
12	4	101	64	0.040	17.1	7.087E+04	1.789E+06	9.6± 4.9
13	1	139	36	0.007	42.0	3.150E+04	4.378E+06	1.7± 1.8
14	7	212	30	0.033	76.8	2.646E+05	8.013E+06	8.0± 3.1
15	1	142	36	0.007	42.9	3.150E+04	4.473E+06	1.7± 1.7
16	0	12	100	0.000	1.3	0.000E+00	1.361E+05	0.0± 0.0
17	0	21	100	0.000	2.3	0.000E+00	2.381E+05	0.0± 0.0
18	1	43	32	0.023	14.6	3.543E+04	1.524E+06	5.6± 5.7
19	0	58	60	0.000	10.5	0.000E+00	1.096E+06	0.0± 0.0
20	1	52	24	0.019	23.5	4.725E+04	2.457E+06	4.7± 4.7
	51	2049			23.0	5.974E+04	2.400E+06	

Area of basic unit = 8.819E-07 cm-2

CHI SQUARED = 328.209 WITH 19 DEGREES OF FREEDOM
P(chi squared) = 100.0 %
CORRELATION COEFFICIENT = -0.001
VARIANCE OF SQR(Ns) = 1.465642
VARIANCE OF SQR(Ni) = 17.1237

Ns/Ni = 0.025 ± 0.004
MEAN RATIO = 0.060 ± 0.036

POOLED AGE = 6.0 ± 0.9 Ma
MEAN AGE = 14.5 ± 8.8 Ma

Ages calculated using a zeta of 355 ± 4 for SRM612 glass
RHO D = 1.367E+06cm-2; ND = 3014